This is to certify that the

dissertation entitled

MECHANISMS OF SNAKE LOCOMOTION:
AN ELECTROMYOGTAPHTC STUDY

presented by

BRUCE CARTER JAYNE

has been accepted towards fulfillment
of the requirements for

pHD degree in zoology

James L. Edwards
Major professor

Date 10/17/85

MECHANISMS OF SNAKE LOCOMOTION: AN ELECTROMYOGRAPHIC STUDY

By

Bruce Carter Jayne

A DISSERTATION

Submitted to
Michigan State University
in partial fulfillment of the requirements
for the degree of

DOCTOR OF PHILOSOPHY

Department of Zoology

1985

ABSTRACT

MECHANISMS OF SNAKE LOCOMOTION: AN ELECTROMYOGRAPHIC STUDY

By

Bruce Carter Jayne

Quantitative techniques were developed to distinguish lateral undulatory, sidewinding, and concertina modes of limbless terrestrial locomotion based on analysis of cinematographic films of five species of snakes and one amphisbaenian crawling on a variety of substrates. Concertina locomotion was the only one of these three modes used by the amphisbaenian, Rhineura floridana. Concertina locomotion of snakes is described for Acrochordus javanicus and Nerodia fasciata. Sidewinding is described for N. fasciata, Cerberus rynchops and Crotalus cerastes. An example of sidewinding combined with lateral undulation is described for a Cerberus rynchops moving on sand.

Electromyography of major epaxial muscles was used to determine muscular mechanisms of locomotor modes. Mechanisms of concertina locomotion and terrestrial and aquatic locomotion were determined for N. fasciata and E. obsoleta, and mechanisms of sidewinding were determined for N. fasciata and C. cerastes. For terrestrial locomotion most muscle activity occurred as descending, alternating, unilateral contractions. Muscle activity usually initiated in a lateral region of the snake when it was maximally convex and continued until the region was maximally

concave (flexed) on the side of the active muscle. During concertina locomotion, some muscle activity also maintained concave regions of the snake as it pressed against the sides of the tunnel. Bilateral activity of the M. semispinalis-spinalis and M. multifidus occurred during sidewinding of snakes as the body was lifted above the substrate. The timing of bilateral muscle activity relative to the kinematic profile differed for Nerodia and Crotalus during sidewinding. The wave of muscle contraction showed a constant phase relation to lateral vertebral flexion during terrestrial lateral undulation, whereas this phase relation changed along the length of the snake during aquatic lateral undulation.

Samples of skin from the mid-ventral, ventrolateral and mid-dorsal regions of five species of snakes, including generalists and aquatic and arboreal specialists, were mechanically tested in uniaxial extension. Loading curves revealed substantial variation in loads and maximum stiffnesses among samples from different regions within an individual and anatomically similar regions from different species. The size of the scales within a skin sample was an inadequate predictor of mechanical properties.

ACKNOWLEDGMENTS

I am grateful to each of my committee members for their unique contributions towards the completion of my degree. My advisor Dr. James Edwards provided much instructive criticism and professional support throughout my dissertation work in addition to becoming a good friend who was able to tolerate my personal quirks. Dr. Donald Straney provided amiable, insightful advice and patiently allowed continued use of laboratory space despite some disagreements about the asthetic appeal of my limbless subjects. The mechanical testing of snake skin was only made possible by the generous offer of laboratory facilities by Dr. Robert Hubbard. Dr. Joseph Vorro provide a bounty of free film and invaluable loans of emg equipment.

P. Ocello cheerfully assisted with digitizing data, animal keeping chores and many filming sessions. Dr. Harold Voris freely provided advice and opportunities for advancement including an introduction to the rigors of field work with marine snakes in Malaysia. Dr. Carl Gans generously provided prepublication copies of manuscripts on limbless locomotion.

A debt of gratitude is owed to the many following people who helped chasing and filming snakes on emg days: C. D'Haem, C. Cheng, K. McWilliams, P. Occello, S. DosReis, J. Zablotny, C. Griffith and C. Jayne. Technical assistance with the mechanical testing of snake skin was provided by M. Sacks, T. Segula and D. Petryga. J. Zablotny

skillfully prepared the muscle illustrations.

I am also most grateful to my parents who realized that potentially much could be learned from my once flourishing menagerie. Finally, my wife Carole deserves tribute for her unflagging moral and material support which allowed me to pursue my interests with a sometimes oppressive single-mindedness.

Financial support was provided by National Science Foundation Dissertation Improvement Grant No. BSR-8401874 and grants from the Michigan State University and national chapters of the Sigma Xi, the Scientific Research Society, and NIH grant NS16270 (to J. Edwards).

TABLE OF CONTENTS

Page

LIST OF TABLES v

LIST OF FIGURES vii

GENERAL INTRODUCTION 1

CHAPTER ONE
KINEMATICS OF LATERAL UNDULATION, CONCERTINA AND SIDEWINDING 9

INTRODUCTION 9
MATERIALS AND METHODS 12
RESULTS 20
DISCUSSION 36

CHAPTER TWO
MUSCULAR MECHANISMS OF
LATERAL UNDULATION, CONCERTINA AND SIDEWINDING 49

INTRODUCTION 49
MATERIALS AND METHODS 54
RESULTS 61
Anatomy 61
Terrestrial Lateral Undulation 71
Aquatic Lateral Undulation 80
Concertina 98
Sidewinding 104
DISCUSSION 112
Lateral Undulation 112
Concertina 129
Sidewinding 130
Anatomical Considerations 138

CHAPTER THREE
MECHANICAL BEHAVIOR OF SNAKE SKIN 156

INTRODUCTION 156
MATERIALS AND METHODS 159
RESULTS 165
DISCUSSION 182

SUMMARY 188

BIBLIOGRAPHY 193

LIST OF TABLES

TITLE PAGE

1.1 Motion analysis sample grouped by substrate. Figures in parentheses after species indicate range in total length of animals in cm. lu = lateral undulatory, c = concertina, and sw = sidewinding. Distances listed under substrate indicate widths of tunnels and distances between pegs used. See text for more complete explanation. 15

1.2 Maximum mean forward velocities for snakes performing lateral undulation on pegboard with glass pegs. * indicates snake was gravid. # indicates snake had an incomplete tail. 31

1.3 Maximum mean V_x for snakes sidewinding on sand. 34

1.4 Least squares regressions for $V_x = mf + b$. V_x = mean forward velocity in TL/sec, f = frequency of undulation in Hertz, m = slope, and b = Y-intercept (V_x). lu = lateral undulation, sw = sidewinding, r^2 = coefficient of determination, and n = sample size used for regression. *, from Jayne (1985). 38

2.1 Electromyographic sample. Nerodia fasciata, Elaphe obsoleta and Crotalus cerastes are abbreviated NF, EO and CC, respectively. For substrate, distances indicate spacing between centers of pegs in square arrays or the widths of the tunnels (tnl) used. Abbreviations for locomotor mode are LU, C and SW for lateral undulation, concertina and sidewinding, respectively. 55

2.2 Location of electrodes used in swimming snakes. Location of each site is given as vertebral number (v) and distance from the snout of the snake. 81

2.3 Representative maxima and minima of $\bar{\theta}$ of swimming snakes. For each electrode site values in parentheses after each angle indicate the time in sec when this angle occurred during these illustrated sequences. Angles are listed so that reading a row form left to right enables one to follow a half wave through time as it travels posteriorly along the body of the snake. 94

2.4 Average phase lag times (in sec) of emg's and $\bar{\theta}$. See text for complete explanation. 95

2.5 Average maximum $\bar{\theta}$. Abbreviations for locomotor mode are: LU, terrestrial lateral undulation; ALU, aquatic lateral undulation; C, concertina; and SW, sidewinding. Mean V_x is in TL/sec. Numbers in parentheses after angles indicate the vertebral number of the vertebra centered in the interval of the five vertebrae used to measure $\bar{\theta}$. See text for complete explanation. 146

3.1 Specimens used for uniaxial loading of skin. SVL = snout-vent length in mm. Unless otherwise stated snakes died of unknown causes while in captivity. All refrigeration was 1°C and fozen storage was -5°C. R,L = dorsal scale rows included in right and left ventrolateral samples of skin 161

3.2 Summary of uniaxial loading of snake skin samples. All loads are in N/mm. Stiffness is in N/mm% and maximum stiffness occurred at the strain during beginning of failure. See materials and methods for explanation of sample labels. 166

3.3 Approximate number of scales in longitudinal strips of skin 7 x 70 mm. 178

3.4 Mean values of stress and stiffness for uniaxial loading of snake skin samples. Means were calculated for homologous samples listed in Table 3.2. All stresses are in N/mm^2. Stiffness is in $N/\%mm^2$ and maximum stiffness occurred at the strain during the beginning of failure. See text for more complete explanation. 180

LIST OF FIGURES

TITLE PAGE

1.1 Orientation of axes for digitizing displacements of snakes. The large horizontal arrows indicate the overall direction of travel for each of the locomotor modes. The thick horizontal lines surrounding the snake performing concertina represent the sides of the tunnel. 16

1.2 Modified Figure 10 from the models of Gray (1946) predicting the displacements of a hypothetical snake 24 segments long performing sidewinding (top) and lateral undulation (bottom). Displacements of segment XV are shown for equal intervals of time within one cycle of activity (XVa - XVi). 19

1.3 Velocities versus time for Gray's model of lateral undulation. All velocities are in total lengths/ sec, assuming a frequency of one cycle per sec. CV = coefficient of variation of V_r. 21

1.4 Velocities versus time for lateral undulation for three species of snakes moving across various substrates. The oblique lines are to facilitate recognition of sequential points in time. 22

1.5 Velocities versus time for concertina locomotion. 24

1.6 Velocities versus time for Gray's model of sidewinding. Symbols are as in Figure 1.3. 25

1.7 Velocities versus time for snakes sidewinding on sand. 27

1.8 Velocities versus time for Cerberus rynchops combining lateral undulation and sidewinding while moving on sand. 29

2.1 Method of measuring lateral vertebral flexion from tracings of films (Note this is an example of vertebrae concave to the right). 60

2.2 Simplified right lateral view of the major epaxial muscle segments of Nerodia f. pictiventris. Anterior is to the right of the figure. SP and SSP respectively indicate the spinalis and semispinalis portions of the M. semispinalis-spinalis, and AT is the anterior tendon of the SSP-SP. LD represents the M. longissimus dorsi and MT, TA, and LT are the medial tendon, tendinous arch, and lateral tendon of LD. MIC and LIC respectively are the

medial and lateral heads of the M. iliocostalis and IT is the intermediate tendon of this muscle. See text for more detailed description. From Jayne (1985). 62

2.3 Simplified right lateral view of the major epaxial muscle segments of Elaphe o. quadrivitatta. Anterior is to the right. Abbreviations are as in Figure 2.2. 65

2.4 Simplified right lateral view of the major epaxial muscle segments of Crotalus cerastes. Anterior is to the right. Abbreviations are as in Figure 2.2. 67

2.5 Simplified right lateral view of deeper epaxial muscle segments of Nerodia f. pictiventris. Anterior is to the right. The M. semispinalis-spinalis has been removed. The M. multifidus and M. interarticularis superior are abbreviated M and IAS, respectively. 69

2.6 Emg and movement records from sequence 53.7 of Nerodia 35 performing terrestrial lateral undulation with 10 cm peg spacing. Right and left are abbreviated R and L. Oblique lines connecting dots are only to facilitate recognition of successive points in time. Numbers in parentheses after muscle abbreviations indicate the vertebrae spanned by the muscle segments containing electrodes. Horizontal bars represent emg with greater thicknes indicating stronger activity. Emg's of muscles from the right side of the snake are diagrammed above the portion of the plot of $\bar{\theta}$ indicating lateral vertebral flexion concave to the right. Velocities are in TL/sec and are for the first vertebra (69) in the interval used to determine $\bar{\theta}$. 71

2.7 Emg and movement records from sequence 53.2 of Nerodia 35 performing terrestrial lateral undulation with 10 cm peg spacing. Notation is as in Figure 2.6. 74

2.8 Emg and movement records from sequence 53.3 of Nerodia 35 performing terrestrial lateral undulation with 10 cm peg spacing. Notation is as in Figure 2.6. 75

2.9 Emg and movement records from sequence 61.11 of Nerodia 36 performing terrestrial lateral undulation with 7.5 cm peg spacing. Notation is as in Figure 2.6. 77

2.10 Emg and movement records from sequence 60.2 for two longitudinal sites of Elaphe 18 performing terrestrial lateral undulation with 15 cm peg spacing. Notation is as in Figure 2.6. 78

2.11 Emg and movement records from sequence 47.2 of Nerodia 34 performing aquatic lateral undulation at the surface of the water. At left, $\bar{\theta}$, V_y, and V_r for the site near mid-body. At right, $\bar{\theta}$ for three different longitudinal sites. Notation is as in Figure 2.6. 82

2.12 Emg and movement records from sequence 47.16 of Nerodia 34 performing aquatic lateral undulation below the surface of the water. At left, $\bar{\theta}$, V_y, and V_r for the site near mid-body. At right, $\bar{\theta}$ for three different longitudinal sites. Notation is as in Figure 2.6. 84

2.13 Emg and movement records from sequence 64.16 of Nerodia 38 performing surface aquatic lateral undulation. $\bar{\theta}$, V_y, and V_r are shown for a site near mid-body, and at top, $\bar{\theta}$ is also shown for a more anterior site. Notation is as in Figure 2.6. 86

2.14 Emg and movement records from sequence 65.7 of Nerodia 39 performing aquatic lateral undulation at the surface of the water. At left, $\bar{\theta}$, V_y, and V_r for the site near mid-body. At right, $\bar{\theta}$ for three different longitudinal sites. Notation is as in Figure 2.6. 87

2.15 Sample emg's from the left side of Nerodia 39 swimming during sequence 65.7. Horizontal and vertical lines indicate time and voltage scales, respectively. Arrows indicate time = 0 for Figure 2.14. Note the decrease in emg amplitude. 88

2.16 Emg and movement records from sequence 64.5 of Elaphe 20 performing aquatic lateral undulation at the surface of the water. At left, $\bar{\theta}$, V_y, and V_r for the site near mid-body. At right, $\bar{\theta}$ for four different longitudinal sites. Notation is as in Figure 2.6. 90

2.17 Sample emg's from the right side of Elaphe 20 during sequence 64.5 of swimming. The arrows indicate time zero used for Figure 2.16. The horizontal and vertical lines indicate the time and voltage scales, respectively. Sites 1 - 4 were 29, 45, 60 and 70 cm from the snout of the snake, respectively. Electrodes 1 - 4 were in contractile tissue near vertebrae 73, 116, 153 and 192, respectively. 91

2.18 Emg and movement records from sequence 63.1 of Elaphe 19 performing aquatic lateral undulation at the surface of the water. At left, $\bar{\theta}$, V_y, and V_r for the site near mid-body. At right, $\bar{\theta}$ for three different longitudinal sites. Notation is as in Figure 2.6. 92

2.19 Emg and movement records from sequence 43.7 of Nerodia 33 performing concertina locomotion in an 8 cm wide tunnel. Notation is as in Figure 2.6. 99

2.20 Emg and movement records for three body regions near site 1 of Elaphe 15 (sequence 43.4) performing concertina locomotion in an 8 cm wide tunnel. Notation is as in Figure 2.6. 101

2.21 Emg and movement records for three body regions near site 2 of Elaphe 15 (sequence 43.4) performing concertina locomotion in an 8 cm wide tunnel. Notation is as in Figure 2.6. 102

2.22 Emg and movement records from sequence 61.3 of Nerodia 36 performing right-handed sidewinding on a linoleum floor. Notation is as in Figure 2.6. 105

2.23 Sample emg's from 0.55 to 2.50 sec during sequence 61.3 (Figure 2.22) of Nerodia 36 sidewinding. The top three emg's are from the left side and the others are from the right side of the snake. Horizontal and vertical lines indicate time and voltage scales, respectively. The voltage scale = 400 uV for the right LD and IC. Arrows indicate beginning and end of static contact. Note weak early activity of the left IC and time of bilateral activity. 106

2.24 Emg and movement records from sequence 49.4 of Crotalus 6 performing right-handed sidewinding on sand. Notation is as in Figure 2.6. 108

2.25 Emg and movement records for sequence 49.1 from two sites in Crotalus 6 performing left-handed sidewinding on sand. Notation is as in Figure 2.6. 110

2.26 From Gray and Lissmann (1950). A. Figure 8(i) indicates changing lengths of muscles with shaded regions showing segments about to become shorter. B. Figure 8(ii) shows Gray and Lissmann's assumptions about sections of snakes functioning as lever arms. 113

2.27 Figure 9 from Gray and Lissmann's (1950) model of the muscular mechanism of a snake performing lateral undulation through a channeal with rectangular bends. Shaded areas indicate active muscles. 115

2.28 From Gray and Lissmann (1950). A. Figure 10 showing muscular mechanism for gliding past one peg. B. Figure 11 showing muscular effort for gliding past two pegs. Shaded areas indicate active muscles. 117

2.29 Figure 12 from Gray and Lissmann's (1950) model of the muscular mechanism of terrestrial lateral undulation. Shaded regions indicate active muscle. 118

2.30 Figure 7 from Gray's (1953) model of the muscular mechanism of lateral undulation. Shaded areas indicate active muscles, and the width of these areas represents the degree of tension. 120

2.31 Representative postures of snakes moving past a limited number of pegs. At left, illustrations are modified from Figure 7 of Gray and Lissmann's (1950) tracings of films. At right are illustrations from tracings of films of Nerodia from this study. The circles represent pegs and the arrows indicate approximate regions of maximum lateral displacement. 123

2.32 Working model of the muscular mechanism of left-handed sidewinding of Crotalus cerastes. Shaded regions indicate active contractile tissue. See text for more detailed description. 131

2.33 Representative postures of snakes performing right-handed sidewinding. Illustrations were made from tracings of films. A. From sequence 61.3 (Figures 2.22 and 2.23) of Nerodia on a linoleum floor. From bottom to top the images are from .83, 1.48 and 2.11 sec in the sequence. The arrows indicate the electrode site near mid-body (vertebra 66). B. From Crotalus 5 on sand. From bottom to top, the images are at 0, 1.08 and 1.75 sec. Cross-hatched regions indicate static contact with the substrate. Arrows indicate near mid-body (vertebra 70). See discussion for more complete explanation. 134

3.1 Loading curves for skin from Nerodia fasciata pictiventris. A: ventral sample NfB2V, B: ventrolateral sample NfB2L and C: dorsal sample NfB1D. 169

3.2 Loading curves for skin from Ahaetulla prasina. A: ventral sample ApB1V, B: ventrolateral sample ApB2L, C: ventrolateral sample ApB4L and D: dorsal sample ApB3D. 171

3.3 Loading curves for skin from Laticauda colubrina. A: ventral sample LcA2V, B: ventrolateral sample LcA1L and C: dorsal sample LcA2D (Note vertical scale is different from all other figures). 172

3.4 Loading curves for skin from Hydrophis melanosoma. A: Ventral sample HmA1V, B: Ventrolateral sample HmA2L and C: dorsal sample HmA1D. 173

3.5 Loading curves for skin from Enhydrina schistosa. A: ventral sample EsA2V, B: ventrolateral sample EsA2R and C: dorsal sample EsA3D. 175

3.6 Loading curves for skin from Acrochordus granulatus. A: ventral sample AgA1V, B: ventrolateral sample AgA2R and C: dorsal sample AgA1D. 176

GENERAL INTRODUCTION

By most standards, snakes are an evolutionarily successful group. The suborder Serpentes contains over 2200 species representing more than 400 genera and 14 families (Duellman, 1979). This is about comparable to the species diversity shown by lizards which comprise the other major group of squamate reptiles with about 3300 species, 360 genera and 17 families (Duellman, 1979). Both groups of squamates are ecologically and phylogenetically diverse. Allowing for some limitations imposed by ectothermy, squamate reptiles are found in almost every conceivable habitat, including desert, rain forest, arboreal, fossorial and even marine habitats (Bellairs, 1970).

Despite the similar phylogenetic and ecological diversity of snakes and lizards, it is not uncommon for lizards to be viewed as morphologically more diverse than snakes (Young, 1981). Lizards occur with or without limbs and great variation is also found among lizards in the elongation of the trunk, robustness of the limbs, scalation of the body and morphology of the feet (Bellairs, 1970). To a great extent, snakes are defined by the reduction or loss of anatomical structures (Bellairs, 1972). For example, snakes have only vestiges of limbs or no limbs, the left lung is reduced or absent, the epipterygoid bone is absent and no interorbital septum is present (Bellairs, 1972). Because so much morphological diversity may be found in the anatomical stuctures that are present in lizards and absent in snakes, it is easy to

understand how snakes may be viewed as morphologically less diverse than lizards.

While the limbless condition causes some similarity of appearance among snakes, additional characters can be found that contribute to some overall uniformity of appearance of the vast majority of snake species. For example, nearly all snakes have imbricate (overlapping) scales over almost the entire body surface. Notable exceptions to this occur in fully aquatic snakes such as Acrochordus and select species of Hydrophiidae (Smith, 1943). In contrast, lizards may have either imbricate scales as in most Iguanidae and Agamidae or granular scales as in Helodermatidae and Varanidae (Bellairs, 1970). Whereas lizards most often have no correspondence between the arrangement of scales and underlying body segments, nearly all booid and colubroid snakes have a 1:1 correspondence between the ventral scales and the numbers of vertebrae (Alexander and Gans, 1966). The ventral scales of snakes are also usually very smooth upon gross examination and show relatively little varation even when viewed microscopically (Gans, 1974). Once again, the Acrochordidae and Hydrophiidae provide exceptions to these general trends. Snakes also are somewhat unified by having high numbers (>160) of vertebrae (Hoffstetter and Gasc, 1969).

Thus, the question arises of how a group with such similar overall morphology has exploited ecologically diverse habitats. Perhaps there is only superficial morphological similarity among snakes and more detailed study of infrequently used characters would reveal correlations with ecological specialization. Alternatively, behavioral and physiological specialization could be more important for exploitation of diverse habitats, or the general morphology of a snake may be versatile

enough that specialized morphologies are unnecessary for different habitats.

Probably the two most conspicuous aspects of ophidian biology are feeding and locomotion. Many species of snakes are rather secretive or difficult to maintain in captivity, and this complicates the study of more subtle aspects of their natural history. Numerous morphological correlates with function have been found for the feeding apparatus of snakes. In part this probably resulted from an historical emphasis on the use of cranial morphology in systematic studies. For example, of the 50 characters used by Marx and Rabb (1972) in their phyletic anlysis of colubroid snakes, 41 characters involved cranial morphology and 25 of these dealt with cranial osteology.

Although snakes are a strictly carnivorous group, considerable diversity of diet exists (Bellairs, 1970), and often different species of snakes may be quite specialized in their prey preference (e.g. Voris and Voris, 1983). As prey preference is correlated with cranial morphology, some general trends can be found, by comparing convergence of phylogentically diverse lineages of snakes with similar prey type (Savitzky, 1983).

The relation between cranial morphology and prey size has been extensively studied (Albright and Nelson, 1959; Gans, 1961; Kardong, 1977). As a group, snakes have the ability to swallow whole large prey items and this has long been the subject of much interest. Even within snakes, however, considerable diversity in the cranial morphology and size of prey taken indicates there are stout-bodied species apparently specialized for consuming prey that is large relative to the mass of the snake (Pough and Groves, 1983). Furthermore, snake venom may facilitate

the digestion of such large prey (Thomas and Pough, 1979). Many detailed studies have examined the cranial musculature of snakes (eg. Haas, 1962; Varkey, 1979), and recently electromyography has been used to determine the role of certain cranial muscles during swallowing (Cundall, 1983). Reasonable morphological diversity has been found in the cranial region of snakes, and some characters such as dentition, venom, gape (size of mouth opening) and cranial osteology and myology correlate with feeding specializations.

Studies of snake feeding often allude to important correlated changes in the body form of snakes (Pough and Groves, 1983). For example, the stout stature of the vipers specialized for consumption of large prey is generally believed to limit their ability to perform different locomotor modes (Gans, 1974). Indeed, one often can observe stout snakes performing rectilinear locomotion; however, generalities regarding the effect of weight-length ratio on locomotor mode have not been studied. In fact, the functional morphology of the trunk of snakes has been largely neglected when compared to the cranial region.

Much of the morphological diversity seen in the trunk of snakes involves differences of degree rather than of kind. For example, the maximum length of different snake species varies from about 20 cm for certain Leptotyphlopidae (Broadley, 1983) up to nearly 10 m for some Boidae (Pope, 1967). The ratio of total length to maximum diameter gives some indication of stoutness, and this quantity may be 15 for some vipers of the genus Bitis (Pough and Groves, 1983) compared to about 100 for the highly arboreal colubrid Imantodes (personal observation). Although all snakes have relatively high numbers of vertebrae compared to lizards, within snakes the number of total vertebrae ranges from 160

to 400 (Hoffstetter and Gasc, 1969). These total numbers of vertebrae do not just correlate with the maximum length of a species (Johnson, 1955). Instead, some of this variation in vertebral number correlates with specialized habits such as constricting prey (Jayne, 1982). Considerable variation has been documented in the morphology of those axial muscles believed important for locomotion (Mosauer, 1935a; Gasc, 1974). Some of these differences in the axial musculature do correlate with habitat specialization (Gasc, 1974; Voris and Jayne, 1976; Jayne, 1982); however, the function of the epaxial muscles has not been directly observed for snake locomotion. The shape of the vertebral processes onto which major axial muscles attach varies widely among snake taxa and to some extent correlates with habitat specialization (Johnson, 1955), but the functional consequences of this vertebral variability remain unclear. Hence, more detailed examinations of the trunk of snakes indicate that there is considerable morphological diversity, yet there has been considerable difficulty interpreting the functional consequences of this variability. Ultimately it is desirable to determine if the limbless condition may constrain morphological diversity, or if there are significant differences within the general body plan of limbless species.

Because of the lack of information on the functional morphology of the trunk during snake locomotion, a number of different levels of approach can be productive. At the simplest level, one may study species varying in the musculo-skeletal anatomy of the trunk and attempt to determine differences in performance for a particular locomotor mode. Necessarily, one must first develop some method of determining which locomotor mode is being performed, and then some measure of performance

such as maximum forward velocity can be meaningfully compared between species. Chapter 1 outlines a quantitative system for determining locomotor mode and then compares maximum speeds of snakes with different numbers of vertebrae. This method of measuring performance of whole organisms can be complicated by the behavior and physiology of the species, but this approach may at least indicate potential functional morphological differences which can then be pursued in greater detail.

Another approach is to directly observe the function of an anatomical structure during the activity of an intact animal. Electromyography provides a direct means of observing the activity of muscles, and when this is combinied with a cinematographic record of movement, correlations with mechanical events in the body of the snake can be determined. The axial muscles of snakes are large enough that gross dissection reveals much information about the anatomy of the system whose activity is being observed. In Chapter 2 the most integrated approach is used for understanding the functional morphology of snake locomotion, using electromyography to determine muscle activity, cinematography to determine mechanical events, and dissection to describe the anatomy of the system.

A third approach is to directly determine the mechanical behavior of some isolated element of the snake's anatomy in order to explore whether significant functional differences can be found between species specialized for different habitat. By isolating some element from the intact snake one can avoid the complicating influences of behavior and physiology inherent in an organismal approach. In Chapter 3 the mechanical properties of isolated skin samples are examined for various species of snakes. Because of the limbless condition of snakes, the

skin provides the contact with the substrate necessary for the transmission of locomotor forces for all modes of lomomotion. Furthermore, a specific set of muscles attaches the skin of snakes to the skeleton and generates locomotor forces during rectilinear locomotion by moving the skin relative to the skeleton and substrate. Hence, the skin of snakes plays an important role during snake locomotion. Even if one uses somewhat of a "black box" approach (Gans, 1974) for the underlying anatomy of the skin, understanding the elastic properties of skin is likely to provide insight into potentially different roles of skin during different modes of locomotion.

All of the above methods rely to some extent on a comparative approach to begin to isolate the effects of morphological variation. In some cases, species of extremely specialized morphology could be obtained (for example use of sea snake skin in Chapter 3). However, restricted availablility of species limited the comparative scope of this overall study. The variablity (or lack of it) observed in this work should be viewed within the context of the diversity of form found among different snake lineages.

The advanced snakes (colubroids) used in this study are replete with presumed parallelisms and convergence of form, and this has considerably complicated phylogenetic analysis of the major portion of this group formed by the colubrids (Underwood, 1967; Marx and Rabb, 1972). As mentioned earlier, snakes may have some superficial uniformity of morphology, but it remains to be determined if the morphological diversity of the trunk region that emerges under close scruntiny has functional consequences. The functional approach used in this work provides a useful aid for sifting through some of the morphological

diversity found among snakes.

CHAPTER ONE

KINEMATICS OF LATERAL UNDULATION, CONCERTINA AND SIDEWINDING

INTRODUCTION

Four major modes of terrestrial snake locomotion are generally recognized: lateral undulatory, concertina, sidewinding, and rectilinear (Gray, 1946; Gans, 1974). Common to lateral undulation, concertina locomotion, and sidewinding is the generation of propulsive forces by some pattern of vertebral flexion. Lateral undulation is generally used when there are sufficient irregularities of the substrate. The body of the snake pushes against these irregularities to generate anteromedially directed reactive forces great enough to overcome sliding frictional resistance (Gans, 1974). The speed of a laterally undulating snake is equal to the velocity with which the wave of lateral bending propagates posteriorly along the body of the animal. In this mode all points along the body of the snake follow a more or less identical sinusoidal path and all points on the body move simultaneously (Mosauer, 1932; Gray, 1946). In contrast to this is the movement pattern observed during concertina locomotion and sidewinding. In these modes one portion of the body of the snake makes static contact with the substrate while another portion moves relative to the substrate (reviewed in Gans, 1974). Concertina locomotion is often used in tunnels which lack the anteromedially oriented surfaces that are necessary for lateral undulation. Snakes progressing in the concertina mode form a series of lateral bends which are pressed against the sides of the tunnel to generate static points of contact. These points of contact are used to

accelerate adjacent regions of the snake's body. Additionally, concertina locomotion may be used on smooth flat surfaces. Under such conditions, the weight of the snake in the regions of lateral bending is used to generate static frictional forces sufficient to permit the snake to propel itself. Sidewinding is also used on very flat surfaces that lack projections needed to serve as lateral pivotal points. During sidewinding, a combination of lateral and dorsal vertebral flexion is used to lift a portion of the snake's body from one region of static contact to the next region of static contact.

Good general descriptions of each of these three distinct locomotor modes have been provided by various workers (eg. Mosauer, 1932; Gray, 1946; Gans, 1974). However, quantified kinematic descriptions of these different locomotor modes are scarce or incomplete. After viewing extensive movie footage of snake locomotion, Gray (1946) generated models of each of these three locomotor modes. His models clarified characteristics of each locomotor mode. However, it is not clear from data provided by Gray or others how realistic each of his models are.

Most species of snakes are capable of using all of these three modes of terrestrial locomotion, and individual snakes will often appear to use two modes simultaneously (Gans, 1974). For such observations, it is not always obvious whether different regions within a snake are performing discrete locomotor modes or if the entire snake is simultaneously combining characteristics of one or more distinct modes. This versatility in the locomotor repertoire is a major obstacle to comparative investigations of the terrestrial locomotion of snakes because without cinematography, observers are unlikely to distiguish discrete locomotor modes from combinations of locomotor modes.

In addition to the different modes of snake locomotion, comparisons of the maximum speeds attained by snakes have been of interest to many authors who have related speed to differences in species, substrates, snake size and temperature. Mosauer (1935b) timed six species of snakes crawling on substrates similar to those naturally encountered by the different species. Heckrote (1967) timed Thamnophis s. sirtalis crawling through an array of pegs, in order to investigate the influence of temperature and snake size on speed. Bennet et al (1974) also timed snakes travelling measured distances to investigate the effects of peg spacing on snake speed. Unfortunately, none of these studies records the locomotor mode used by the snakes and the lack of cinematographic records of these studies prevents the determination of locomotor mode. A few speeds can be determined from some publications which include photographs made from films of snake locomotion (Gray, 1946; Gans and Mendelssohn, 1972). Because of uncertainty regarding locomotor mode, the use of different techniques in determining speed, the complicating effects of snake size and peg spacing, and the small number of taxa that have been studied, few valid comparisons can currently be made of the maximum speeds of snakes.

This portion of the study investigates lateral undulatory, concertina, and sidewinding locomotion with four main objectives. First, the characteristics of each of these single modes are clarified. Second, an objective method is developed for detecting the simultaneous use of more than one of these modes. Third, variation in speed and frequency of undulation is quantified. Fourth, comparisons are made for the maximum velocities of different locomotor modes and of different species.

MATERIALS and METHODS

Animals were chosen for this study based on availability and their ability to perform different locomotor modes. Like all amphisbaenians, Rhineura floridana is is an extremely specialized burrower (Gans, 1974). Filming Rhineura presented an opportunity to determine the versatility of its locomotor repertoire compared to the snakes of this study. Acrochordus javanicus is generally considered an aquatic snake; however, I had observed the individual used in this study readily performing concertina locomotion, both underwater and on land. The viperid Crotalus cerastes was chosen as a species that is behaviorally and to some extent morphologically specialized for sidewinding (Gans and Mendelssohn, 1972; Jayne, 1982). The rest of the snakes filmed for this study are all colubrids. The homalopsine Cerberus rynchops is a mostly aquatic species with the relatively short segmental lengths of epaxial muscles characteristic of most aquatically specialized snakes (Jayne, 1982). The natricine Nerodia fasciata pictiventris is a semi-aquatic to terrestrial species whose epaxial musculature is characteristic of nonconstricting terrestrial colubroids, whereas Elaphe obsoleta quadrivittata is a terrestrial to semi-arboreal species of colubrine morphologically representative of constricting colubrids (Jayne, 1982).

Animals were filmed on a variety of substrates. Substrates were chosen which most readily elicited the locomotor mode desired for study. Nerodia were filmed on a layer of sand at least 1.5 cm deep covering a

46 x 110 cm area. Because of the greater size of Cerberus and Crotalus, these snakes were filmed in a larger arena (120 x 120 cm) with sand at least 1.5 cm deep. Straight-sided tunnels, used for eliciting concertina locomotion, had a floor of glass placed over a one cm grid which provided points of reference. Pieces of wood 4.4 cm high formed the sides of these tunnels which were 8 or 10 cm wide. For some sequences, strips of dense rubber matting were used to line the tunnel walls to elicit conertina locomotion. For other sequences, the bare surfaces of the wood served as the sides of the tunnel. If animals attempted to crawl out of the tunnel, a sheet of glass was placed over the tunnel.

Several trials were filmed using 5 mm diameter wooden pegs which were arranged on a square grid pattern. These pegs were inserted through the holes of 3 mm thick tempered pegboard into an underlying sheet of stryrofoam that was 2.5 cm thick. About 3.5 cm of each 5 cm peg protruded above the surface of the pegboard. All peg distances given in Table 1.1 refer to the shortest straight-line distance between centers of adjacent pegs. To reduce frictional resistance between the snakes and the pegs, sheaths of glass tubing 5 cm long, with an inside diameter of 6 mm and an outside diameter of 8 mm, were placed over the pegs. Because Rhineura seemed to slip when the glass sheaths were in place, they were removed when filming this species. A piece of pegboard 60 x 240 cm was used for filming all snakes, but Rhineura was filmed in a 45 x 60 cm arena.

A Bolex H16 16 mm movie camera with a 12 V DC motor drive, operated at 50 f.p.s. with an exposure time of 1/300 sec was used. Films were made with either Kodak Tri-X (ASA 200) or 4-X (ASA 400) black and white

reversal stock and developed comercially (Filmcraft Labs, Detroit, MI). All animals were filmed indoors with a Vario-Switar 100 POE zoom lens and with the camera positioned directly above the test surface to eliminate parallax. Target-to-camera distance was 3 m. Film transport speed was verified by including in the field of view a specially constructed neon light (with R-C circuit) blinking at 2.0 flashes/sec. Four floodlights provided illumination, and the air temperature at the time of filming approximated 25°C. Paint marks were placed at regular intervals along the mid-dorsal line of each animal to provide points of reference. Table 1.1 indicates the number of locomotor sequences that were analyzed for the single amphisbaenian and the five snake species.

The films were projected with a Lafayette stop-action movie projector and a single paint mark (usually from the middle 1/3 of the animal's body) was traced over a period of time. The resulting record of displacement was then placed on a graphics tablet interfaced with an Apple II+ microcomputer for digitizing. As illustrated in Figure 1.1, tracings were oriented so that the overall direction of travel was in the positive x direction. The overall direction of travel was determined by drawing a straight line through two points that were 360° out of phase. After digitizing, changes in displacement were divided by the time between traced points to calculate average velocities. Each resultant velocity, V_r, was then resolved into longitudinal (V_x) and lateral (V_y) components. Hence, positive and negative values of V_x indicate forward and backward movements, respectively. Positive and negative values of V_y respectively indicate movement to the right and left. All velocities were converted to total lengths (of animal)/ sec to facilitate comparisons among different size individuals. For each

Table 1.1. Motion analysis sample grouped by substrate. Figures in parentheses after species indicate range in total length of animals in cm. lu = lateral undulatory, c = concertina, and sw = sidewinding. Distances listed under substrate indicate widths of tunnels and distances between pegs used. See text for more complete explanation.

SPECIES	No. animals	No. trials	MODE	SUBSTRATE
Acrochordus javanicus(74)	1	3	c	linoleum
Nerodia f. pictiventris(84-110)	2	13	c, c+lu	8, 10 cm tunnel
Crotalus cerastes(33-36)	3	17	sw	sand
Cerberus rynchops(46-50)	2	10	sw, lu, lu+sw	sand
Nerodia f. pictiventris(30)	2	4	sw, lu+sw	sand
Elaphe o. quadrivittata (120-147)	3	27	lu	7.5, 12.5 cm pegs
Nerodia f. pictiventris(70-91)	9	49	lu, lu+sw	7.5,10,12.5 cm pegs
Rhineura floridana(29)	1	9	c	2.5, 5.0 cm pegs

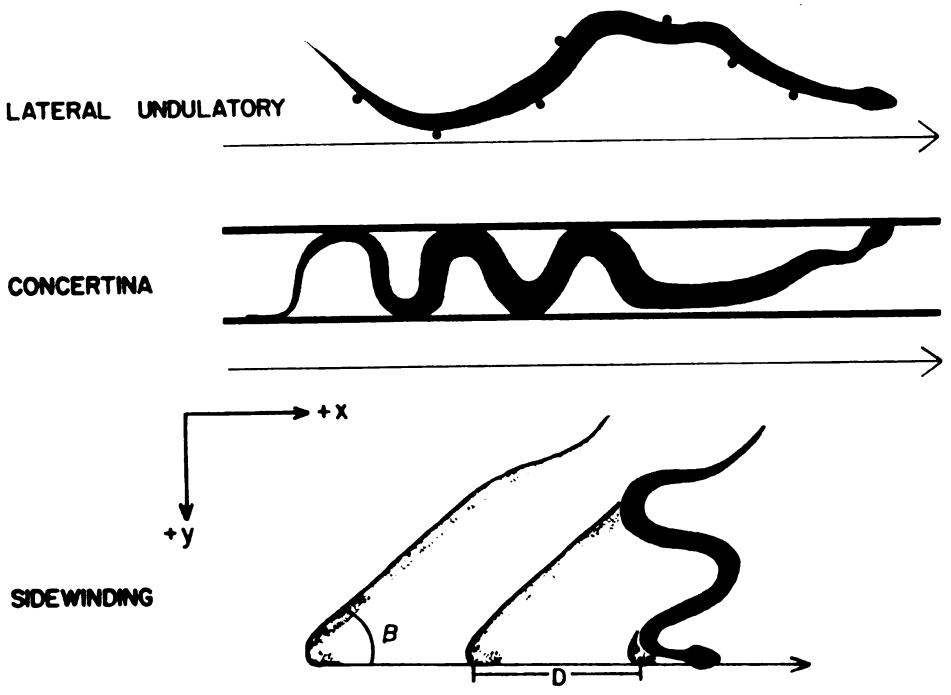

Figure 1.1. Orientation of axes for digitizing displacements of snakes. The large horizontal arrows indicate the overall direction of travel for each of the locomotor modes. The thick horizontal lines surrounding the snake performing concertina represent the sides of the tunnel.

film sequence, V_x, V_y, and V_r were plotted versus time.

Velocity profiles of film sequences were compared with those predicted from descriptions and models proposed by Gray (1946). Gray's models of lateral undulation and sidewinding were digitized in a fashion similar to that of the film tracings. A photocopy of Figure 10 from Gray (1946) was placed on the digitizing tablet with the orientation of axes as indicated in Figure 1.2. For both models, the point at one end of the line representing segment XV provided the record of displacement. This point was digitized for two cycles of activity for each model assuming the period of motion was equal to 1 sec. The length of the 24 segment line representing a snake was used to convert velocities into lengths/ sec. Operational definitions of each mode were then developed based on the observed patterns of V_x, V_y and V_r and previous definitions (Gray, 1946; Gans, 1974). After determining the locomotor mode of each trial, mean forward velocity was calculated for one or more complete periods of motion.

Two procedures were used to estimate errors associated with the digitizing process. First, to assess error resulting from inaccurate placement of the digitizing pen on the graphics tablet, various series of equally spaced points on graph paper were digitized, with the spread between points representative of the range in values found in the tracings made from the actual films of snake locomotion. Error from inaccurate placement of the digitizing pen produced a coefficient of variation (CV) of less than 5% in V_r. Second, tracings were made from a single film sequence of snake locomotion. The film sequence contained a range of displacements comparable to those observed among all of the film sequences. For each equivalent estimate of V_r, the CV was

calculated for the replicates. This yielded CV values less than 13% for V_r.

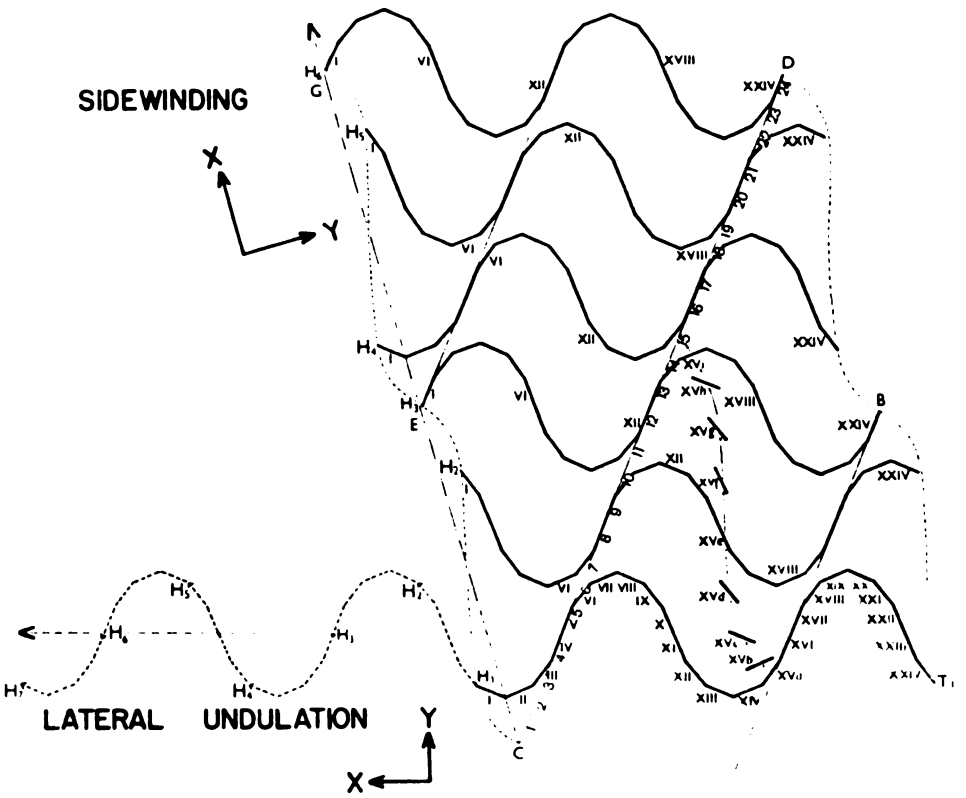

Figure 1.2. Modified Figure 10 from the models of Gray (1946) predicting the displacements of a hypothetical snake 24 segments long performing sidewinding (top) and lateral undulation (bottom). Displacements of segment XV are shown for equal intervals of time within one cycle of activity (XVa - XVi).

RESULTS

Figure 1.2 illustrates Gray's (1946) mathematical model of lateral undulatory locomotion which was digitized for analysis. For this example of lateral undulation, V_x and V_y behave sinusoidally (Figure 1.3). The period of the sinusoidal function of V_x is one-half the period for V_y, and the absolute value of V_x is always at a maximum when V_y equals zero. For the digitized data from this model, V_r had little variation (CV = 10%). Considering the error of the digitizing procedure, V_r is effectively constant.

Figure 1.4 illustrates velocity profiles for lateral undulation of snakes filmed in this study. A slight difference can be seen in the pattern of V_x for Nerodia compared to Elaphe and Cerberus. The Nerodia was not travelling in a regular sinusoidal path as were the Elaphe and the Cerberus. Hence, V_x shows a somewhat irregular pattern which reflects these rather irregular changes in direction. However, V_x is still always at a maximum when V_y equals zero. V_r for this sequence of Nerodia was also effectively constant with the small coefficient of variation of 27.1%, and respective values of this quantity were 11.1% and 27.6% for the sequences of Elaphe and Cerberus. For other sequences of lateral undulatory locomotion, there was not always a clear periodic pattern of variation in V_x. However, for many of the sequences with no clear pattern of V_x, V_r was effectively constant and this should indicate that the mode was lateral undulation.

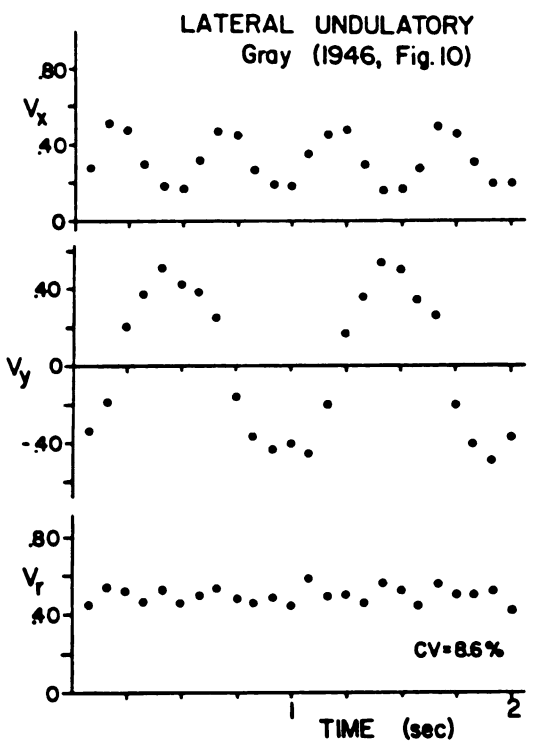

Figure 1.3. Velocities versus time for Gray's model of lateral undulation. All velocities are in total lengths/ sec, assuming a frequency of one cycle per sec. CV = coefficient of variation of V_r.

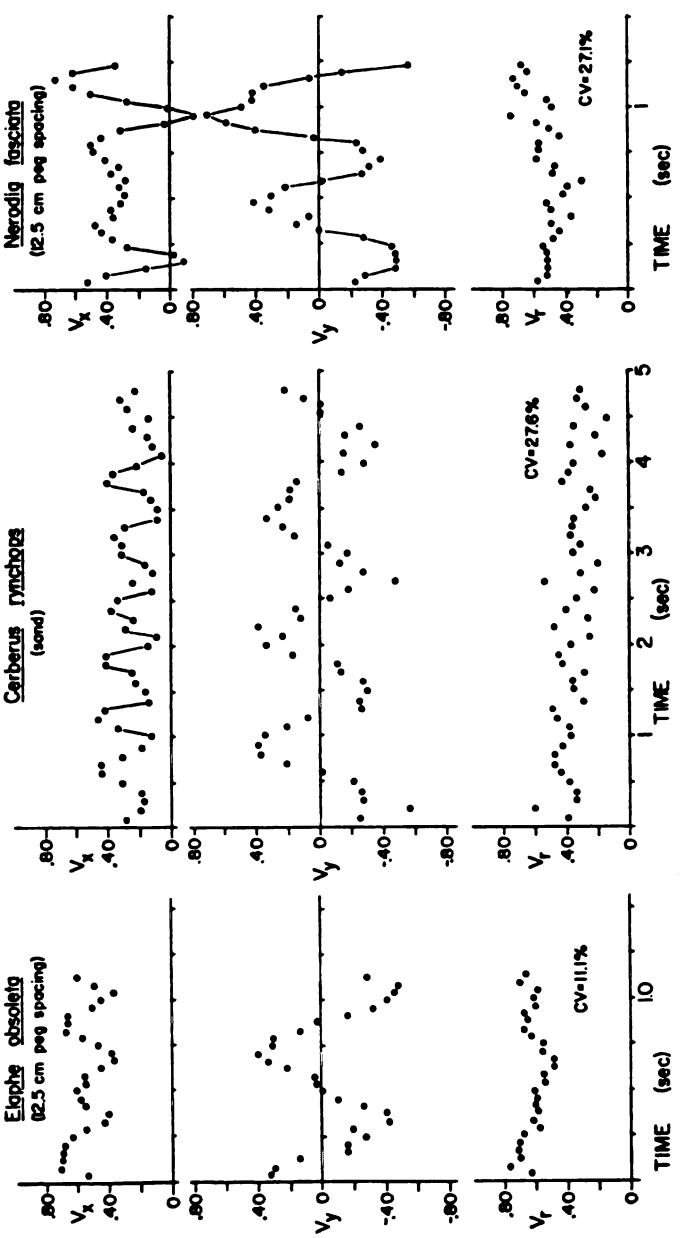

Figure 1.4. Velocities versus time for lateral undulation for three species of snakes moving across various substrates. The oblique lines are to facilitate recognition of sequential points in time.

Gray (1946) did not provide sufficient detail in his model of concertina locomotion to allow digitizing. However, his model of this mode did suggest a single point on the snake would move left, then right, and then stop ($V_r = 0$) during one cycle of activity.

Figure 1.5 illustrates velocity profiles for three sequences of concertina locomotion filmed in this study. For all three sequences, the snakes stopped periodically causing rather high coefficients of variation for V_r (121.7 - 102.7%). In the period from 4 - 6 sec into the sequence of Acrochordus performing concertina locomotion on the floor, the snake moved to the left (L), stopped, moved to the right (R), and then stopped. For the middle diagram of Nerodia performing concertina locomotion in a tunnel, a similar pattern of R, stop, L, stop was used from 6 - 10 sec. However, during earlier points in time for these sequences of Acrochordus and Nerodia, a pattern of R, L, stop was used. The righthand diagram, showing concertina locomotion of Nerodia in a tunnel, has three bimodal curves for V_r in the three periods from 2 - 10 sec. A close examination of the film of this sequence revealed that the first and second peaks corresponded to pushing and pulling phases, respectively. In other words, the point on the snake that was being observed was first pushed forward from a more posterior point of static contact and then pulled forward from a more anterior point of static contact. In most other sequences of concertina locomotion, it was not possible to distinguish distinct pushing and pulling phases because the body of the snake was in close proximity to the walls of the tunnel at points anterior and posterior to the point which was being observed.

Figure 1.6 illustrates the velocity profiles for Gray's (1946,

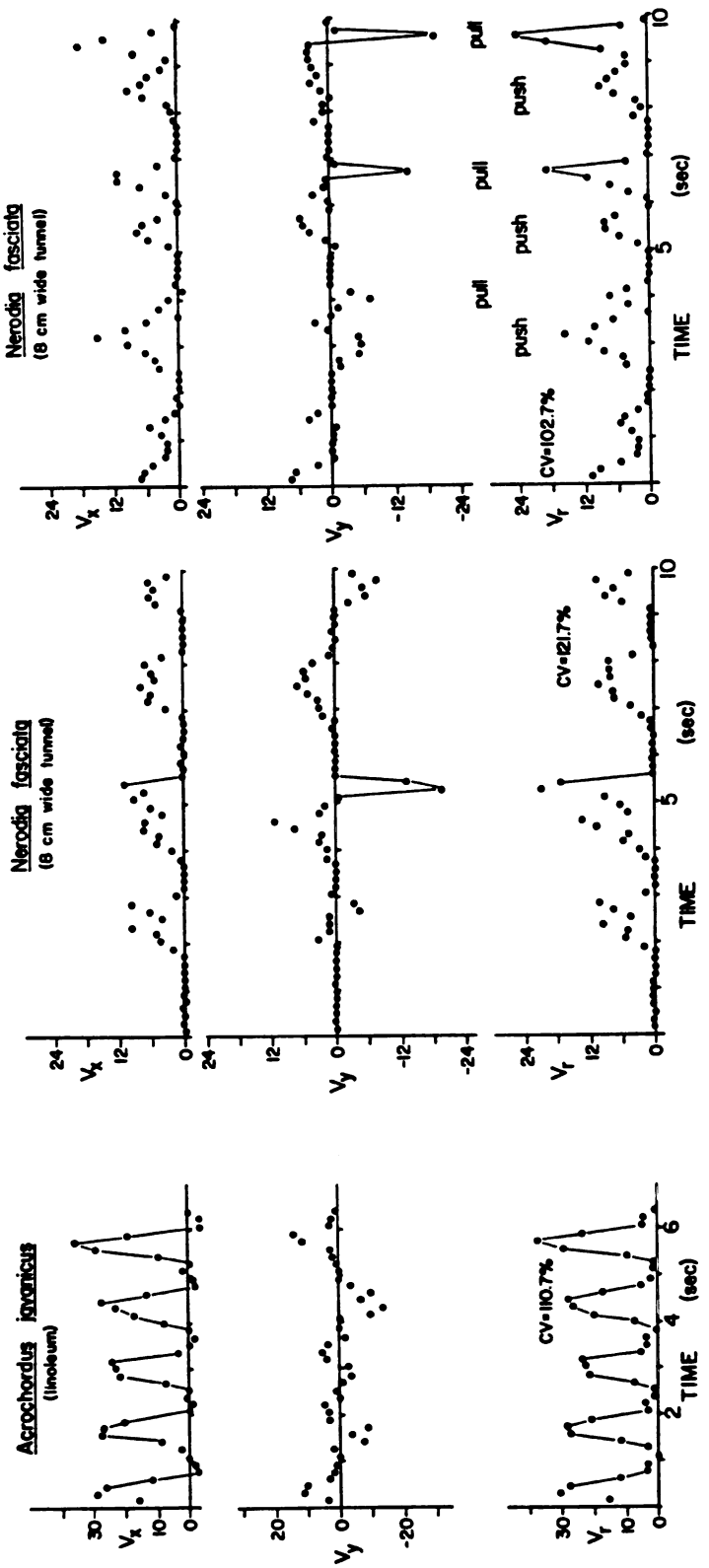

Figure 1.5. Velocities versus time for concertina locomotion.

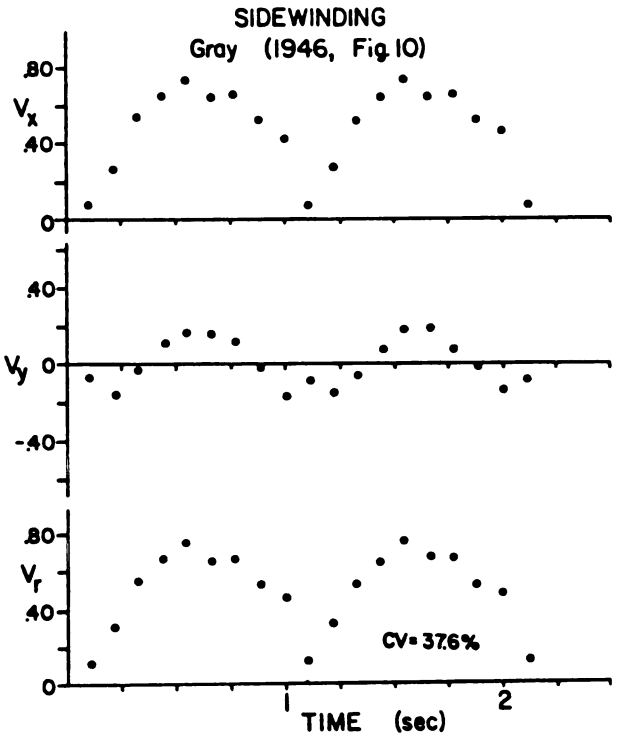

Figure 1.6. Velocities versus time for Gray's model of sidewinding. Symbols are as in Figure 1.3.

Figure 10) model of sidewinding. Gray's (1946) verbal description of sidewinding indicated that the snake used static contact with the substrate during this mode. However, V_r was never equal to zero for the illustration of Gray's model of this mode (Figure 1.2; Figure 1.6). Presumably, the reason for this discrepency is that the time of static contact in the model is shorter than the time interval that was used to generate the displacements of segment number fifteen (Figure 1.2). Hence, for Gray's model, the snake should periodically come to a stop ($V_r = 0$). This stop would cause the range in V_r during one cycle to be larger than that illustrated in Figure 1.3. Consequently, the CV of V_r, during Gray's model of sidewinding, should be even greater than the 36.7% that was calculated after digitizing Figure 1.2. The period of V_x equals the period of V_y and V_r with R, L, R movements occurring between times of static contact.

Figure 1.7 shows the velocity profiles for Crotalus, Cerberus, and Nerodia sidewinding on sand. Because the snakes periodically stopped in all three of these examples, the coefficient of variation of V_r was rather large (46.3 - 63.1%). The Cerberus did come to a stop at the 1 sec point of its sequence, but the time of static contact was shorter than the time interval that was used for making tracings. During one cycle of activity for each of these sequences, there are R, L, R movements between times of static contact. Crotalus cerastes consistently attained maximum speeds (V_r) approximately midway between times of static contact (Figure 1.7). In contrast, Cerberus rynchops always decelerated about midway between times of static contact followed by a second acceleration before the snake came to a stop (Figure 1.7). The sidewinding of Nerodia fasciata pictiventris was the most variable

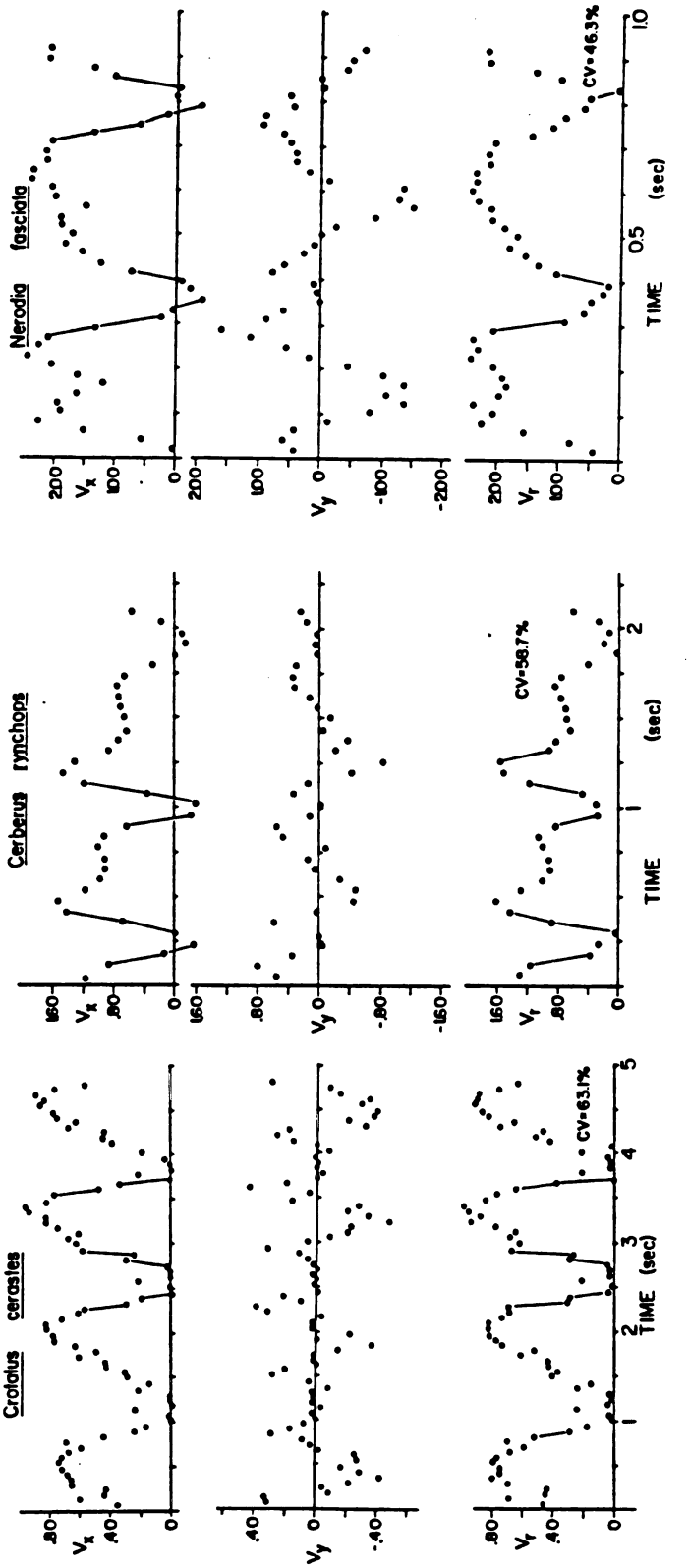

Figure 1.7. Velocities versus time for snakes sidewinding on sand.

of the three species. Nerodia occasionally decelerated midway between times of static contact, but most often the maximum speed was attained at this midway point in a cycle of activity (Figure 1.7). Nerodia and Cerberus both tended to remain in static contact with the substrate for only a very brief time (Figure 1.7) and this was quite similar to the pattern of movement predicted by Gray's model of sidewinding (Figure 1.6). In contrast, Crotalus generally had longer times of static contact with the substrate.

For at least one sequence of each locomotor mode or combination of modes performed by a species, the velocity profiles were compared for two or more different points along the body of the snake. With the exception of concertina locomotion, the only differences in velocity profiles within the body of the snake were attributable to the phase lag one would expect for a periodic pattern of movement travelling from anterior to posterior within the snake. For some sequences of concertina locomotion, the patterns of left and right movement varied along the length of the snake. However, all such points along the snake still displayed patterns characteristic of concertina locomotion, with increasing phase lag from anterior to posterior for the times of static contact. No instances were observed where different regions of the snake were performing different modes. Hence, all reference to the simultaneous use of locomotor modes indicates that the entire body of the snake displayed velocity profiles with characteristics of more than one discrete locomotor mode.

Figure 1.8 illustrates the velocities for a Cerberus rynchops combining locomotor modes while moving on sand. During this sequence,

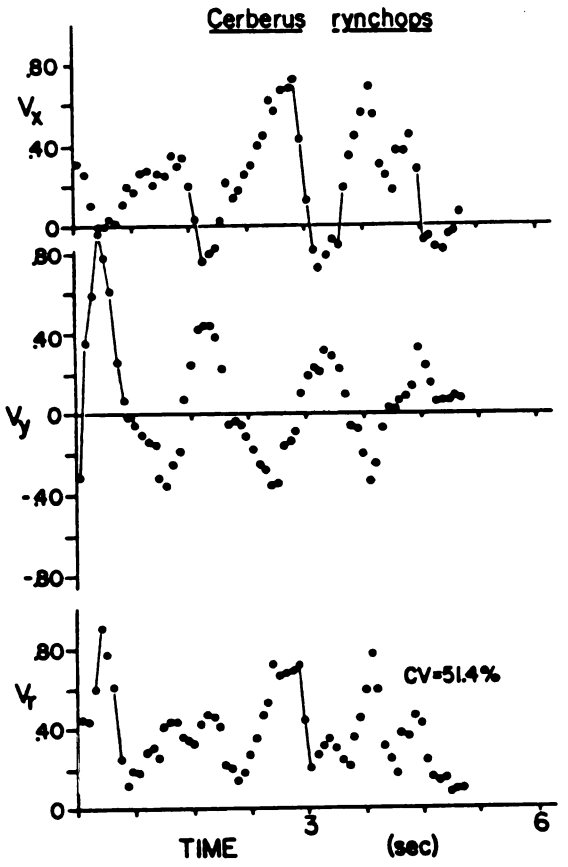

Figure 1.8. Velocities versus time for Cerberus rynchops combining lateral undulation and sidewinding while moving on sand.

the snake made a series of parallel tracks in the sand that would normally be indicative of sidewinding locomotion (Figure 1.1). During one cycle of activity (from 1.5 - 3.0 sec), the snake displayed R, L, R movement which is also normally indicative of sidewinding. Yet as indicated by the graph of V_r, this snake never remained in static contact with the substrate (Figure 1.8). Hence, this snake was combining aspects of sidewinding with lateral undulation. Rather than coming to a stop as it touched the sand (making a track), the snake was sliding within each track. Consequently, the length of the track left in the sand was less than the total length of the snake.

For snakes, the rotating glass pegs and pegboard were a very effective substrate for eliciting good lateral undulation over a wide range of speeds. Table 1.2 summarizes the mean maximum forward velocities attained by snakes performing lateral undulation on this apparatus. For each digitized film sequence, mean forward velocity was calculated for each period of V_y. The space between pegs affected the maximum mean V_x. All five of the Nerodia that performed lateral undulation with the 12.5 cm peg spacing had their fastest speed with this spacing. Similarly, all of the Elaphe were fastest with the 12.5 cm spacing. Not one of the Nerodia attained its fastest speed at the smallest peg spacing (7.5cm). An 87 cm long Nerodia had the fastest mean absolute speed (164.1 cm/sec) and the second fastest mean specific speed (1.89 TL/sec). For Elaphe, the longest snake recorded the fastest mean absolute (110.0 cm/sec) and specific (0.75 TL/sec) forward velocities. The slowest sequence of lateral undulation for Elaphe was for a 123 cm snake moving through the 12.5 cm peg spacing with a mean V_x = 0.19 TL/sec. The slowest V_x of a Nerodia performing simple lateral

Table 1.2. Maximum mean forward velocities for snakes performing lateral undulation on pegboard with glass pegs. * indicates snake was gravid. # indicates snake had an incomplete tail.

SPECIES	TOTAL LENGTH (cm)	MASS (gm)	MAXIMUM MEAN Vx (TL/sec) PEG SPACING 7.5 cm	10.0 cm	12.5cm
Nerodia fasciata	91	218	-	0.47	-
pictiventris	88#	643*	-	0.53	1.19
	87	183	-	0.46	1.89
	84	218	-	0.22	-
	81	278*	-	-	1.03
	80#	238	0.36	0.97	1.89
	73#	235*	0.97	1.51	-
	70#	154	0.51	0.22	0.76
Elaphe obsoleta	147	454	0.62	-	0.75
quadrivittata	123#	627	0.32	-	0.61
	120#	517	0.39	-	0.56

undulation was 0.17 TL/sec for a 70 cm snake moving through pegs with a spacing of 7.5 cm. For all of the other slowest sequences (mean V_x < 0.20 TL/sec) of Nerodia on the glass peg apparatus, V_r was quite variable within each of these sequences (CV > 40%). Despite the accelerations and decelerations during these slowest sequences, the Nerodia did not stop and no vertical flexion of the vertebral column was observed. Hence, this highly variable V_r may indicate Nerodia was combining lateral undulation with concertina locomotion in these cases.

In contrast to the snakes, Rhineura floridana used concertina locomotion when moving on the pegboard and wooden pegs (without the glass sheaths). The range in the mean V_x of Rhineura was 0.17 - 0.28 TL/sec for 2.5 cm peg spacing and 0.13 - 0.20 TL/sec for 5.0 cm peg spacing. Even though wooden pegs were used to minimize slippage of the Rhineura, some backward slipping was still evident in nearly every cycle of activity and occurred to the greatest extent for the 5 cm peg spacing. For Rhineura, an estimate of mean V_x without slippage can be calculated by converting all of the negative V_x's to zero. This estimated mean V_x ranged from 0.18 - 0.29 TL/sec for 2.5 cm peg spacing and from 0.19 - 0.31 TL/sec for 5 cm peg spacing.

Acrochordus javanicus used concertina locomotion on a linoleum floor, and the mean V_x for this snake ranged from 0.04 - 0.11 TL/sec. During the first (and fastest) filmed sequence of Acrochordus, practically no backward slippage was observed; however, as the ventral surface of the snake gathered dust, backward slipping became apparent. When Nerodia were placed in tunnels with rubber sides, concertina locomotion was readily performed and backward slipping was extremely uncommon. Nerodia 84 - 110 cm long attained mean V_x from 0.03 - 0.05

TL/sec in the 8 cm wide tunnel. For a large Nerodia (110 cm), the tunnel with a 10 cm width and wooden sides was not very satisfactory for eliciting pure concertina locomotion. In this apparatus, mean V_x varied from 0.02 - 0.04 TL/sec, and the Nerodia did not usually come to a complete stop. Instead the Nerodia usually continued to glide forward even while contacting the sides of the tunnel. However, the coefficients of variation of V_r for these trials were usually too large for the mode to be considered pure lateral undulation. This suggests some combination of lateral undulation and concertina was used.

When Crotalus cerastes, Cerberus rynchops, and small Nerodia f. pictiventris (Table 1.3) were placed on fine sand, sidewinding locomotion could be observed. The ranges in mean V_x for the sidewinding of these three species were 0.26 - 1.70, 0.39 - 1.20 and 0.42 - 1.36 TL/sec, respectively. Table 1.3 summarizes the maximum mean V_x and size of each snake that performed sidewinding on sand. Figure 1.1 illustrates the determination of the angle between the track and the direction of travel (β) and the distance between tracks along the direction of travel (D), using the notation of Gans (1974). For all of the sidewinding sequences of Crotalus, Cerberus, and Nerodia, the mean β (range) and mean D (range) were 26.5° (16 - 42), 0.60 TL (.56 - .67); 38.2° (28 - 47), 0.57 TL (.50 - .66); and 48.3° (34 - 55), 0.50 TL (.46 - .60), respectively. Using a two-tailed T-test, all mean β's were significantly different from each other (P always at least $< .01$). When the mean β's (21.8° and 30.0°) of two smallest Crotalus cerastes were compared over a comparable range of mean V_x (0.29 - 0.76 and 0.35 - 0.75 TL/sec), a two tailed T-test showed they were significantly different ($t = 5.01$, $P < .01$). The only significant difference among the mean D's

Table 1.3. Maximum mean V_x for snakes sidewinding on sand.

SPECIES	TL (cm)	MASS (gm)	MAX MEAN V_x (TL/sec)
Crotalus cerastes	30.1	27.0	0.75
	33.5	27.0	1.70
	35.7	41.0	0.76
Cerberus rynchops	46.0	28.0	0.73
	49.5	24.0	1.20
Nerodia f. pictiventris	30.0	9.9	1.36

for each species was between Cerberus and Nerodia ($t = 2.67$, $P < .05$).

Crotalus cerastes always performed sidewinding on a smooth unobstructed sand surface. However, occasionally when the Crotalus encountered the sides of the sandbox, rectilinear locomotion could be observed. As the surface of the sand became more convoluted, all three species were likely to shift to lateral undulation, but this was extremely rare for Crotalus and no footage of this presumed lateral undulation could be obtained for Crotalus. Analysis of velocity plots (eg. Figure 1.8) revealed both Cerberus and Nerodia readily combined sidewinding and lateral undulation while moving on the sand. The range in mean V_x of Cerberus performing lateral undulation on sand (0.15 - 0.29 TL/sec) did not overlap with the range in mean V_x for sidewinding, whereas the range in V_x for combined lateral undulation and sidewinding on sand (0.23 - 0.67 TL/sec) overlapped with the ranges in V_x both for sidewinding and lateral undulation on sand.

DISCUSSION

Three key steps were performed to determine which locomotor mode was being used by an individual snake. First, if variation in V_r was low (CV < 37%) during one cycle of activity, then the snake was considered to be performing lateral undulatory locomotion. For this mode, if periodic patterns were discernable for both V_x and V_y, then the period of V_x was one-half that of V_y. Second, if V_r periodically equalled zero (and CV of V_r > 37%), then the locomotor mode was concertina or sidewinding. Third, these two modes were distinguished from each other because of the different patterns of lateral movement. During concertina locomotion there was a pattern of L, R, stop or L, stop, R, stop. When the former pattern was displayed there was a 1:1 ratio of the period of V_x to V_y, whereas the latter pattern caused this ratio to be 1:2. For sidewinding, the periods of V_x, V_y and V_r were always equal, and there was always a L, R, L pattern of movement between times of static contact with the substrate. In addition, for flat surfaces, sidewinding is the only mode that utilizes vertical flexion of the vertebral column. If a sequence of locomotion did not meet these operational criteria for single locomotor modes, then I presumed that the snake was simultaneously combining two or more locomotor modes.

This procedure was successful for distinguishing locomotor modes despite two complications caused by the errors from the digitizing process. First, when snakes performing lateral undulation travelled a

path with a low ratio of amplitude to wavelength, error in determining V_x obscured periodic variation in this quantity. Second, the magnitude of V_y was often very small during concertina locomotion (the slowest mode); therefore, small absolute errors in determining V_y often obscured periodic patterns of variation in V_y.

For pure lateral undulation and pure sidewinding, the period of V_y was easily determined. The inverse of this period roughly corresponds to the frequency of undulation (f). Table 1.4 summarizes the regressions of V_x as a function of f for snakes performing lateral undulation and sidewinding. To compare the predicted values (V_x) of any two regressions, each regression was plotted with its 95% confidence limits and then superimposed on the other regression for comparison. Regions with non-overlapping confidence limits were considered significantly different. The spacing of the pegs affected the relation of V_x to f by enabling snakes to go faster for a given frequency as the distance between pegs increased. For Nerodia with the 12.5 cm spacing, a greater V_x is predicted compared to V_x for the 10.0 cm spacing (for $f > 1.4$ Hz) and compared to V_x predicted for the 7.5 cm spacing (for $f > 1.2$ Hz). Similarly, for Elaphe with the 12.5 cm peg spacing, a greater V_x is predicted compared to that for the 7.5 cm spacing (for $f > 1.3$ Hz). The predicted V_x's for Nerodia were greater compared to the V_x's for Elaphe with both the 7.5 and 12.5 cm peg spacing (for $f > 1.3$ Hz). There were no significant differences in V_x predicted from f among any of the three species when sidewinding was used. For Nerodia, there were no significant differences for V_x predicted for sidewinding versus 12.5 cm peg spacing versus swimming (Jayne, 1985). For the swimming of Elaphe guttata (Jayne, 1985) compared to the closely related Elaphe

Table 1.4. Least squares regressions for $V_x = mf + b$. V_x = mean forward velocity in TL/sec, f = frequency of undulation in Hertz, m = slope, and b = Y-intercept (V_x). lu = lateral undulation, sw = sidewinding, r^2 = coefficient of determination, and n = sample size used for regression. *, from Jayne (1985).

SPECIES (range length)	MODE	SUBSTRATE	m	b	r^2	n
N. f. pictiventris(70-80 cm)	lu	7.5 cm pegs	.331	.022	.78	14
(70-88 cm)	lu	10.0 cm pegs	.369	-.054	.70	31
(70-88 cm)	lu	12.5 cm pegs	.721	-.282	.55	42
(71-99 cm)*	lu	water	.450	.056	.77	15
(30cm)	sw	sand	.497	0	.92	8
(22-39 cm)*	lu	water	.459	-.087	.85	21
E. o. quadrivittata(120-147 cm)	lu	7.5 cm pegs	.117	.173	.24	19
(120-147 cm)	lu	12.5 cm pegs	.261	.072	.72	19
E. g. guttata(100-142 cm)*	lu	water	.329	.001	.92	17
Cerberus rynchops(46-50 cm)	sw	sand	.650	-.129	.98	8
Crotalus cerastes(33-36 cm)	sw	sand	.529	.053	.94	34

obsoleta using the 12.5 cm peg spacing, a greater V_x was predicted over all common values of f. These differences in the relation of V_x to f imply differences in waveform. For example, if a greater V_x is attained for a given f, then the wave of undulation should be larger. For example, as interpeg distance increases for both *Nerodia* and *Elaphe*, the waves of undulation appear to become larger (in wavelength and amplitude) and approach the size of undulations used during swimming. Furthermore, the waveform of sidewinding *Nerodia* appears to approach the waveform during swimming and terrestrial lateral undulation using a minimal number of pivotal points. Finally, similarities are suggested for the waveform of all three species that displayed sidewinding.

Because of the variable patterns of lateral movement during concertina locomotion, determining f is most problematic for this mode. If f is to indicate the rate of repetition of a pattern of movement, then the inverse of the longest period of V_x or V_y should be used. However, for a given sequence of this mode, the period of V_y can show a two-fold difference whereas the period of V_x is usually less variable and more readily determined (Figure 1.5). In some sequences of *Rhineura* and *Acrochordus*, slippage created especially complicated patterns of V_y compared to V_x (and V_r). Consequently, the values of f listed below were calculated as 1/(period of V_x). For *Rhineura*, f ranged from 1.1 - 3.1 Hz for 2.5 cm peg spacing and from 1.5 - 2.2 Hz for 5.0 cm peg spacing. For *Acrochordus*, f ranged from 0.31 - 0.48 Hz. For *Nerodia* performing concertina in an 8 cm wide tunnel, f ranged from 0.24 - 0.55 Hz.

The concertina locomotion of snakes was characterized by very slow mean V_x (0.03 - 0.11 TL/sec) and extremely low frequency of movement

(0.21 - 0.55 Hz). Plate 5 of Gray (1946) illustrates the concertina locomotion of a 75 cm Tropidonotus natrix and can be used to estimate V_x and f. This snake was filmed in glass tubes with widths of 3.75 and 5.63 cm. In the smaller tunnel, mean V_x = 0.05 TL/sec and f = 0.5 Hz, whereas in the large tunnel, this snake had V_x = 0.02 TL/sec and f = .125 Hz. Just as peg spacing affects the speed of lateral undulation, one might expect tunnel width to affect the speed of concertina locomotion. Interestingly, the speeds of concertina locomotion attained by Nerodia using a given f while in a 10 cm wide tunnel are somewhat similar to the V_x predicted for Nerodia performing lateral undulation with the 10 cm peg spacing. For example, in a 10 cm wide wooden tunnel an 84 cm Nerodia performed concertina with mean V_x = 0.04 TL/sec and f = 0.31 Hz. The regression for V_x during lateral undulation (Table 1.4) predicts V_x = 0.06 TL/sec for this frequency. However, the snakes filmed during this study did not perform lateral undulation using such low frequencies of movement. In contrast to snakes, Rhineura used much higher frequencies while performing concertina locomotion, and the V_x attained for such f was generally much slower than the V_x that would be predicted for the lateral undulation of snakes (Table 1.4). For concertina locomotion, future studies clarifying the effects of tunnel width and comparing snakes with amphisbaenians should prove very informative.

The tremendous difference between maximum V_x attained by Nerodia performing concertina (0.05 TL/sec) and terrestrial lateral undulation (1.88 TL/sec) illustrates the need to document the locomotor mode before comparing maximum speeds. Perhaps, different locomotor modes partially

account for the different maximum speeds reported by Mosauer (1935b) for Lichanura (10 cm/sec) compared to Masticophis (166 cm/sec). The relationships between substrate, locomotor mode and maximum speed are likely to further complicate comparisons of maximum speeds among species. Gans and Mendelssohn (1972) described a hierarchy of locomotor modes that were used by snakes in response to increased coarseness of the substrate. For lizards with reduced limbs, Gans (1985) suggested that the choice of locomotor mode is dependent on velocity. Similarly, for a given substrate, snakes might have a hierarchy of locomotor modes that is used to attain increased velocity. For example, as Cerberus increased its speed while moving on sand, pure lateral undulation, lateral undulation combined with sidewinding, and then pure sidewinding were used. Interspecific comparisons of maximum speeds (attained with a given mode on comparable sustrates) should help to determine if the relationship between substrate, locomotor mode and speed differs among species.

The maximum mean V_x of Nerodia f. pictiventris and Elaphe o. quadrivittata performing terrestrial lateral undulation in this study can be compared to the maximum mean V_x during aquatic lateral undulation of N. f. pictiventris and Elaphe g. guttata (Jayne, 1985). Both studies recorded Vx over short time intervals, usually less than one second. The air temperature in this study was 25°C. During filming, Jayne (1985) kept snakes at an air temperature of 25°- 27°C before releasing them for brief periods (usally less than 30 sec) into water with temperatures of 20°- 22°C. Although sidewinding is often presumed to be a very rapid mode of snake locomotion, the maximum mean V_x of a 30 cm Nerodia sidewinding was only 1.34 TL/sec compared to 2.54 TL/sec

attained by a 28 cm Nerodia swimming. In this study an 80 cm Nerodia performing lateral undulation with the 12.5 cm peg spacing attained a maximum mean V_x of 1.89 TL/sec and forward speeds over 1.50 TL/sec were attained by two other adult Nerodia on the substrate with pegs. A slightly slower mean maximum V_x of 1.47 TL/sec has been recorded for the swimming of a Nerodia 77 cm long with a mass of 242 gm (Jayne, 1985). Elaphe obsoleta and Elaphe guttatta are very similar in terms of their behavior, weight-length proportions, numbers of vertebrae, and segmental lengths of major epaxial muscles. In this study, an E. o. quadrivittata 147 cm long attained a maximum mean V_x of 0.75 TL/sec compared to a maximum mean V_x of 1.32 TL/sec attained by a swimming E. g. guttata 142 cm long with a mass of 803 gm. Adult E. g. guttatta commonly attained swimming speeds greater than 0.75 TL/sec (Jayne, 1985).

In this study, the relative forward velocity of the terrestrial lateral undulation of Nerodia was consistently faster than that of Elaphe (Table 1.2). A number of factors could possibly confound this result. First, because the V_x is expressed in TL/sec, scaling considerations suggest that Elaphe, which are generally larger snakes, would be expected to move slower. However, an increase in mass should be the most important factor affecting scaling, and the heaviest snake was a gravid Nerodia (643 gm) which still managed to move 0.40 TL/sec faster than the fastest Elaphe. Second, Bennet et al (1974) and this study found that peg spacing affects maximum velocity of snakes. Presumably, the relationship of peg spacing to snake length is the major factor affecting the speed of a snake. If there is some optimal waveform and number of pivotal points for maximum speed, then for a given peg spacing, the shortest snakes may not encounter enough pivotal

points and the longest snakes may encounter too many pivotal point in order to attain maximum speed. If the space between pegs divided by the length of the snake is a constant, then peg spacing is comparable for snakes of different lengths. The 7.5 cm peg spacing was 10.3% of the 73 cm length of a Nerodia and this snake attained a maximum mean V_x of 0.97 TL/sec on this substrate. The two shortest Elaphe only reached maximum mean V_x of 0.56 and 0.61 TL/sec while crawling through pegs spaced at 10.4 - 10.2 % of their total length. Hence, peg spacing differences do not appear to be sufficient to account for the different maximum V_x's between these two species. Third, behavioral and motivational differences between the two species could affect the determination of maximum V_x. Because the snakes were harassed to make them crawl as fast as possible, if certain snakes were not as readily frightened as others, then they might not crawl as fast. The number of attempts of snakes to bite their handlers could be interpreted as a measure of the degree of agitation of those snakes. All of the Elaphe repeatedly attempted to bite during the filming, whereas only the 73 cm Nerodia attempted to bite. Thus, it seems unlikely that behavioral differences between Elaphe and Nerodia were sufficient to account for different V_x. Therefore, morphological or physiological differences between Elaphe and Nerodia probably cause the different maximum forward velocities for terrestrial lateral undulation.

After comparing Lichanura roseofuscus with Masticophis flagellum, Ruben (1977) suggested that musculo-skeletal adaptations for locomotor speed and constriction may be mutually exclusive. Nerodia and Elaphe are both colubrid snakes; hence they have qualitatively similar major epaxial musculature (Mosauer, 1935a; Gasc, 1974). Nerodia and Elaphe do

possess differences in the numbers of vertebrae and segmental lengths of major epaxial muscles that are characteristic of non-constricting and constricting colubroid snakes, respectively (Jayne, 1982). Hence, the different speeds during the terrestrial lateral undulation of Nerodia and Elaphe in this study support Ruben's (1977) suggestion, if locomotor speed is limited to speed during terrestrial lateral undulation. However, after correcting for snake size, when the maximum V_x's were compared for the swimming of Nerodia versus Elaphe, no significant differences were found (Jayne, 1985). This, and the fact that adult Nerodia were faster on land than in water while the reverse was true for adult Elaphe, emphasizes the need to differentiate between terrestrial and aquatic lateral undulation of snakes in addition to recognizing the different terestrial modes.

An enhanced abilty to determine locomotor mode may have bearing on some of the more general conclusions about snake locomotion. For example, an elegant experiment of Gray and Lissmann (1950) determined the ratio of lateral to longitudinal forces exerted by a snake crawling through experimental chambers with different numbers of pegs to provide lateral pivotal points. This ratio of lateral to longitudinal forces increased with an increase in the number of pivotal points. Figure 7 of Gray and Lissmann (1950) illustrates the position of snakes while crawling with one and two pivotal points, and the posture of the snakes in these two diagrams appears somewhat different from that of Nerodia while performing pure lateral undulatory locomotion in this study (eg. Figure 1.1). Consequently, Gray and Lissmann's (1950) conclusion regarding the ratio of lateral to longitudinal forces might be complicated by their comparing snakes using different locomotor modes.

Ruben (1977) used the number of lateral pivotal points to compare locomotor performance of snakes, but this comparison was incomplete because of the lack of additional kinematic data.

Data from previous studies of the sidewinding of Crotalus cerastes agree closely with this study. Mosauer (1935b) reported a maximum velocity of 91 cm/sec and a prowling velocity of 14 cm/sec for a C. cerastes of unknown size. Crotalus c. cerastes average 17.5 cm at birth, mature at some 48.5 cm, and 55 cm is considered a large individual (Klauber, 1972). Thus, it is likely that C. cerastes can attain a maximum V_x greater than some 2.0 TL/sec compared to the 1.7 TL/sec found in this study. Gans and Mendelssohn (1972) reported a speed on sand of 45 cm/sec for a 38 cm C. cerastes with a body temperature of 39.5°C. For C. cerastes about 30 cm long, Brain (1960) found β ranging from 17° to 40°, with a mean of 26°. The minimum length of snake that must be lifted between tracks is equal to the perpendicular distance between tracks ($= D*\sin\beta$). Based on the mean β and D for Crotalus, Cerberus, and Nerodia, these estimated lengths are 26.9, 35.1, and 37.3 %TL, respectively. Assuming only an average of 10% of the snake length touches each track, the maximum number of simultaneous points of static contact that any of these snakes could have would be three. Occasionally, just as the neck of Crotalus cerastes contacted the substrate, three points of static contact could be observed. However, two regions of static contact were by far the most common situation for C. cerastes, and this was the only situation observed for the sidewinding of Cerberus and Nerodia.

The three species of snakes which performed sidewinding in this study do not appear to all be equally proficient sidewinders. The

combination of lateral undulation and sidewinding was most easily elicited from small Nerodia on sand, whereas small Nerodia on this substrate usually had to be frightened in order to perform pure sidewinding. In contrast to Nerodia on smooth sand, Cerberus readily performed pure sidewinding and pure lateral undulation as well as simultaneously combining these two modes. During field work on tidal mud flats in Malaysia, I have also frequently observed sidewinding by Cerberus that were undisturbed. This suggests sidewinding is a regular part of the locomotor repertoire of Cerberus rather than just an infrequently used escape response. Hence, Nerodia was the least proficient sidewinder in this study. Crotalus cerastes has long been known to belong to a group of desert viperids which are extremely proficient sidewinders (Gans and Mendelssohn, 1972). Finally, this study suggests Cerberus may belong to another distinct group of proficient sidewinders and Wall's (1919) observation of sidewinding in this species is supported.

The relationship of sidewinding to other modes of locomotion is not well understood. Based on the observations of the sidewinding of Tropidonotus natrix, Gray (1946) emphasized the similarity of sidewinding to lateral undulation, and suggested that normal forces, opposing movement, acted equally along the entire length of a snake during lateral undulation. Gray then proposed that the pattern of motion characteristic of sidewinding could be predicted if the external normal forces only acted upon regions of the snake that were in phase and in static contact with the substrate while no external forces opposed the movement of the snake while it was above the substrate.

Hence, by superimposing a wave of vertical vertebral flexion on a wave of lateral flexion, characteristic of lateral undulation, the new resulting pattern of external resistive forces would predict sidewinding motion (Gray, 1946). Using similar reasoning, Brain (1960) also considered sidewinding to be derived from lateral undulation.

Gans (1962, 1974) suggested that sidewinding more closely resembles concertina locomotion because of the similar use of static contact. Gans (1974) stated that at a given instant during either of these modes, there are generally two regions of the snake's body that are in static contact with the substrate. Consequently, the other portions of the snake are being accelerated forward either by being pushed away from a more posterior point of static contact or by being pulled toward a more anterior point of static contact.

In this study, the pattern of sidewinding shown by Nerodia (Figure 1.7), the least proficient sidewinder, is very similar to that predicted by Gray (1946) (Figure 1.6). Both of these diagrams illustrate sidewinding where static contact with the substrate is extremely brief. Another observation that tends to support the suggestion of Gray (1946) and Brain (1960) is the transition from lateral undulation to sidewinding for Cerberus and Nerodia moving on sand. If the muscular mechanisms of sidewinding and lateral undulation are fundamentally similar, then one might expect to see the combined use of lateral undulation that was commonly displayed by Cerberus and Nerodia. On the other hand, because the simultaneous use of sidewinding with lateral undulation can be quite common for certain colubrids, observations of this combined mode could possibly be mistaken for pure sidewinding and lead one to conclude that pure sidewinding is derived from pure lateral

undulation. Gray (1946) did not film any of the specialized sidewinders studied by Gans and Mendelssohn (1972). In fact the sidewinding of Crotalus cerastes (Figure 1.7) differs slightly from the model of Gray (Figure 1.6) by having a longer time of static contact between the snake and the substrate. The sidewinding of Cerberus (Figure 1.7) was different from Crotalus cerastes and the model of Gray because of the second acceleration within each cycle of activity. This second acceleration strongly resembles the pushing and pulling phases that were evident in three cycles of activity of a sequence of concertina locomotion of Nerodia (Figure 1.5). Thus, for each cycle, a point on Cerberus may be pushed from a posterior track and then pulled to the next successive region of static contact (track). Therefore, the sidewinding of Cerberus supports the suggestion of Gans. Furthermore, if the pulling phase immediately followed or overlapped with the pushing phase, the patterns of sidewinding shown by Crotalus and Nerodia could be predicted. Figure 1.7 emphasizes that all sidewinding is not alike, and the study of different taxa may have complicated the resolution of the relationships of major locomotor modes. Electromyographic studies of the different modes of snake locomotion should help resolve this question.

CHAPTER TWO

MUSCULAR MECHANISMS OF LATERAL UNDULATION, CONCERTINA AND SIDEWINDING

INTRODUCTION

The diversity of snake locomotor modes has been well documented. Lateral undulation, concertina and sidewinding are three of the most common modes for which various patterns of vertebral flexion generate propulsive forces (Gray, 1946; Gans, 1974). In addition to these distinct modes, the existence of certain less common and transitional modes has been discussed (Gans, 1974; 1984). To date most work on snake locomotion has dealt with categorizing different locomotor modes and discussing the patterns of force transmission and the interrelationships between the different modes (Mosauer, 1932; Gray and Lissmann, 1950; Gans, 1974, 1985).

Concurrent with the study of snake locomotion, workers have clarified the anatomy of snake axial muscles believed important for locomotion. The individual segments of snake axial muscles usually have a 1:1 correspondence with the underlying vertebrae. Each of the individual muscle segments has distinct tendinous and contractile tissue portions. These serially homologous muscle segments often collectively form distinct longitudinal columns of muscle which are apparent upon gross examination (Mosauer, 1935a; Gasc, 1974).

Mosauer's (1935a) pioneering work on the axial muscle segments of snakes documented considerable interspecific variation. Individual segments of axial muscles vary in their shape, interconnections with nonhomologous muscle segments and the relative proportion of tendon and

contractile tissue. Mosauer attempted to correlate this variation in muscle segments with a phylogenetic scheme based on the familial lines of the boids, colubrids and viperids. The more recent detailed studies of Gasc (1967, 1974) have illustrated that Mosauer's phylogenetic scheme was greatly oversimplifed. A major dichotomy does exist between booid and colubroid snakes and this is clearly manifested in the axial muscles as qualitative differences in shapes and interconnections among muscles segments (Mosauer, 1935a). However, within colubroid snakes there is much gross qualitative similarity in the shape of the contractile tissue for largest epaxial muscles such as the Mm. semispinalis-spinalis, multifidus, longissimus dorsi and iliocostalis. Furthermore, these major epaxial muscles of colubroids display a continuum of variation in their interconnections with each other, and this has obscured Mosauer's earlier distinctions between the colubrid and viperid myological types within the colubroid snakes (Gasc, 1974). Substantial quantitative differences also exist in the lengths of the tendinous portions of the various muscles, and this variation is associated with specialization in habitat and habits (Gasc, 1974; Jayne, 1982). A tendon of a single segment of the M. semispinalis-spinalis may exceed 30 vertebrae in length in certain arboreal species compared to a length of only 6 vertebrae in some aquatic species (Jayne, 1982).

Despite the parallel study of snake locomotion and musculature, a muscular mechanism has not been directly observed for any of the modes of snake locomotion that use vertebral flexion. After measuring coefficients of friction and reactive forces generated by a snake performing terrestrial lateral undulation, Gray and Lissmann (1950) proposed models for the muscular mechanisms of this mode for snakes

crawling through a tube with rectangular bends and past various numbers of pegs. For their modelling, Gray and Lissmann assumed the locomotor muscles of snakes spanned only one body segment and that a specific posture was used by snakes gliding past pegs. They concluded that snakes performed this terrestrial mode by using alternating, unilateral, descending muscle contractions. Furthermore, the initiation of muscle contraction was not just dependent on the extent of lateral vertebral flexion, but it was also dependent on the position of the snake relative to the lateral pivotal points.

Gray (1953) provided another detailed discussion and model for the mechanisms of most types of animal undulatory locomotion including the swimming of snakes. In this review, Gray stressed the similarity between terrestrial and aquatic lateral undulation. According to Gray, the primary difference between these two modes is that the waves of lateral flexion move posteriorly with a velocity equal but opposite to the velocity of forward progression during terrestrial movement, whereas the wave of bending travels faster than the forward speed of the swimming snake. Hence, the wave of bending remains stationary to the ground for terrestrial undulation but slips backward through the water during swimming. Gray included observational data on the waveform of snakes swimming in media with differrent viscosities and noted that the external resistive forces encountered by swimming snakes did affect the waveform of the animal. However, Gray did not suggest that this would affect the underlying muscular mechanism of propulsion. More recently, Blight (1977) suggested that a balance between the active and passive properties of the body of the swimmer and of the resistence of the medium determine the nature of the swimming mechanism. Blight

particularly emphasized elongate swimmers, whose bodies he predicted to be stiffness-dominated rather than flexibility-dominated. The models of Gray and the concepts of Blight will be discussed in more detail later.

Although Gray and Lissmann (1950) modelled aspects of sidewinding and concertina locomotion, muscular mechanisms have been predicted only for terrestrial and aquatic lateral undulation. Gray and Lissmann were careful to state their assumptions and simplifications when discussing snake locomotion, and their explicit detail provides an excellent theoretical framework which can now be tested experimentally.

This study uses synchronized electromyography and cinematography to determine the muscular mechanisms of terrestrial and aquatic lateral undulation, concertina and sidewinding locomotion. The activity of the three largest epaxial muscles, the Mm. semispinalis-spinalis, longissimus dorsi and the iliocostalis, is the primary focus of this work. Emg's are analyzed only for colubroid snakes to minimize the extent of qualitative variation of these three muscles. The colubrids Nerodia fasciata pictiventris and Elaphe obsoleta quadrivittata were chosen because their segmental muscle lengths and numbers of vertebrae are representative of nonconstricting and constricting colubroids, respectively (Jayne, 1982). The aquatic and terrestial lateral undulation and concertina locomotion of these two taxa are compared primarily to isolate the effects of increased numbers of body vertebrae (Elaphe 240 vs. Nerodia 125) when segmental lengths of major axial muscle segments are similar. For swimming, Elaphe may be considered a more flexible animal in the sense of Blight (1977). Within both of these species, aquatic and terrestrial lateral undulation are studied to clarify the distinctions between these two rather similar modes.

Crotalus cerastes was chosen as a behaviorally and morphologically specialized sidewinder (of Mosauer's viperid muscle type) that could be compared with the relatively unspecialized *Nerodia* (of Mosauer's colubrid muscle type).

MATERIALS AND METHODS

Various species of colubroid snakes snakes were chosen for this study based on practical considerations as well as the ability of a species to perform a desired locomotor mode. The primary species studied were Nerodia fasciata pictiventris, Elaphe obsoleta quadrivittata and Crotalus cerastes. The Nerodia and Elaphe were obtained from commercial suppliers in southern Florida and the Crotalus were from a dealer in southern California. Animals were maintained in a light and temperature controlled room that complied with local guidelines for the housing of snakes. When possible, large individuals of each species were preferentially chosen so that size of the epaxial muscle mass was maximized. Table 2.1 summarizes the lengths and masses of snakes used in the electromyographic portion of this study.

Based on the previous kinematic analysis of snake locomotion, substrates were chosen which best elicited a particular locomotor mode. Table 2.1 summarizes the substrates used for particular individuals. Tempered peg board with rotating glass pegs proved most effective for eliciting terrestrial lateral undulation. A pool 1.6 x 4 m with water depth of about 20 cm was used for filming aquatic lateral undulation. A straight-sided tunnel with a glass floor and rubber sides was used for concertina locomotion. Sand and a linoleum floor were good substrates for sidewinding and some transitional modes of locomotion. Snakes were filmed moving at ambient room temperature (24 - 28°C).

After filming, snakes were killed with an injection of sodium

Table 2.1. Electromyographic sample. Nerodia fasciata, Elaphe obsoleta and Crotalus cerastes are abbreviated NF, EO and CC, respectively. For substrate, distances indicate spacing between centers of pegs in square arrays or the widths of the tunnels (tnl) used. Abbreviations for locomotor mode are LU, C and SW for lateral undulation, concertina and sidewinding, respectively.

SNAKE	SUBSTRATE	MODE	SEX	MASS (gm)	LENGTH (cm) Total	SV	VERTEBRAE Total	Body	AREA (cm^2) Total	Body
NF36	7.5cm pegs linoleum	LU SW	M	76	68	48	212	126		
NF37	7.5cm pegs linoleum	LU SW	F	88	65	49	192	130		
NF35	10cm pegs	LU	M	124	73	52	204	125		
NF39	water	LU	M	79	62	47	190	126	75	64
NF38	water	LU	F	152	73	55	199	129	107	97
NF34	water	LU	F	260	85	67	171	125	146	138
NF33	8cm tnl	C	F	280	91	71	176	125		
NF30	10cm tnl	C	F	267	87	75	165	132		
NF32	8cm tnl	C	F	253	81	75	142	126		
NF31	8cm tnl	C	F	389	107	80	198	127		
EO18	15cm pegs	LU	F	353	153	118	326	242		
EO17	15cm pegs	LU	F	604	158	131	320	235		
EO20	water	LU	F	165	112	91	330	245	146	137
EO19	water	LU	M	455	149	121	321	235	263	242
EO15	8cm tnl	C	F	510	126	118	265	240		
EO16	8cm tnl	C	M	695	141	128	271	238		

Table 2.1 (cont'd)

CC9	sand	SW	F	67	42	39	164	121
CC7	sand	SW	M	95	53	48	167	146
CC8	sand	SW	M	93	55	50	163	141
CC10	sand	SW	F	94	56	52	164	145
CC5	sand	SW	F	140	57	53	160	145
CC6	sand	SW	M	155	58	53	165	146

pentabarbitol. Snout-vent (SV) and tail lengths were then measured to the nearest cm and mass was determined to the nearest gm. For snakes that had been filmed swimming, midsagittal area, to the nearest cm^2, was calculated from measurements of the mid-dorsal to mid-ventral heights of the relaxed snake taken at intervals of 10% of its length. Snakes were then fixed in 10% formalin and stored in 70% ethanol.

The electrodes used for electromyography were made of .002 gauge, poly-coated, stainless steel wire. A cyanoacrylate glue was used to bond together about the first 10 cm of the strands of the bipolar electrodes. With the aid of a dissecting microscope, a razor blade was used to scrape the insulation from the first 0.8 to 1.2 mm of the electrode wire. Bipolar electrodes were inserted through the skin and into muscles by using hypodermic needles. A unipolar ground wire was implanted lateral to the ribs. During early attempts to implant electrodes with 25 gauge needles, snakes were anesthetized with a mixture of halothane and nitrous oxide. This procedure was quickly abandoned after discovering that manual restraint of the snake and implantation with 26 gauge needles gave better results. After insertion, the electrode wires were glued to the skin of the snake using a cyanoacrylate glue with a viscous formula (advertised for bonding leather and wood). Small pieces of plastic were pressed against the glue to facilitate strong bonding. Plastic cement was then used to glue together the two strands of each electrode and to bond the electrodes to each other to form a single cable which was glued to the back of the snake. The lengths of electrode wire from the snake to the probes of the polygraph ranged from 1.5 to 3.0 meters, averaging about two meters. Lengths of wire were used which allowed unimpeded locomotion by the snakes. The number of electrodes implanted in a single snake ranged

from four to ten. Small pieces of tape were used to label the ends of the electrodes that were connected to the probes of the polygraph. Placement of electrodes was confirmed by dissection of the preserved specimens.

The emg's were processed by a Grass model 7D polygraph with wide band EEG alternating current amplifiers (models 7P5B and 7P3B). Emg's were not integrated and amplifiers were calibrated weekly. Low and high filter settings were 10 Hz and 40 kHz, respectively. A 60 Hz filter was also used to minimize noise. Depending on the availability of equipment, emg's were recorded from four or six muscles simultaneously. The sensitivities of the pre-amplifiers varied from 50 to 300 uV/cm. The amplified signals were recorded on magnetic tape at 15 i.p.s. with a Honeywell model 5600 eight channel tape recorder.

Emg's were played back from the tape recorder at 1 7/8 i.p.s. to the pens of the polygraph to provide a paper copy of the signals for which the mechanical response of the pens did not limit frequency response. These emg records were analyzed for the onset and offset of muscle activity (to nearest 0.01 sec).

A Bolex H16 movie camera operated at 50 f.p.s. with a shutter speed of 1/300 sec was used to obtain 16 mm black and white films of snakes. The camera was always positioned vertically above the surfaces upon which the snakes crawled. Within the view of the camera, a light blinked every one-half second and simultaneously sent a signal to the tape recorder to insure synchronization of the film and emg records.

Films were projected using a Lafayette stop action projector. At regular time intervals, tracings were made of paint marks along the middorsal scales of the snakes. For each resulting tracing, lines about 4 cm long were drawn beginning at the anterior portion of a traced paint

mark and tangent to the curve formed by the paint marks representing the vertebrae (Figure 2.1). These modified tracings were then digitized using a graphics tablet interfaced to an Apple II+ microcomputer. Each tangentially constructed line on the tracings was digitized by entering its two endpoints. Thus, the more anterior endpoint of each line represented a single point on the moving snake which allowed determination of linear displacement for this region of the snake. Each pair of endpoints was used to generate the equation of the tangential line, and hence calculate angular displacement relative to the adjacent tangential lines (representing vertebrae). Hence a record of angular and linear displacements through time was generated for several vertebrae along each snake. Angles between the tangential lines were divided by the number of intervening vertebral joints to calculate mean lateral vertebral flexion ($\bar{\theta}$) over intervals of every four vertebrae (Figure 2.1). Positive values of $\bar{\theta}$ indicate the vertebral column is concave (flexed) to the animal's right. Tracings were oriented so that the overall direction of travel was in the positive X direction and movement to the right was in the positive Y direction (Figure 1.1). Hence, each overall velocity (V_r) could be resolved into forward (V_x) and lateral (V_y) components. Plots of V_x, V_y and V_r versus time were used to determine locomotor mode (see Chapter 1). Muscle activity was superimposed on plots of $\bar{\theta}$, V_y and V_r versus time to determine the mechanical correlates of emg.

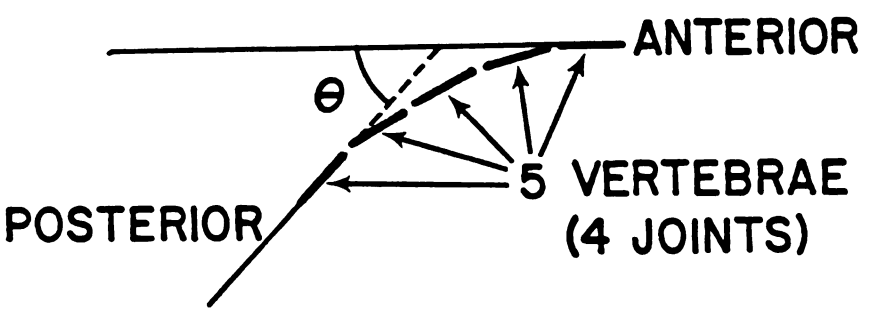

$\bar{\theta} = \theta/4$ = Mean Lateral Flexion

$\bar{\theta} > 0$ concave (flexed) right (R)

$\bar{\theta} = 0$ straight

$\bar{\theta} < 0$ concave (flexed) left (L)

Figure 2.1. Method of measuring lateral vertebral flexion from tracings of films (Note this is an example of vertebrae concave to the right).

RESULTS

Anatomy

The following descriptions of muscles are based on the average measurements taken from at least three individuals each of Nerodia f. pictiventris, Elaphe obsoleta quadrivittata and Crotalus cerastes. Terminology follows that of Gasc (1981).

In snakes the three largest and most superficial longitundinal columns of epaxial muscles are comprised of segments of the Mm. semispinalis-spinalis, longissimus dorsi and the iliocostalis. In all three of these colubroid species, the muscular segments of the Mm. semispinalis-spinalis, longissimus dorsi, and iliocostalis each receive the majority of muscle fibers from two adjacent vertebral units (e.g., see spinalis origin on vertebrae 19 and 20 in Figure 2.2). Despite this, certain tendinous portions of all three muscles exhibit a 1:1 correspondence with the number of vertebrae. These tendinous portions are 1) the long anterior tendon of the M. semispinalis-spinalis, 2) the anterior tendinous arch of the M. longissimus dorsi, and 3) the intermediate tendon between the medial and lateral heads of the M. iliocostalis (= AT, TA and IT on Figure 2.2). Rather than describing all of the deeper epaxial muscles, descriptions are only provided for those into which electrodes were implanted. For more complete accounts of the axial musculature, the reader is referred to Mosauer (1935a) and Gasc (1974; 1981).

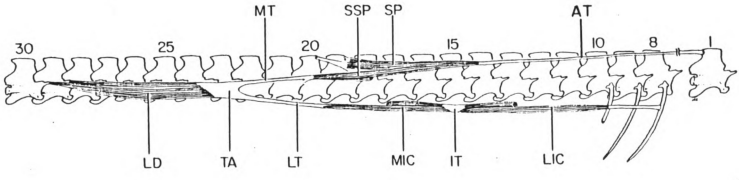

Figure 2.2. Simplified right lateral view of the major epaxial muscle segments of Nerodia f. pictiventris. Anterior is to the right of the figure. SP and SSP respectively indicate the spinalis and semispinalis portions of the M. semispinalis-spinalis, and AT is the anterior tendon of the SSP-SP. LD represents the M. longissimus dorsi and MT, TA, and LT are the medial tendon, tendinous arch, and lateral tendon of LD. MIC and LIC respectively are the medial and lateral heads of the M. iliocostalis and IT is the intermediate tendon of this muscle. See text for more detailed description. From Jayne (1985).

To facilitate comparisons, the vertebra onto which the anterior tendon of the M. semispinalis-spinalis inserted was counted as number one and the subsequent numbering of vertebrae proceeded posteriorly. Figure 2.2 illustrates a simplified view of the arrangements of the major epaxial muscle segments of Nerodia fasciata pictiventris. The thin anterior tendon (AT) of the M. semispinalis-spinalis extends posteriorly to end lateral to the 14th vertebra of Nerodia. The muscle tissue of the dorsomedial head (spinalis) of the M. semispinalis-spinalis continues posteriorly for five more vertebrae. The muscle fibers then terminate on the posterior tendons of the segments of the M. multifidus, which extend posteriorly for an additional one or two vertebrae and attach to the lateral surface of the neural spine. Thus, the resulting span of vertebrae for one segment of the spinalis is 20, including the vertebrae of origin and insertion. Muscle fibers from the ventrolateral head (semispinalis) of the M. semispinalis-spinalis terminate on a tendinous sheet at the 20th vertebra of Nerodia. Part of this tendinous sheet contributes to an intermuscular septum (between the Mm. semispinalis-spinalis and longissimus dorsi). This septum forms a diffuse connection to the vertebra in the region of the prezygapophysis. Another portion of the tendinous sheet extends ventrolaterally to form the medial tendon of the M. longissimus dorsi.

Muscle tissue from a single segment of the M. longissimus dorsi extends anteriorly from its origin on the 30th vertebra to insert into a tendinous arch lateral to the 24th vertebra of Nerodia. The tendinous arch gives rise to a dorsomedial tendon (MT) that connects with the semispinalis and a ventrolateral tendon (LT) that connects with the

medial head of the M. iliocostalis. Between the lateral and medial heads of the iliocostalis is an intermediate tendon that is less than one vertebra long; this tendon is lateral to the 15th vertebra. The muscle tissue of one segment of the M. iliocostalis extends anteriorly from the 20th to 10th vertebra of Nerodia. The tendon from the lateral head extends anteriorly until it attaches to the rib of the eighth vertebra. Hence the total number of vertebrae spanned by a single unit of the M. longissimus dorsi - M. iliocostalis is 23.

Figure 2.3 illustrates the arrangement of major muscle segments of Elaphe obsoleta. In this species, the anterior tendon of the M. semispinalis-spinalis extends posteriorly to end lateral to the 11th vertebra and the muscle tissue of the spinalis continues posteriorly for four to five vertebrae. The muscle fibers then terminate on the posterior tendons of the segments of the M. multifidus, which extend posteriorly for almost two additional vertebrae. Thus, the resulting span of vertebrae for one segment of the spinalis is 18 in Elaphe. At the 18th vertebra of Elaphe muscle fibers from the semispinalis terminate on a tendinous sheet similar to that of Nerodia. In Elaphe muscle tissue from a single segment of the M. longissimus dorsi extends anteriorly from the 27th to the 21st vertebra. The origin, insertion and intermediate tendon of the M. iliocostalis of Elaphe are similar to those of Nerodia. The muscle tissue of one segment of the M. iliocostalis extends anteriorly from the 17th to the seventh vertebra of Elaphe, and the tendon from the lateral head extends anteriorly until it attaches to the rib of the fifth vertebra. The total number of vertebrae spanned by a single unit of the M. longissimus dorsi - M. iliocostalis is 23.

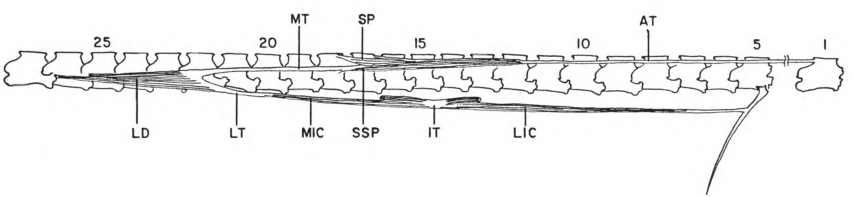

Figure 2.3. Simplified right lateral view of the major epaxial muscle segments of Elaphe o. quadrivitatta. Anterior is to the right. Abbreviations are as in Figure 2.2.

Figure 2.4 shows the axial muscle segments of Crotalus cerastes. The anterior tendon of the M. semispinalis-spinalis extends to the 10th vertebra and the muscle tissue extends for about an additional four vertebrae before inserting onto the tendon of the M. multifidus. The total segmental length of the spinalis is thus 15 vertebrae. Unlike the semispinalis of Nerodia and Elaphe, the semispinalis of Crotalus attaches directly to the 15th vertebra via a distinct ribbon-like tendon (Figure 2.4) that is shared with the M. interarticularis superior. Muscle tissue of the M. longissimus dorsi extends anteriorly from its attachment to the prezygapophysial process (accesory process of Mosauer, 1935a) for about five vertebrae at which point a tendinous arch is formed. Unlike Nerodia and Elaphe, the medial tendon of the longissimus dorsi extends anterodorsally for three vertebrae and forms a diffuse attachment to the neural spines of the vertebrae (Figure 2.4). The exact point of attachment of this medial tendon to the vertebrae is difficult to determine because the tendon becomes part of a connective tissue sheath surrounding the M. semispinalis-spinalis. The span of the M. longissimus dorsi from the prezygapophysial process to its rather indistinct attachment to the neural spines is nine vertebrae. The lateral tendon of the M. longissimus dorsi extends anteriorly for two vertebrae whereupon a weak connection extends medially to the proximal portion of a rib. A more robust portion of this tendon extends ventrolaterally for an additional vertebra at which point the muscle fibers of the iliocostalis begin and continue anteriorly for 11 vertebrae. The posterior muscle fibers of the M. iliocostalis terminate on a distinct tendon, slightly longer than a vertebra, that attaches to a rib. The span of the M. iliocostalis segment by itself is 14

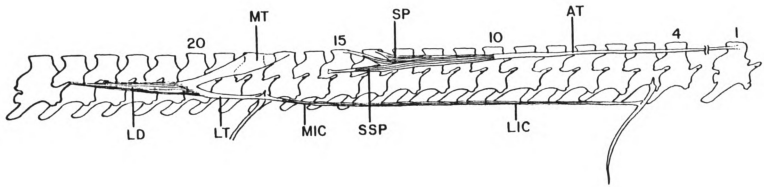

Figure 2.4. Simplified right lateral view of the major epaxial muscle segments of Crotalus cerastes. Anterior is to the right. Abbreviations are as in Figure 2.2.

vertebrae and with the associated M. longissimus segment is 21 vertebrae. The M. iliocostalis of Crotalus cerastes does not have a distinct intermediate tendon and this somewhat complicates the dissection of this muscle.

Deeper muscles occasionally implanted with electrodes included the Mm. multifidus, interarticularis superior and interarticularis inferior. The M. multifidus was effectively identical in the above mentioned three species. This triangular shaped muscle lies deep to the spinalis. Anteriorly, the multifidus fibers form a wide attachment to the posterior portion of the postzygapophysial wing and these fibers taper posteriorly as they join a triangular tendon until a total of five vertebrae are spanned by a complete segment (Figure 2.5).

The M. interarticularis superior (M. digastricus of Mosauer, 1935a) was occasionally encountered in Nerodia and Elaphe, and it has comparable morphology in these two taxa (Figure 2.5). Segments of this muscle originate from the posterior margin of the postzygapophysis just ventral to the fibers of the M. multifidus. As the fibers extend posteriorly, they bifurcate to form two distinct spindle-shaped heads. Each of these heads attaches to the posterior portion of the postzaygapohphysis via thin tendons about one vertebra long. Including the vertebrae of origin and insertion, four vertebrae are spanned by these segments.

The M. interarticularis inferior lies deep to the M. longissimus dorsi of Elaphe. This muscle extends anteriorly four vertebrae from its origin on the prezygapophysial process to its insertion on the most proximal portion of a rib. Each segment receives some fibers from each of the vertebrae it spans.

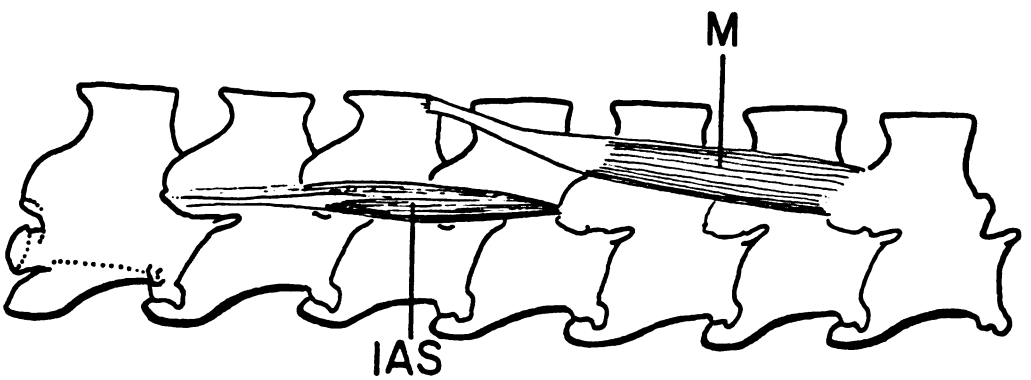

Figure 2.5. Simplified right lateral view of deeper epaxial muscle segments of Nerodia f. pictiventris. Anterior is to the right. The M. semispinalis-spinalis has been removed. The M. multifidus and M. interarticularis superior are abbreviated M and IAS, respectively.

Hereafter, for the sake of brevity, the following abbreviations will be used to indicate the location of an electrode from which an emg was obtained.

SSP-SP - M. semispinalis-spinalis (anterior to the formation of the spinalis and semispinalis heads)

SP - spinalis head of M. semispinalis-spinalis

SSP - semispinalis head of M. semispinalis-spinalis

LD - M. longissimus dorsi

IC - M. iliocostalis

M - M. multifidus

IAS - M. interarticularis superior

IAI - M. interarticularis inferior

In graphic summaries of results, spans of muscle segments containing electrodes are given in parentheses after the muscle abbreviation. Muscle spans indicate the positions of the anterior-most and posterior-most vertebrae to which the muscle attaches, counting posteriorly from the skull. If an electrode was in more than one adjacent muscle segment, the span included the most anterior and posterior origins and insertions of all the contractile tissue containing the uninsulated electrode wire. Span of the IC of Nerodia and Elaphe includes the asociated segmental length of LD. Span of the SSP does not include the associated LD in any of the studied taxa.

Terrestrial Lateral Undulation

Figures 2.6, 2.7 and 2.8 illustrate movement and emg records for the terrestrial lateral undulation of Nerodia 35 crawling through a square array of rotating glass pegs spaced 10 cm apart. Figure 2.6 shows the emg's from contractile tissue of segments of the SP, LD and IC from the right side of the snake near midbody. In this figure, mean lateral vertebral flexion ($\bar{\theta}$) was calculated for the four joints between vertebrae 69 and 73. In all similar figures that follow, the linear velocities (V_y; V_r) are shown for the most anterior vertebra of the body segments used to determine $\bar{\theta}$ (e.g., vertebra 69 in Figure 2.6). For this sequence the overall mean V_x from 0 to 3.26 sec was 0.29 total lengths (TL)/ sec. For the same time interval the value of CV (coefficient of variation) of V_r was a rather small 21% indicating that the snake was performing fairly good lateral undulation. Two complete periods of motion were evident from 0.62 to 2.05 and 2.05 to 3.15 sec and means of V_x for these time intervals were 0.28 and 0.30 TL/sec, respectively. The three cycles of activity of the right side segments of the SP, LD and IC began when vertebrae 69 to 73 were maximally flexed to the left (= convex to the right) and ended when these veterbrae were maximally concave to the right. Activity of these three muscles with contractile tissue at the same level of the body was generally synchronous. The plot of $\bar{\theta}$ versus time did not show a perfect sinusoidal function. Instead, the first two flexions to the right showed decreases roughly midway through flexion to the right. These momentary decreases in right side flexion were caused by the snake forming a rather low amplitude - long wavelength flexion to the right.

Figure 2.6. Emg and movement records from sequence 53.7 of Nerodia 35 performing terrestrial lateral undulation with 10 cm peg spacing. Right and left are abbreviated R and L. Oblique lines connecting dots are only to facilitate recognition of successive points in time. Numbers in parentheses after muscle abbreviations indicate the vertebrae spanned by the muscle segments containing electrodes. Horizontal bars represent emg with greater thickness indicating stronger activity. Emg's of muscles from the right side of the snake are diagrammed above the portion of the plot of $\bar{\theta}$ indicating lateral vertebral flexion concave to the right. Velocities are in TL/sec and are for the first vertebra (69) in the interval used to determine $\bar{\theta}$.

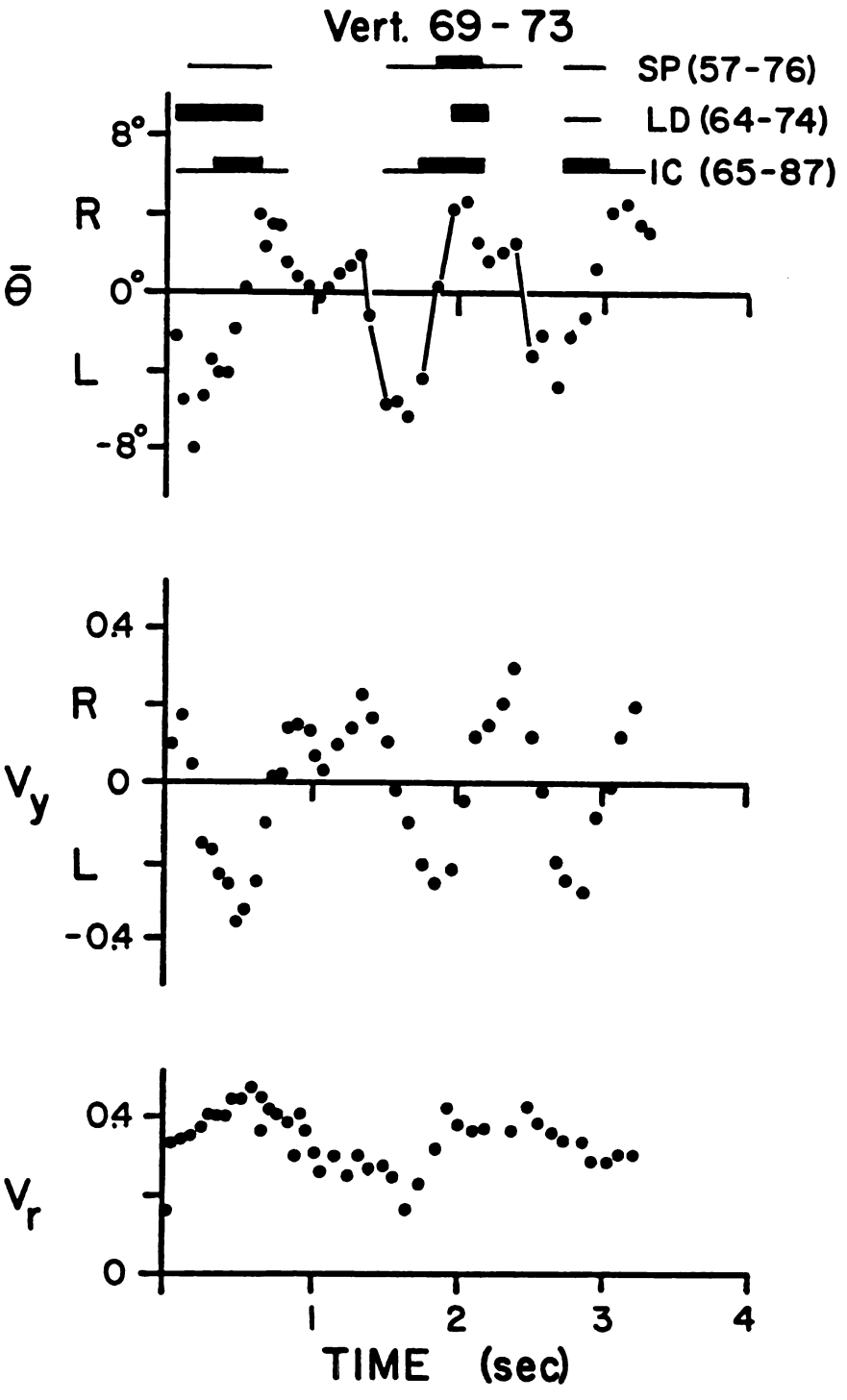
Vert. 69 - 73
SP (57-76)
LD (64-74)
IC (65-87)
8°
R
0°
L
-8°
θ̄
0.4
R
0
L
-0.4
Vy
0.4
0
Vr
1
2
3
4
TIME (sec)

Figure 2.6.

In other words the crest of this half wave was very shallow with the vertebrae nearly becoming straight as they approached maximum lateral displacement.

Figure 2.7 illustrates a rather slow sequence of lateral undulation for the same snake and activity of a segment of the LD on the left side of the snake near mid-body. For this sequence from 0 to 3.86 sec, mean V_x was 0.11 TL/sec and CV of V_r was 40%. The large coefficient of variation of overall speed was primarily the result of a slow start by this snake and a steady acceleration as the sequence progressed. For the complete period of motion from 0.62 to 3.15 sec mean V_x was 0.08 TL/sec and CV of V_r was 21%. For the half periods from 0.62 to 1.86 and 1.86 to 3.05 sec mean V_x was 0.10 and 0.07 and CV of V_r was 11 and 18%, respectively. As suggested by these similar mean values of V_x, the steady increase in V_r was primarily caused by increases in V_y (Figure 2.7). The snake also displayed greater lateral vertebral flexion as time increased ($\bar{\theta}$ = 8° at 2.29 sec and 10° at 3.18 sec). Hence, this sequence may still be considered good lateral undulation although the wave form of the snake changed through time. As before, the muscle was active beginning when the region was maximally convex and ending when the region was maximally concave to the left.

Figure 2.8 shows another sequence of lateral undulation of NF35 and activity from a right side SP and left side LD. Mean V_x is 0.27 TL/sec and CV of V_r is 19% from 0 to 2.10 sec. Mean V_x during the half periods between 0.62, 1.11, 1.77 and 2.10 sec was 0.25, 0.24 and 0.31 TL/sec, respectively. The contractile tissue of these two muscle segments was nearly at the same longitudinal position along the body of the snake. Muscle fibers of the right SP spanned vertebrae 70 to 75 and the those

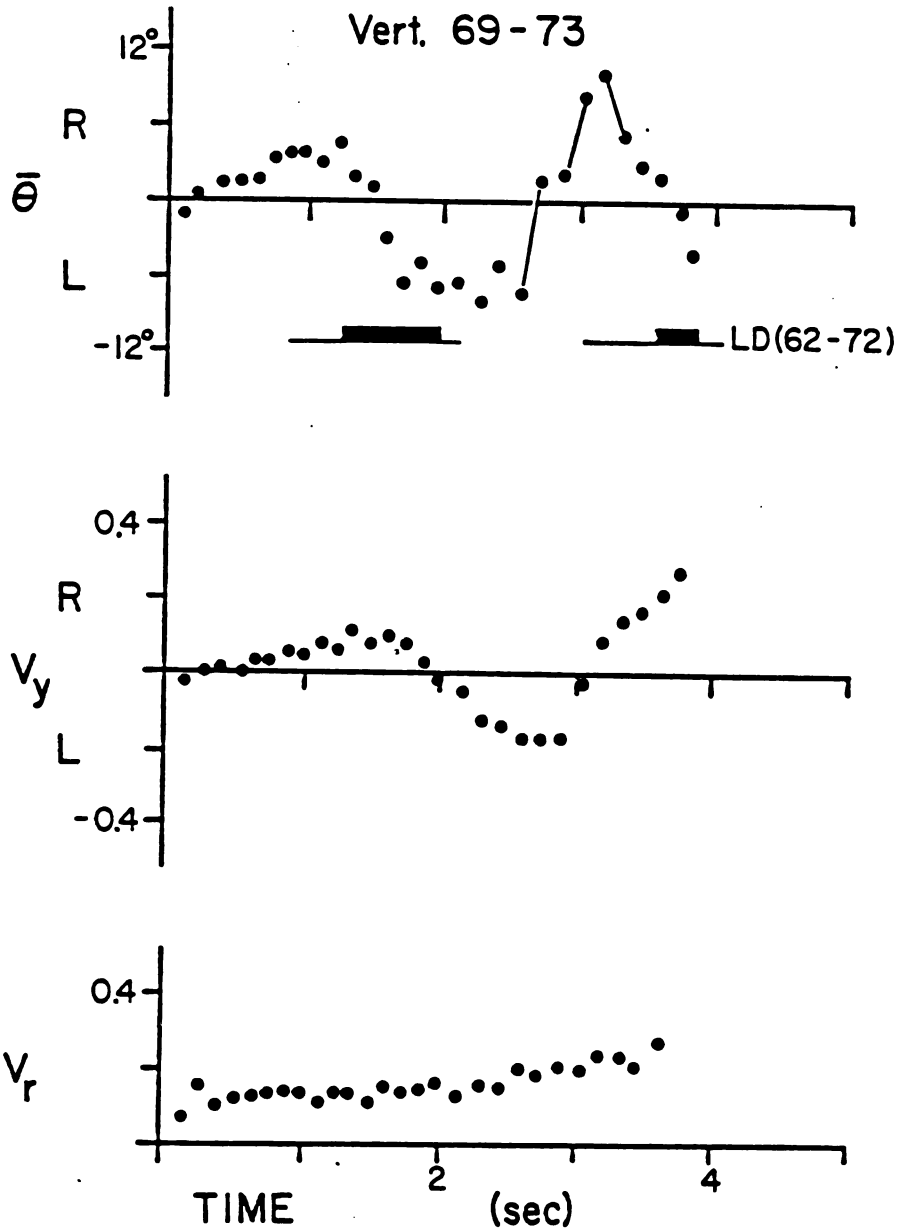

Figure 2.7. Emg and movement records from sequence 53.2 of Nerodia 35 performing terrestrial lateral undulation with 10 cm peg spacing. Notation is as in Figure 2.6.

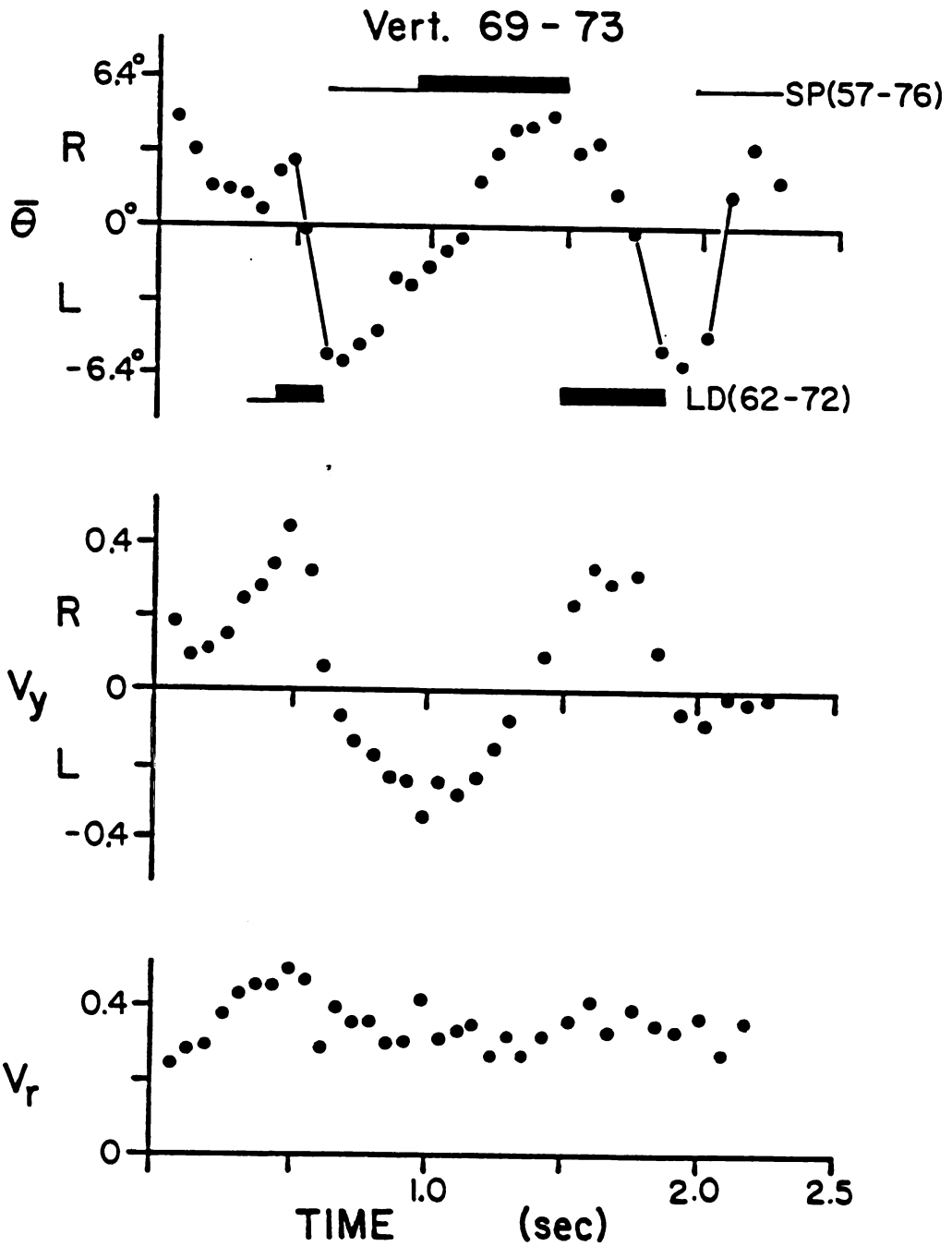

Figure 2.8. Emg and movement records from sequence 53.3 of Nerodia 35 performing terrestrial lateral undulation with 10 cm peg spacing. Notation is as in Figure 2.6.

of the left LD spanned vertebrae 66 to 72. Almost immediately after the cessation of right side activity, left side contraction began. The activity of both sides began with maximal convexity and ended when maximal concavity was reached on the side of the active muscle.

Figure 2.9 shows emg and movement records for almost three cycles of activity for the lateral undulation of Nerodia 36 moving through pegs spaced 7.5 cm apart. Mean V_x and CV of V_r for the entire sequence were .47 TL/sec and 34%, respectively. For the two periods between 0.13, 0.63 and 1.71 sec the values of mean V_x and CV of V_r were .63 TL/sec, 17% and .43 TL/sec, 21%, respectively. Hence, the snake was performing good lateral undulation although it decelerated significantly during this sequence. Activity of the SP, LD and IC of the same side was generally synchronous. Some overlap of strong activity of the left and right SP was evident from .66 to.82 sec and 1.69 to 1.84 sec. Left side activity almost immediately followed right side activity; however, there was a slight pause of major activity from the end of left side contraction near 1.05 sec until the start of right side activity near 1.67 sec. This momentary cessation of major activity occurred as this region of the snake remained nearly straight forming the crest of low amplitude long wavelength lateral flexion. Minor activity of the right IC correlated with this slight straightening of the snake's body. Major activity occurred as regions were maximally convex and continued until maximally concave.

Figure 2.10 illustrates emg and movement records for two sites in Elaphe 18 performing lateral undulation past pegs with 15 cm spacing. Near the middle of this sequence, the anterior portion of the snake began to turn left. For the more posterior site (vert. 169), which

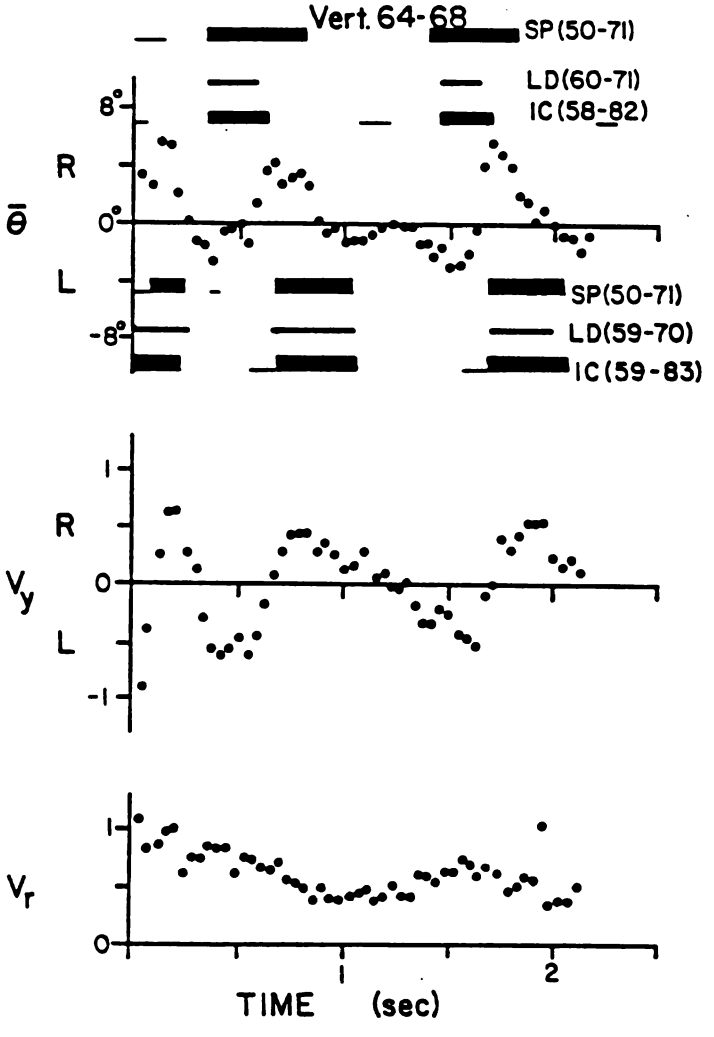

Figure 2.9. Emg and movement records from sequence 61.11 of Nerodia 36 performing terrestrial lateral undulation with 7.5 cm peg spacing. Notation is as in Figure 2.6.

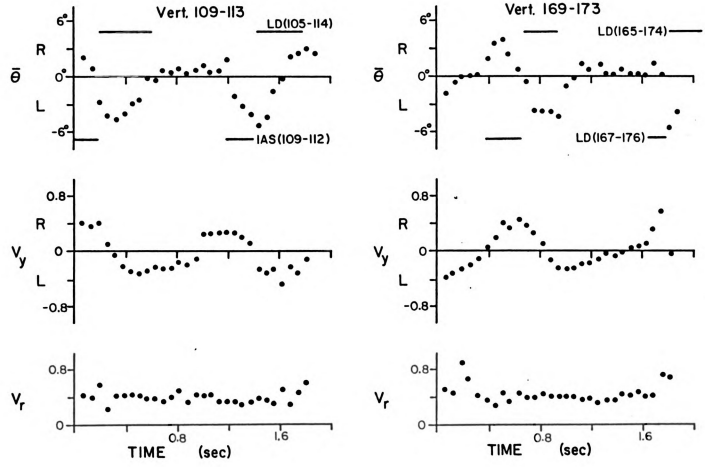

Figure 2.10. Emg and movement records from sequence 60.2 for two longitudinal sites of Elaphe 18 performing terrestrial lateral undulation with 15 cm peg spacing. Notation is as in Figure 2.6.

travelled a slightly straighter path, overall mean V_x and CV of V_r were .33 TL/sec and 29%, respectively. For the period from .19 to 1.00 sec and the half-period from 1.00 to 1.76 sec, values of mean V_x and CV of V_r were .27 TL/sec, 34% and .36 TL/sec, 23%. Two cycles of muscle activity were observed at each of these sites. For both sites, right side activity immediately followed left side activity, but no activity occurred for about .5 sec while these regions of the snake were nearly straight (Figure 2.10). Allowing for the complication of the momentary straightness of the vertebral column, all four of these muscles became active when the region was about maximally convex and activity ceased when the region was about maximally concave. For the first cycle of activity of both sites, the transition from left to right side activity did slightly precede maximal concavity to the left side. However, when comparing activity between the two sites, transitions of left to right muscle activity occurred at comparable postions on the graph of $\bar{\theta}$ vs time. In other words, the lag time was the same for muscle activity and the mechanical response of lateral flexion, as these two events travelled posteriorly along the snake.

To summarize, the mechanism of terrestrial lateral undulation past a limited number of pegs involved alternating, descending, unilateral muscle contractions. These contractions were correlated with a change in lateral flexion of the vertebrae towards the side of the active muscle. Muscles began activity on a side that was maximally convex and ceased activity when the region of the muscle contractile tissue was maximally concave to the same side. When snakes moved without occasional straightenings of the body, the transition of activity to the opposite side was usually immediate.

Aquatic Lateral Undulation

Aspects of the swimming of snakes have been discussed in detail elsewhere (Gray, 1953; Hertel, 1966; Jayne, 1985). When intrepreting the electromyographic results of snake swimming, the following relevant points from these studies are helpful to remember. Snakes swim by propagating waves of lateral flexion posteriorly along the body. The amplitude, wavelength and speed of these waves increases from anterior to posterior along the snake. During swimming, the speed of the waves travelling along most of the body is greater than the forward speed of the snake through the water and this is unlike terrestrial lateral undulation where the snake's forward speed is equal to the wave speed.

The snakes used in this study usually swim along the surface of the water at a slight angle to its surface with the head often being held entirely out of the water while the more posterior portions of the snake remain completely submerged (Jayne, 1985). I will refer to this posture as normal surface swimming.

To document the nature of wave propagation during the swimming of snakes, electrodes were usually implanted in at least three longitunal positions along the body of the snake. Table 2.2 lists the locations of the electrodes as confirmed after their dissection out of the contractile tissue. For the sake of brevity these sites will be referred to by their site number (Table 2.2) for which numbering proceeded from anterior to posterior.

Figure 2.11 shows $\bar{\theta}$, V_y and V_r for left side segments of SSP-SP, SP and LD near midbody of Nerodia 34 and $\bar{\theta}$ for left side segments of LD at additional sites near 2/5 and 4/5 of the body length. NF34 was the

Table 2.2. Location of electrodes used in swimming snakes. Location of each site is given as vertebral number (v) and distance from the snout of the snake.

Snake	Site 1	Site 2	Site 3	Site 4
NF34	46v 25cm	70v 39cm	94v 53cm	
NF38	29v 12cm	64v 28cm		
NF39	30v 11cm	64v 24cm	97v 39cm	
E020	76v 29cm	116v 45cm	153v 60cm	192v 74cm
E019	65v 32cm	119v 59cm	165v 86cm	

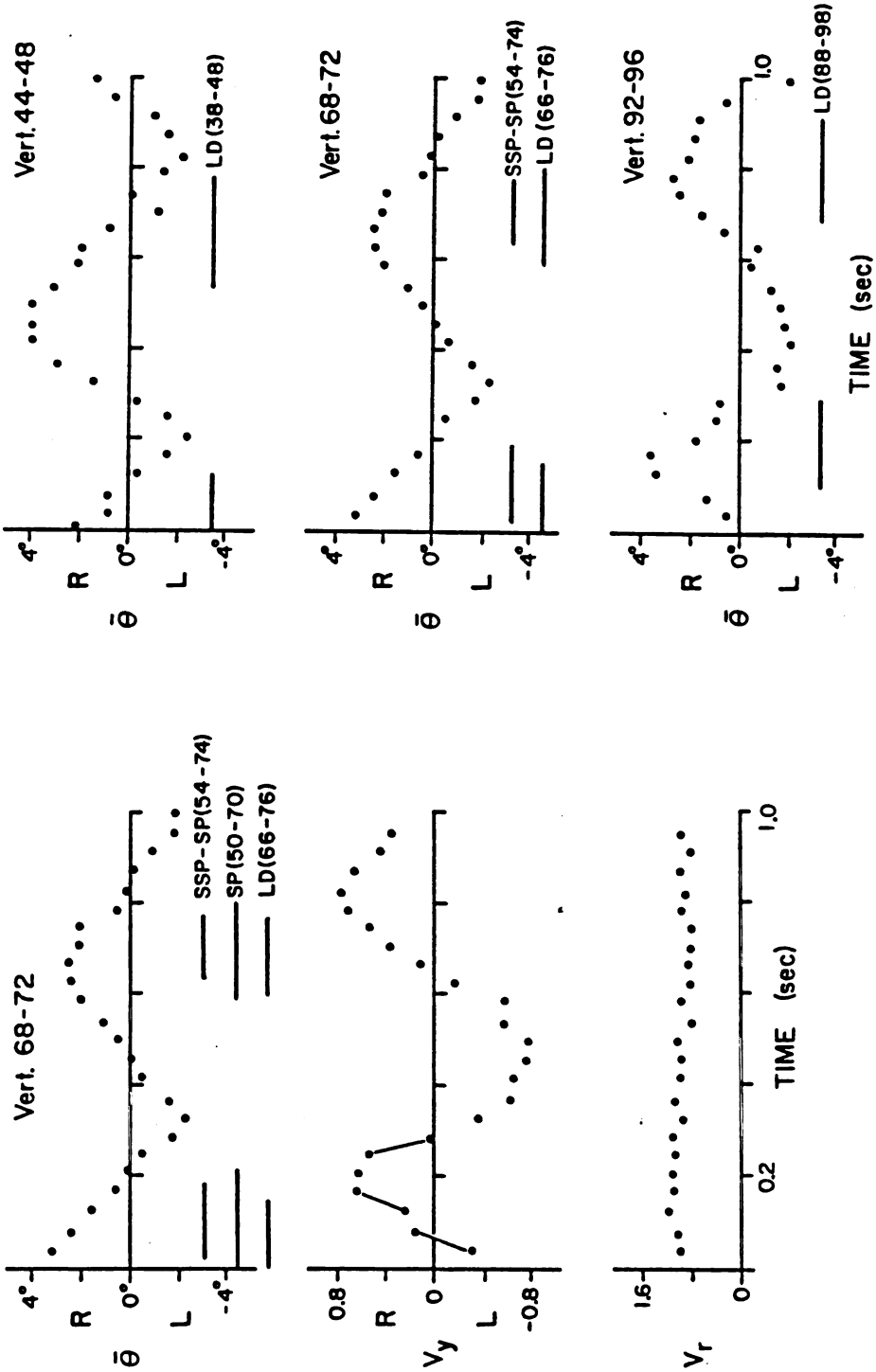

Figure 2.11. Emg and movement records from sequence 47.2 of Nerodia 34 performing aquatic lateral undulation at the surface of the water. At left, $\bar{\theta}$, V_y, and V_r for the site near mid-body. At right, $\bar{\theta}$ for three different longitudinal sites. Notation is as in Figure 2.6.

largest Nerodia used for the observations of swimming, and this snake performed normal surface swimming for the entire sequence. For site 2, mean V_x was 0.81 TL/sec and CV of V_r was 13.6% from 0 to 1.0 sec. For the two half periods between 0.21, 0.50 and .83 sec mean V_x was 0.85 and 0.67 TL/sec, respectively. The left side site 1 LD initiated activity when its region was convex to the left and activity ceased as the region became concave to the left. The site 2 muscles on the left side began contraction nearly when the region was maximally convex to the left and ceased firing about when the region was straight. The left side site 3 LD began contraction almost when the region was straight, continued while the region was convex to the left, and ceased just before the region became straight again. At all three sites the duration of the emg burst was slightly less than the interval between bursts. For example, the second contraction of the site 2 LD lasted .22 sec compared to the .37 sec of inactivity that preceded it. The plots of $\bar{\theta}$ versus time for the three positions along the snake illustrate the travelling of the emg and mechanical waves from anterior to posterior within the body of the snake.

Figure 2.12 diagrams emg's and movement of Nerodia 34 swimming below the surface of the water throughout the sequence. In this interesting trial, the entire length of the snake was submerged with the head deepest below the surface while about the most posterior 20 cm of the snake were close enough to the surface to cause ripples in the water. For site 2 between .23, .84 and 1.5 sec, two cycles of movement occurred with values for mean V_x and CV of V_r .64 TL/sec, 12% and .56 TL/sec, 7%, respectively. Within each of the three sites, the relation of the emg to $\bar{\theta}$ remained about constant through time. The site 1 LD from the left

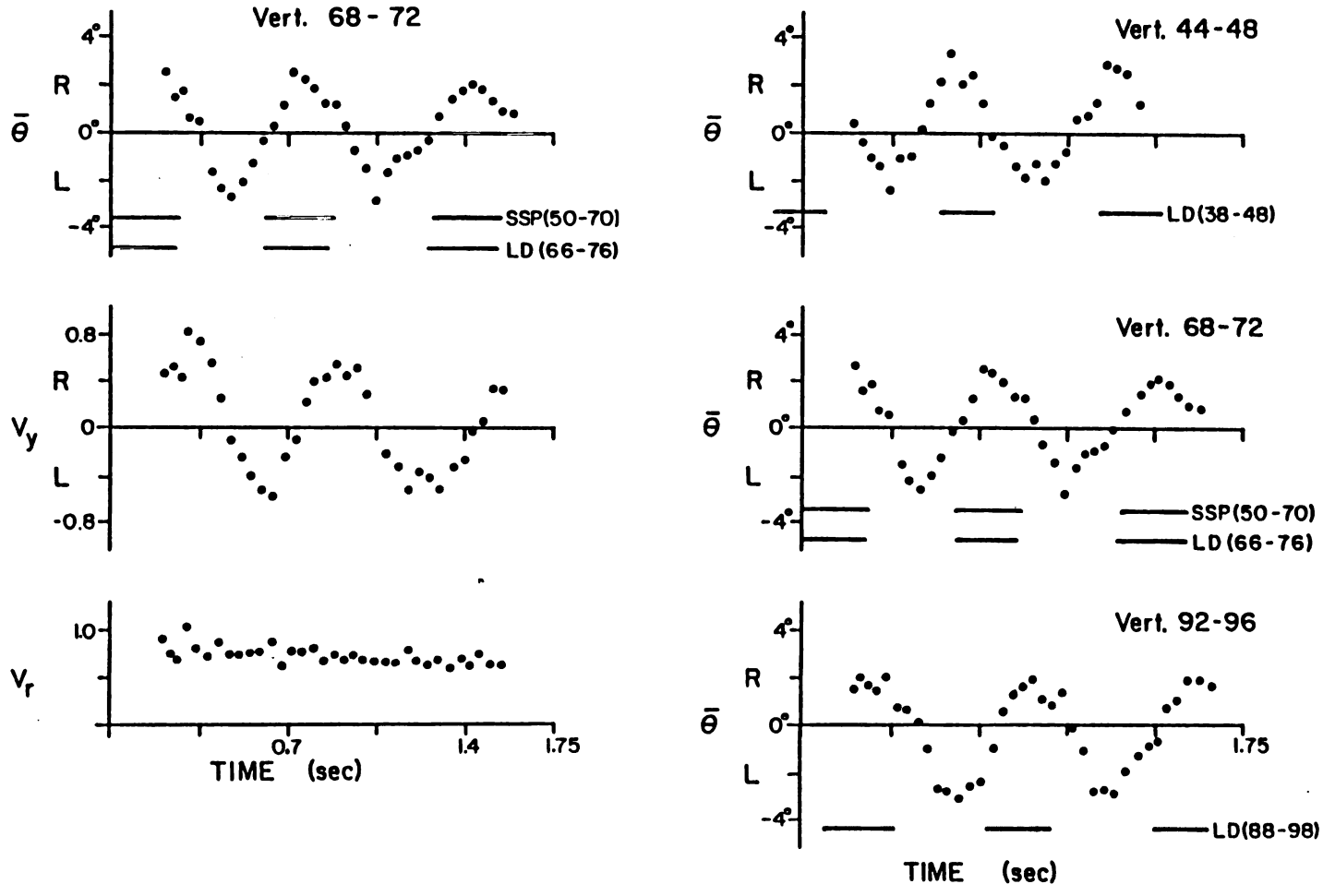

Figure 2.12. Emg and movement records from sequence 47.16 of Nerodia 34 performing aquatic lateral undulation below the surface of the water. At left, $\bar{\theta}$, V_y, and V_r for the site near mid-body. At right, $\bar{\theta}$ for three different longitudinal sites. Notation is as in Figure 2.6.

side began activity about when the region was maximally convex to the left and ceased before the region became maximally concave to the left. The muscles of sites 2 and 3 were mainly active when these regions were convex to the left. Table 2.3 lists some values of the maximal lateral flexion attained at each of these three sites of Nerodia 34. For this snake, lateral flexion between adjacent vertebra was usually less than 3° and there was no regular pattern of variation among the values of $\bar{\theta}$ at the three sites despite the different phase relationship between emg and $\bar{\theta}$ at each of the sites..

Figure 2.13 illustrates the movement and emg's for the left and right sides at two sites of Nerodia 38 swimming at the water's surface. At site 2, two complete cycles of movement occurred between .04, .58 and 1.12 sec. For these two periods, the values for mean V_x and CV of V_r were .69 TL/sec, 17% and .65 TL/sec, 24%, respectively. Muscle activity at both sites was always unilateral. For the earlier contractions, there was a slight delay in the transitions from left to right side activity. For example at site 1 the left LD stopped activity at .14 sec, the right SSP-SP was active from .17 to .51 sec, and then the left LD resumed activity at .84 sec. After this point in time, the transition of activity between sides was immediate. The emg's of sites 1 (vert. 29) and 2 (vert. 64) were almost exactly 180° out of phase, implying that 35 adjacent muscle segments were active simultaneously in this region of the snake.

Figure 2.14 illustrates the movements and emg's of Nerodia 39 swimming rapidly on the surface of the water. The body of this snake displayed typical waveform for a Nerodia of this size, but its tail was nearly touching the bottom of the pool even though its head remained out

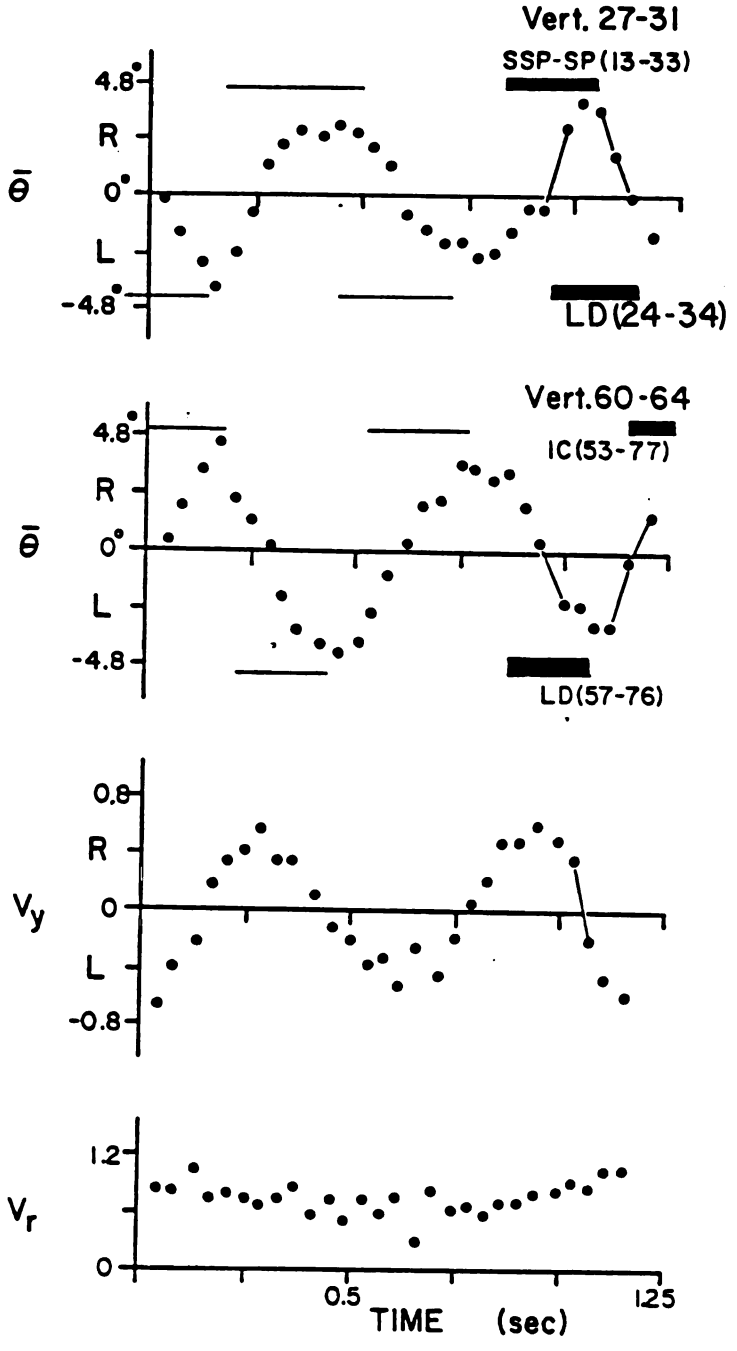

Figure 2.13. Emg and movement records from sequence 64.16 of Nerodia 38 performing surface aquatic lateral undulation. $\bar{\theta}$, V_y, and V_r are shown for a site near mid-body, and at top, $\bar{\theta}$ is also shown for a more anterior site. Notation is as in Figure 2.6.

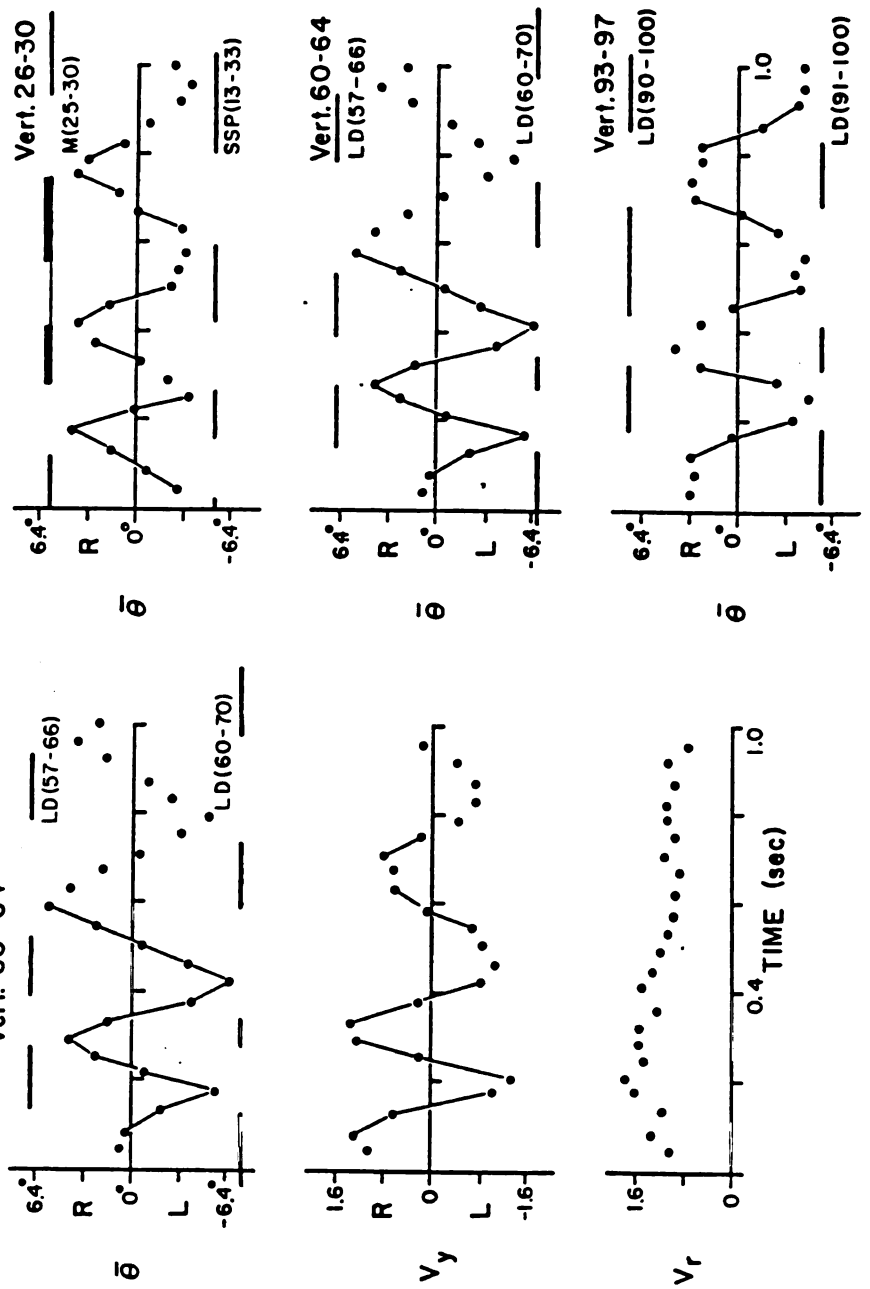

Figure 2.14. Emg and movement records from sequence 65.7 of Nerodia 39 performing aquatic lateral undulation at the surface of the water. At left, $\bar{\theta}$, V_y, and V_r for the site near mid-body. At right, $\bar{\theta}$ for three different longitudinal sites. Notation is as in Figure 2.6.

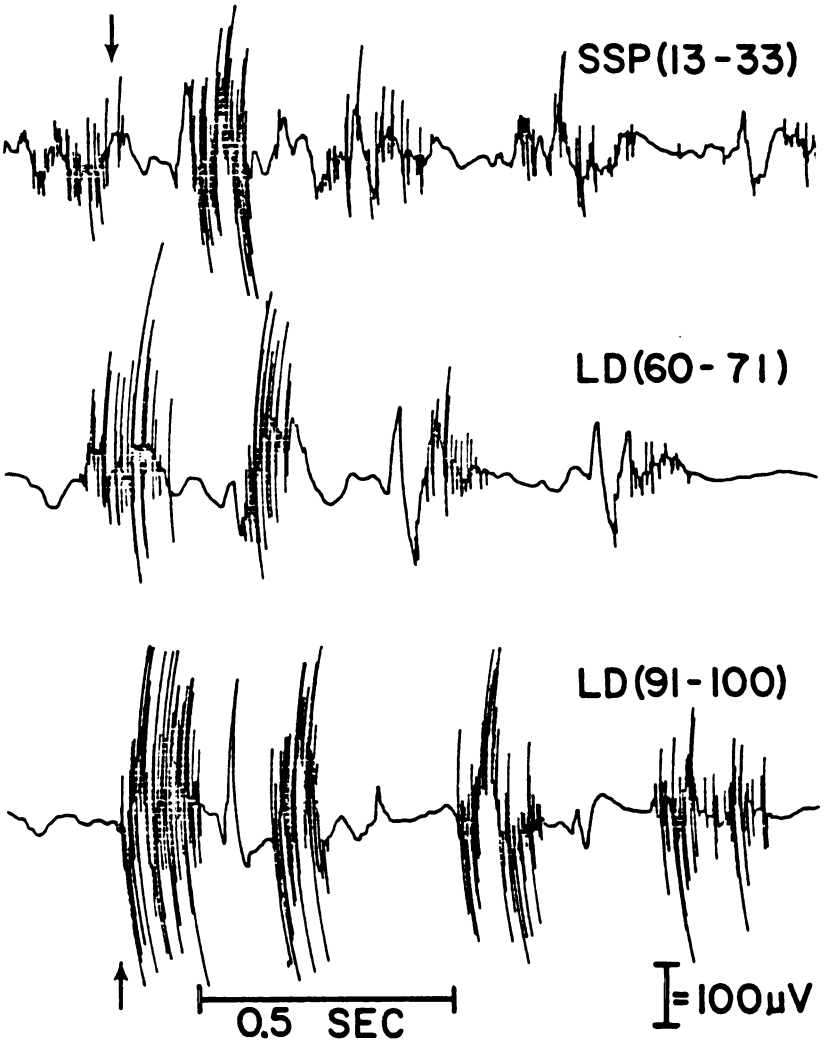

Figure 2.15. Sample emg's from the left side of Nerodia 39 swimming during sequence 65.7. Horizontal and vertical lines indicate time and voltage scales, respectively. Arrows indicate time = 0 for Figure 2.14. Note the decrease in emg amplitude.

of water. The length of the convoluted snake and depth of water were used to estimate an angle of the snake below the water's surface of 18° which was large compared to a more typical values of 5° for this quantity (Jayne, 1985). In all other respects, the swimming of this snake appeared quite normal, and, happily, this particular snake showed a propensity for swimming in a straight path which allowed several cycles to be observed. The snake was performing good lateral undulation as indicated by a value for CV of V_r of 22% for .08 to .92 sec. However, the snake did decelerate from .13 to .79 sec as indicated by the mean values of V_x for the four half-periods during this interval (1.16, .90, .87 and .74 TL/sec, respectively). The emg's were primarily unilateral with the only exception being the weak activity of the right M segment at site 1. The change of the emg relative to $\bar{\theta}$ along the body of the snake was similar to that of other Nerodia.

Figure 2.15 illustrates sample emg's from the left side of sites 1 - 3 in NF39. A consistent decrease in amplitude and increase in the duration of emg bursts was seen as time increased. During the early portion of this sequence, the duration of the emg almost exactly equaled the duration of inactivity. As the snake decelerated, the duration of inactivity exceeded the duration of the emg.

Another interesting aspect of sequence 65.7 was a consistent difference in the maximal lateral vertebral flexion among the different sites (Table 2.3). For a given wave travelling posteriorly along the body the flexion at site 2 exceeded that of sites 1 and 3, with only one exception (Table 2.3). The greatest flexions observed at sites 1 through 3 were 4.2°, 6.4° and 4.8°, respectively.

Figure 2.16 illustrates the movements and muscle activity of the

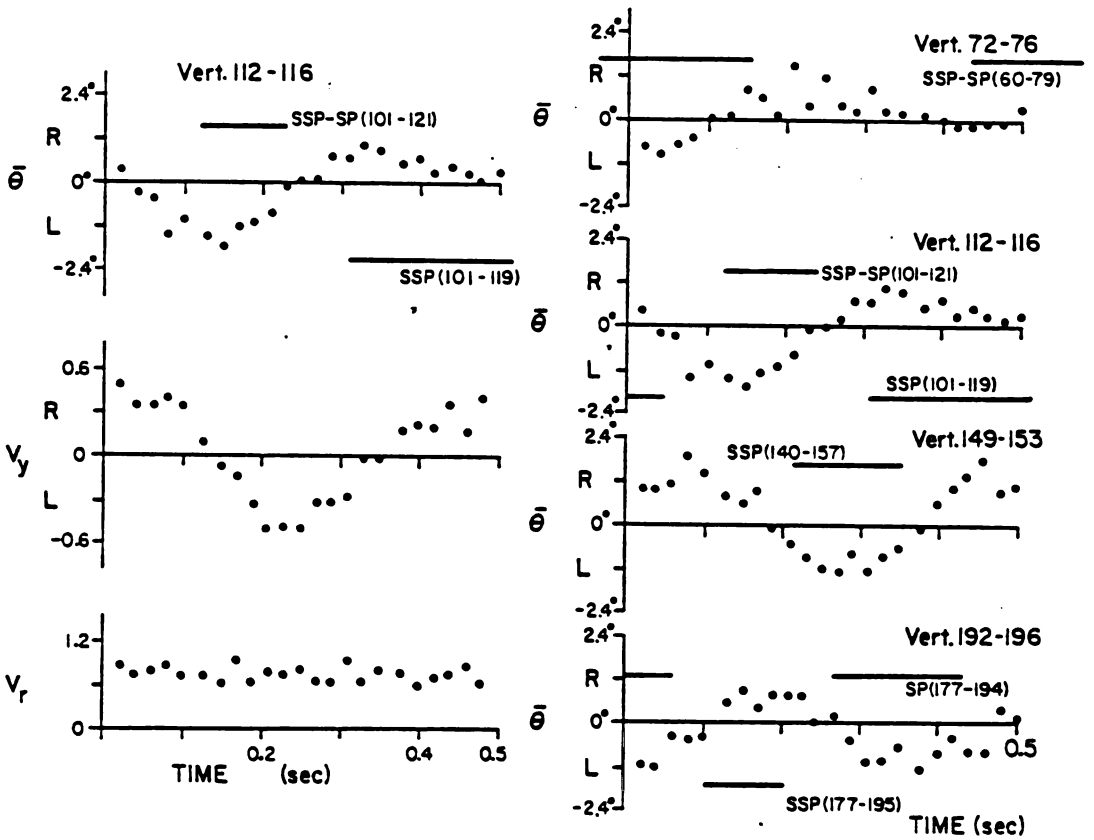

Figure 2.16. Emg and movement records from sequence 64.5 of Elaphe 20 performing aquatic lateral undulation at the surface of the water. At left, $\bar{\theta}$, V_y, and V_r for the site near mid-body. At right, $\bar{\theta}$ for four different longitudinal sites. Notation is as in Figure 2.6.

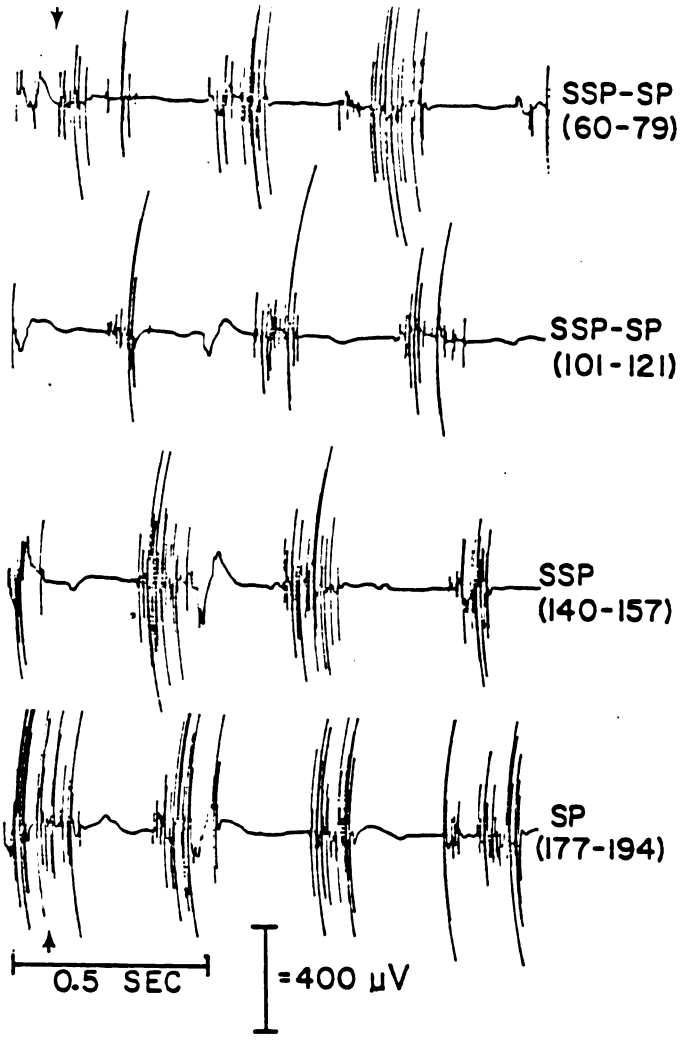

Figure 2.17. Sample emg's from the right side of Elaphe 20 during sequence 64.5 of swimming. The arrows indicate time zero used for Figure 2.16. The horizontal and vertical lines indicate the time and voltage scales, respectively. Sites 1 - 4 were 29, 45, 60 and 70 cm from the snout of the snake, respectively. Electrodes 1 - 4 were in contractile tissue near vertebrae 73, 116, 153 and 192, respectively.

smaller of the two Elaphe specimens that were filmed swimming. E020 used a normal posture relative to the surface of the water as it swam, but it seemed to use waves of bending with exceptionally small lateral displacement compared to that which I have seen for other Elaphe. However, this was consistently characteristic of the swimming of E020 rather than just a peculiarity of sequence 64.5. Two half periods of movement occurred between 0.4, .23 and .42 sec, and the snake maintained very uniform forward and overall speeds as indicated by site 2 values of mean V_x and CV of V_r of .63 TL/sec, 13% and .63 TL/sec, 14% for the two half-periods, respectively. Although the maximal values of lateral vertebral flexion were small compared to those of Nerodia (Table 2.3), Elaphe E020 and Nerodia showed similar relations between the emg's and $\bar{\theta}$. Anteriorly, muscles were active during the transition from convex to concave, and convex region activity predominated posteriorly . The emg's of each pair of adjacent sites overlapped substantially, indicating more than 40 adjacent muscle segments were active simultaneously. Figure 2.17 illustrates sample emg's from E020 during sequence 64.5 and clearly shows the phase lag that occurred as the emg's proceeded posteriorly.

Figure 2.18 diagrams the movements and emg's for the larger Elaphe (E019). This snake performed normal surface swimming with a mean V_x of .78 TL/sec and CV of V_r of 9% over the three half-periods occurring from .04 to .62 sec. Despite the difference in size and speed of snakes for the illustrated sequences of E019 and E020, the relation of the emg's to $\bar{\theta}$ along the length of the snakes was similar. In contrast to E020, the durations of the emg's of E019 were usually about equal to the durations of inactivity between successive emg's. In fact, there was even some

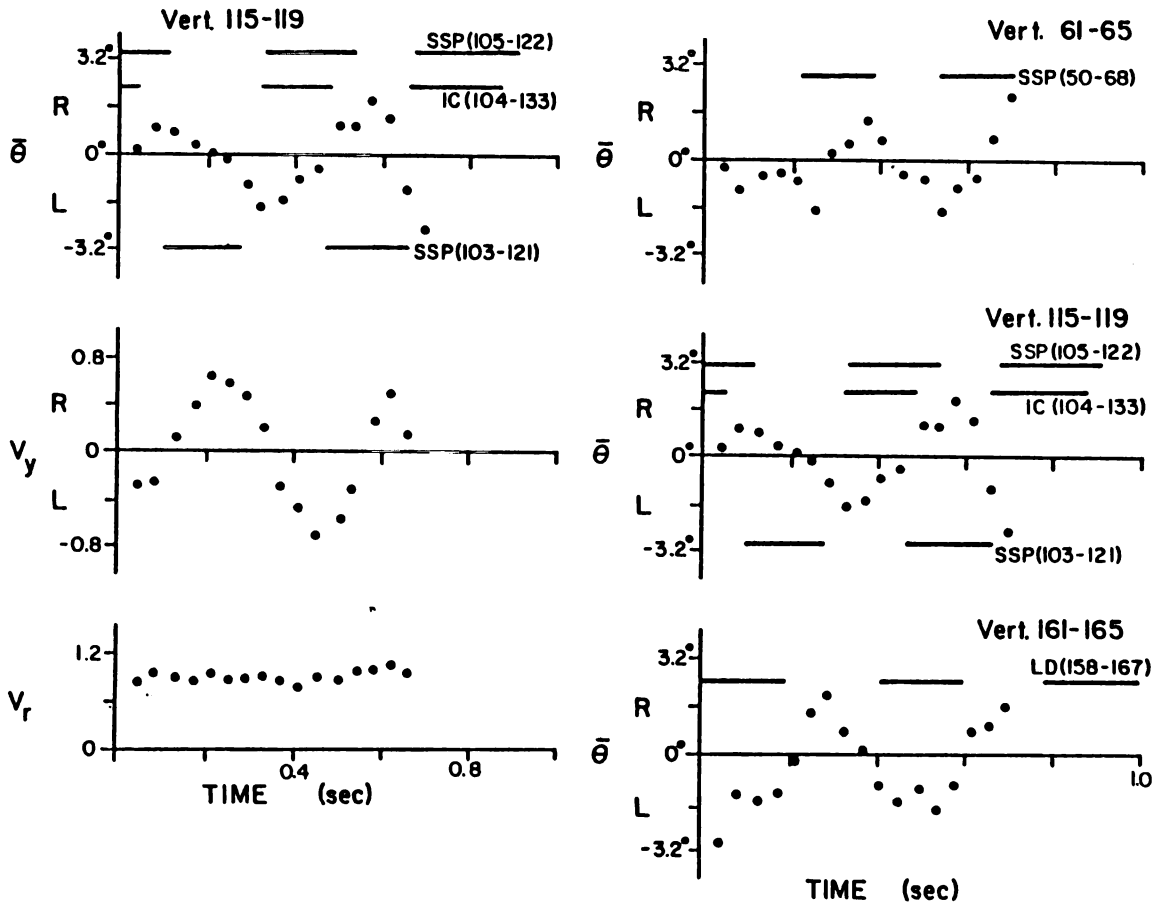

Figure 2.18. Emg and movement records from sequence 63.1 of Elaphe 19 performing aquatic lateral undulation at the surface of the water. At left, $\bar{\theta}$, V_y, and V_r for the site near mid-body. At right, $\bar{\theta}$ for three different longitudinal sites. Notation is as in Figure 2.6.

Table 2.3. Representative maxima and minima of $\bar{\theta}$ of swimming snakes. For each electrode site values in parentheses after each angle indicate the time in sec when this angle occurred during these illustrated sequences. Angles are listed so that reading a row form left to right enables one to follow a half wave through time as it travels posteriorly along the body of the snake.

Snake (Sequence)	Site 1	Site 2	Site 3	Site 4
NF34		2.5° (.20)	2.1° (.33)	
(47.16)	-2.4° (.33)	-2.7° (.46)	-3.1° (.63)	
	3.3° (.58)	2.4° (.84)	1.9° (.92)	
	-2.0° (.96)	-3.0° (1.04)	-3.0° (1.25)	
	2.8° (1.21)	1.9° (1.42)	1.9° (1.54)	
NF39	-4.0° (0)	-5.7° (.17)	-4.8° (.25)	
(65.7)	4.2° (.17)	4.0° (.29)	4.2° (.37)	
	-3.7° (.25)	-6.4° (.42)	-4.7° (.58)	
	3.7° (.42)	5.3° (.58)	3.1° (.75)	
	-3.3° (.58)	-5.2° (.79)	-4.5° (.96)	
E020			1.8° (.08)	0.9° (.15)
(64.5)	-1.0° (.04)	-1.7° (.15)	-1.4° (.29)	-1.3° (.38)
	1.5° (.21)	1.0° (.33)		
E019		0.9° (.08)	2.0° (.29)	
(63.1)	-1.7° (.25)	-1.5° (.37)	-1.9° (.54)	
	1.3° (.37)	1.9° (.58)		

Table 2.4. Average phase lag times (in sec) of emg's and $\bar{\theta}$. See text for complete explanation.

Snake (Sequence)	Site 1 - 2		Site 2 - 3		Site 3 - 4	
	emg	$\bar{\theta}$	emg	$\bar{\theta}$	emg	$\bar{\theta}$
NF34 (47.2)	.08	.16	.09	.10		
NF34 (47.16)	.09	.14	.13	.14		
NF38 (64.16)	.30	.30				
NF39 (65.7)	.15	.17	.06	.14		
EO20 (64.5)	.16	.16	.10	.14	.05	.08
EO19 (63.1)	.15	.20	.09	.15		

overlap in the activity of the left and right side muscles at site 2. Most of this overlap occurred during the latter portion of the right SSP and the early portion of the left SSP.

Common to the swimming of all snakes was the phase lag of muscular and mechanical waves as they moved posteriorly along the snakes. The periodicity of both the emg and mechanical waves allowed easy determination of the phase lag by measuring the time delay for an event to occur from anterior to posterior sites. As illustrated in Table 2.3, the maximal lateral vertebral flexion provided an event that could be followed through time. For each Nerodia the lag times of maximal, minimal and zero $\bar{\theta}$ were determined between adjacent sites. Because of the smaller $\bar{\theta}$ of Elaphe, only $\bar{\theta} = 0$ was used as an event to determine mechanical lag. Similarly the onsets of emg's were used to calculate emg phase lags. The resulting phase lags for each pair of adjacent sites were averaged for an entire sequence.

The average phase lags of emg's and mechanical events are listed in Table 2.4. For a given pair of sites within a single snake during a single sequence, the phase lag of the emg was always less than or equal to that of the mechanical event. In other words, the emg wave consistently travelled faster than the mechanical wave within the body of the snake. Furthermore, over equal lengths of snake, phase lags often decreased posteriorly (with the exception of sequence 47.16 of submerged swimming). Hence, the velocities of both the emg and mechanical waves usually increased posteriorly along the body of the snake.

In summary, snakes swam by using alternating, descending unilateral muscle contractions. Anteriorly, the muscles were active during the

transition from convex to concave on the side of the active muscle. However, this relation of emg to mechanical event changed posteriorly because the emg wave was travelling faster than the mechanical wave within the body of the snake.

Concertina Locomotion

Figure 2.19 shows emg and movement records of Nerodia 33 peforming concertina locomotion in an 8 cm wide tunnel. This sequence includes three complete cycles of activity between .33, 2.98, 4.82 and 7.10 sec and mean V_x of each of these periods was .06, .08 and .06 TL/sec, respectively. Static contact with the substrate was about .5 sec for each of these periods, causing an expectedly high CV value of V_r (90%) over .33 to 7.10 sec. As indicated by a comparison of V_y and V_r profiles, the lateral excursions of this region of the snake were usually slow. The pattern of motion of concertina locomotion (Chapter 1) can vary widely, and this sequence of Nerodia (Figure 2.19) amply illustrates this point. From the first to second time of static contact, vertebrae 70 to 74 of the snake were concave right, concave left and then straight. During the second period of motion, this region of the snake was straight, concave right, concave left and briefly concave right before remaining concave left. During the third cycle, these vertebrae changed from concave left to concave right. As one might expect from this variable movement record, the pattern of muscle activity was correspondingly variable within a cycle of motion. However, no major muscle activity was bilateral, whereas some weak bilateral activity did occur occasionally. Furthermore, most emg's correlated with lateral vertebral flexion toward the side of the contracting muscle. Muscle activity not correlated with these angular accelerations within the vertebral column occurred on the concave sides of the snake during static contact with the sides of the tunnel. For this sequence, right side muscle activity maintained contact with the

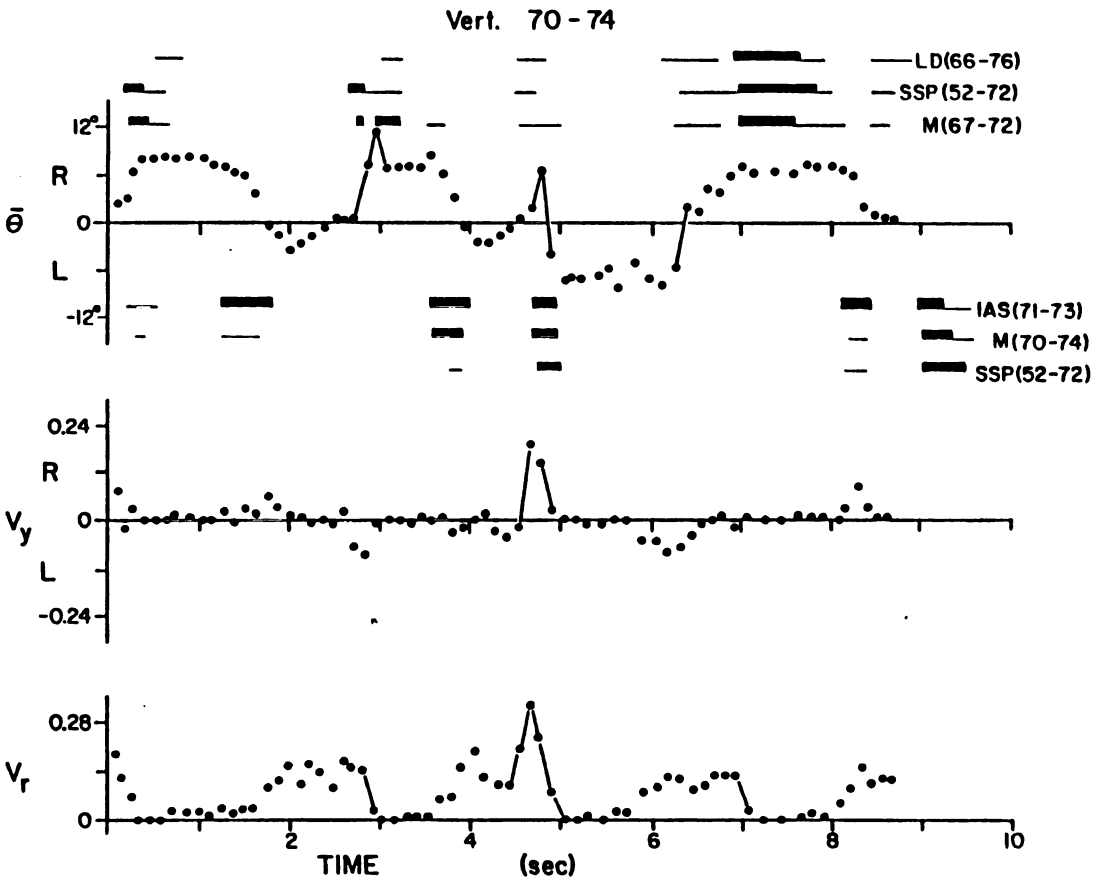

Figure 2.19. Emg and movement records from sequence 43.7 of Nerodia 33 performing concertina locomotion in an 8 cm wide tunnel. Notation is as in Figure 2.6.

sides of the tunnel during the 1st, 2nd and 4th times of static contact and left side activity occurred during the 3rd time of static contact (Figure 2.19).

Figures 2.20 and 2.21 illustrate emg and movement records for two sites of Elaphe 15 performing concertina locomotion in an 8 cm wide tunnel. For vertebra 133, means of V_x for the two periods occurring between .87, 3.40 and 5.83 sec were .04 and .06 TL/sec, respectively. The value for CV of V_r was 81% for the time interval containing these two cycles, and the durations of the three times of static contact with the substrate were about .5, .5 and .3 sec, respectively. The electrodes at sites 1 and 2 were in contractile tissue at the 110th and 130th vertebrae, respectively. For both of these sites, movement records are shown for three vertebral intervals within the span of the muscle segments from which emg's were recorded. As shown in Figure 2.3, the contractile tissue of a SSP-SP muscle segment spans only about five vertebrae beginning about two vertebrae anterior to the origin of fibers on the tendon of the M. multifidus. As shown in Figures 2.20 and 2.21, the most consistent mechanical correlate of emg's occurred in the region spanned by the contractile tissue portions of the muscle segments. In fact the vertebrae adjacent to the most anterior portion of the anterior tendon of the SSP-SP may undergo flexion opposite to the direction expected for left side muscle activity. In the region of contractile tissue of the muscle segment, activity may occur while the region remained convex (1st and 2nd emg's vert. 109 -113, Figure 2.20) or while the region remained concave (1st and 2nd emg's vert. 133 - 137, Figure 2.21). Comparing sites 1 and 2 revealed the time lag of the emg's as they proceeded posteriorly along the snake. The first and second emg's

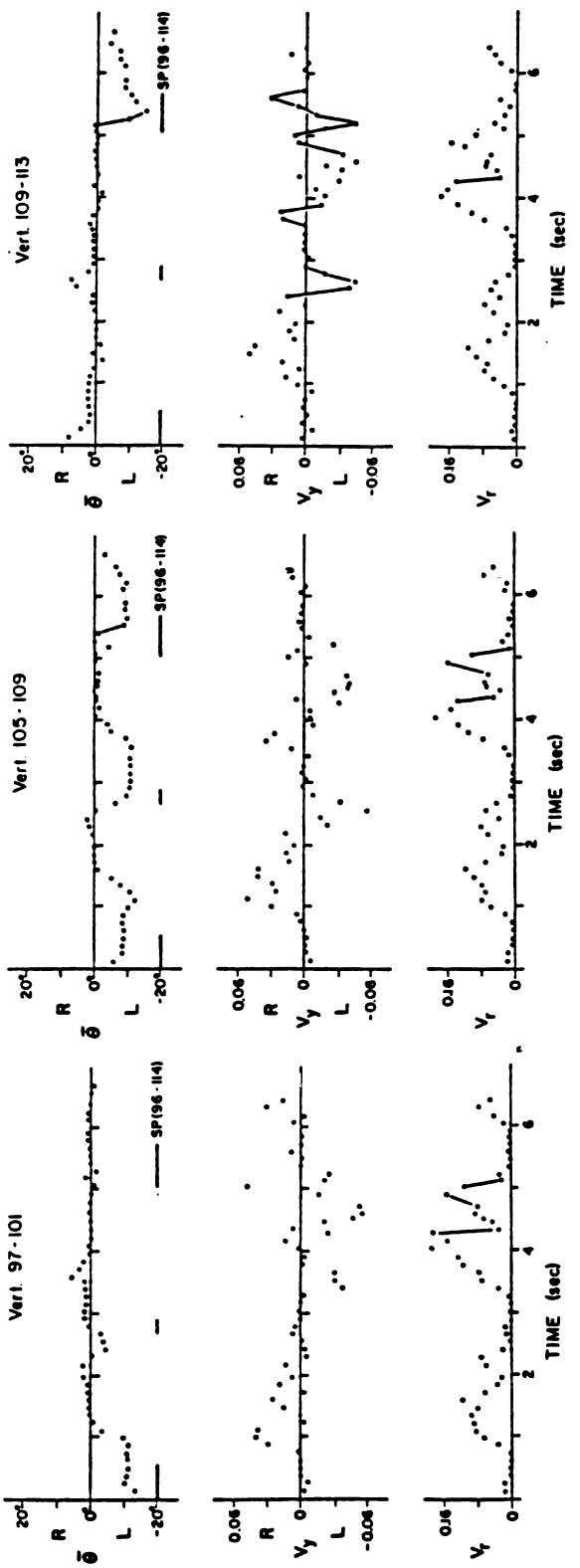

Figure 2.20. Emg and movement records for three body regions near site 1 of Elaphe 15 (sequence 43.4) performing concertina locomotion in an 8 cm wide tunnel. Notation is as in Figure 2.6.

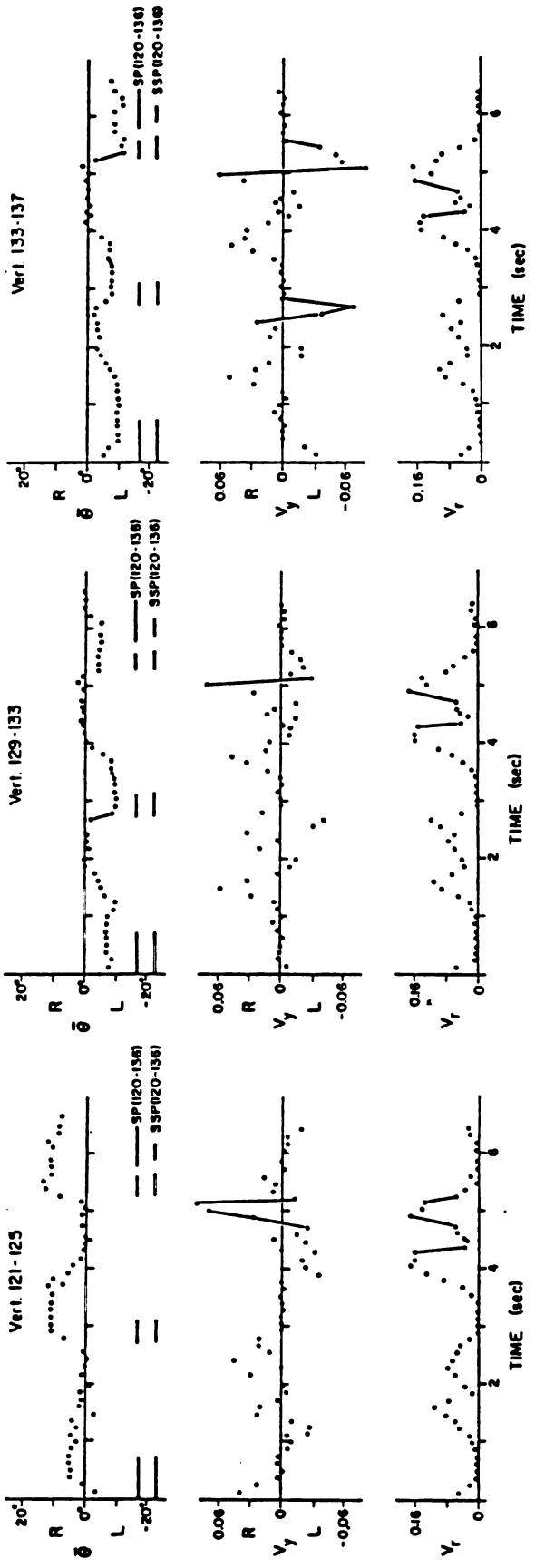

Figure 2.21. Emg and movement records for three body regions near site 2 of Elaphe 15 (sequence 43.4) performing concertina locomotion in an 8 cm wide tunnel. Notation is as in Figure 2.6.

of the SP from site 2 ceased .13 and .25 sec after those of the SP from site 1, respectively. The onset of activity for the third contraction of the SP from site 2 occurred .25 sec after that of the SP from site 1. After 1.8 sec, the activity of the muscles at site 2 differed somewhat from that of the SP at site 1, and this slightly complicates comparison of activity between the two sites. All three contractions of both sites initially correlated with lateral vertebral flexion to the left and did not end until after static contact was established. Because the record of movement was generated over .12 sec time intervals, the exact time lag of the mechanical events is difficult to discern; however, the constant relation between the emg's and $\bar{\theta}$ and initiation of static contact does suggest similarity of time lags between emg's and mechanical events. All three contractions of both sites also showed considerable overlap in time, implying more than twenty adjacent segments of the SP were contracting simultaneously during this sequence.

In summary, concertina locomotion in tunnels was performed by snakes using alternating, descending unilateral muscle contractions. Muscle activity could occur when a region is convex, concave or undergoing the transition from convex to concave. Emg's either were correlated with lateral vertebral flexion towards the side of activity or were associated with the maintainence of a concave posture during static contact with the sides of the tunnel.

Sidewinding

Snakes perform sidewinding locomotion in either a left or right-handed manner. The following features characterize left-handed sidewinding (Figure 1.1). For this variant, the anterior-most portion of the snake is usually flexed to the left. The right side of the snake pushes backwards against the substrate and often forms a windrow when the snake is on loose substrates such as sand. The plot of V_y versus time shows a pattern of right, left and right movement between times of static contact with the substrate (Chapter 1). The movements of right-handed sidewinding are mirror images of those of left-handed sidewinding.

Figure 2.22 illustrates the movement and emg records of Nerodia 36 performing slightly more than two cycles of right-handed sidewinding. For the two periods of sidewinding between .31, 1.50 and 3.31 sec the values of mean V_x and CV of V_r were .29 TL/sec, 57% and .25 TL/sec, 79%, respectively. Allowing for the error of digitizing, static contact with the substrate was about from 1.50 to 1.88 sec and from 3.13 to 3.31 sec. Figure 2.22 includes the activities of left and right segments of SP, LD and IC near midbody of the snake. Figure 2.23 illustrates sample emg's of these six muscles during the interval from .55 to 2.50 sec of the sequence illustrated in Figure 2.22.

For this sequence of Nerodia, most of the major activity correlated with lateral flexion of the vertebrae towards the side of the active muscles. The major activity of the IC was unilateral over the entire duration of the illustrated sequence (Figure 2.22). With the exception of overlap from .09 to .13 sec, the major activity of the LD segments

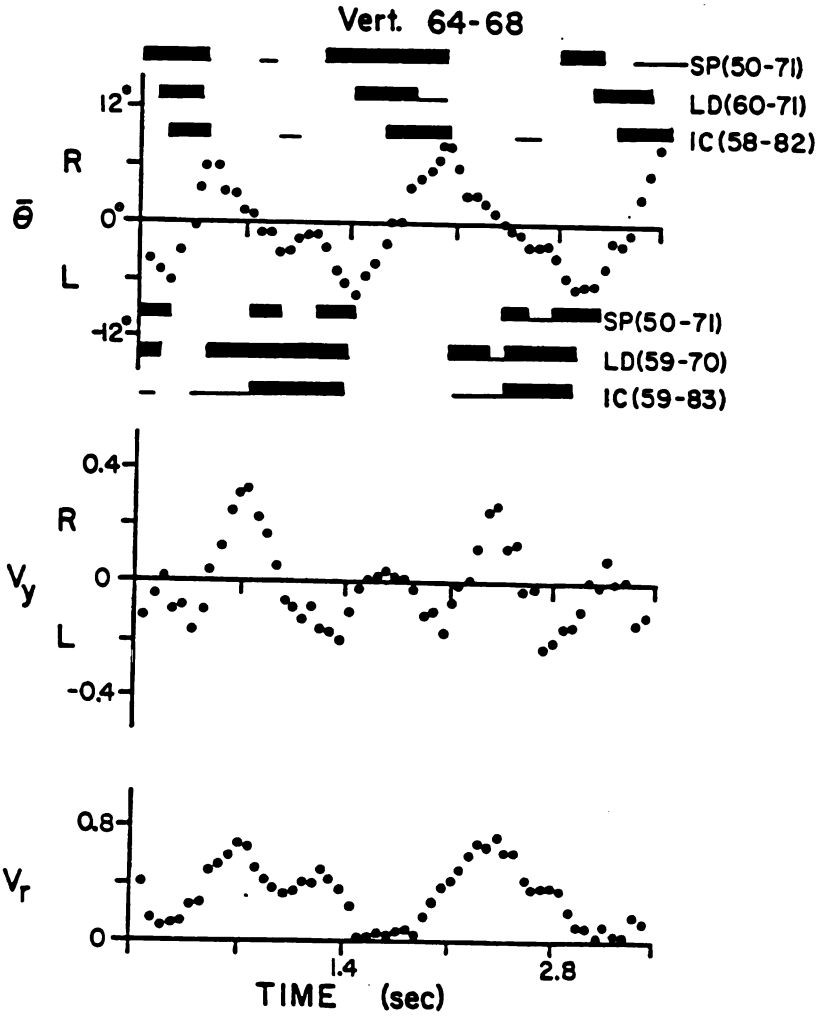

Figure 2.22. Emg and movement records from sequence 61.3 of Nerodia 36 performing right-handed sidewinding on a linoleum floor. Notation is as in Figure 2.6.

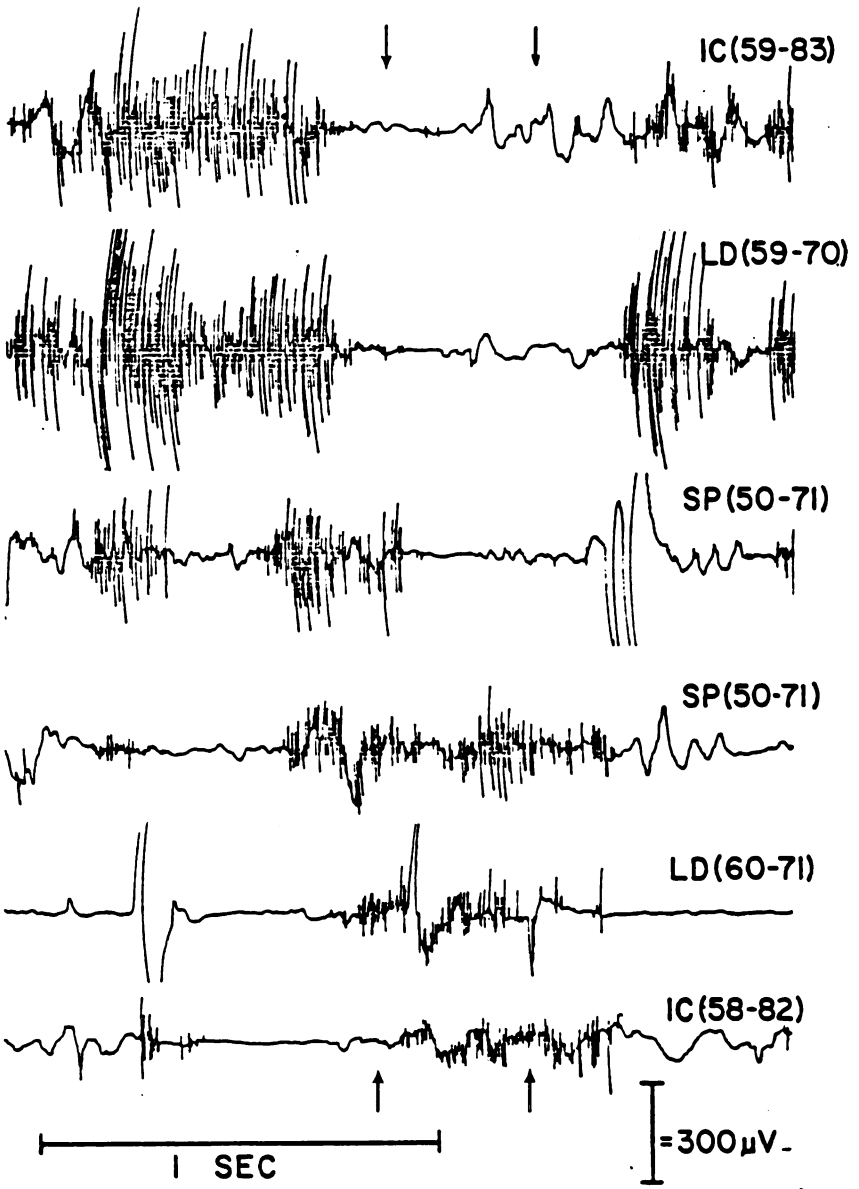

Figure 2.23. Sample emg's from 0.55 to 2.50 sec during sequence 61.3 (Figure 2.22) of Nerodia 36 sidewinding. The top three emg's are from the left side and the others are from the right side of the snake. Horizontal and vertical lines indicate time and voltage scales, respectively. The voltage scale = 400 uV for the right LD and IC. Arrows indicate beginning and end of static contact. Note weak early activity of the left IC and time of bilateral activity.

was also unilateral. Major activity of the right SP consistently began before that of the right LD and IC, and this time of activity overlapped with that of the left SP (Figures 2.22 and 2.23). To a lesser extent, major activity of the left SP and right LD also overlapped. Activity of the left LD and IC ceased slightly prior (about .1 sec) to static contact with the substrate, whereas the activity of the left SP ceased almost exactly at the intitiation of static contact with the substrate. The overlap of activity between the right SP and muscles of the left side occurred mainly before and slightly after initiation of static contact with the substrate. This suggests that bilateral contractions primarily elevated the region of the body posterior to the area of static contact. Some weak activity of the right SP and IC correlated with a slight straightening of the body about midway through the transition from concave right to concave left. To summarize simply, as a collective group the right side muscles were active before, during and after static contact, as the vertebrae flexed from maximally convex to maximally concave to the right. In contrast, the group of the left side muscles was primarily active between times of static contact, as the vertebrae flexed from maximally convex to maximally concave to the left.

Figure 2.24 illustrates emg and movement records of Crotalus 6 performing right-handed sidewinding on sand. Nearly two complete periods of movement are illustrated for this sequence. For the period from .31 to 1.54 sec, mean V_x and CV of V_r were .49 TL/sec and 78%, respectively. Strong activity of the right SP began just before static contact when the region was still convex to the right and continued until the region was maximally concave to the right, whereupon weaker activity continued until the region was almost straight. The major

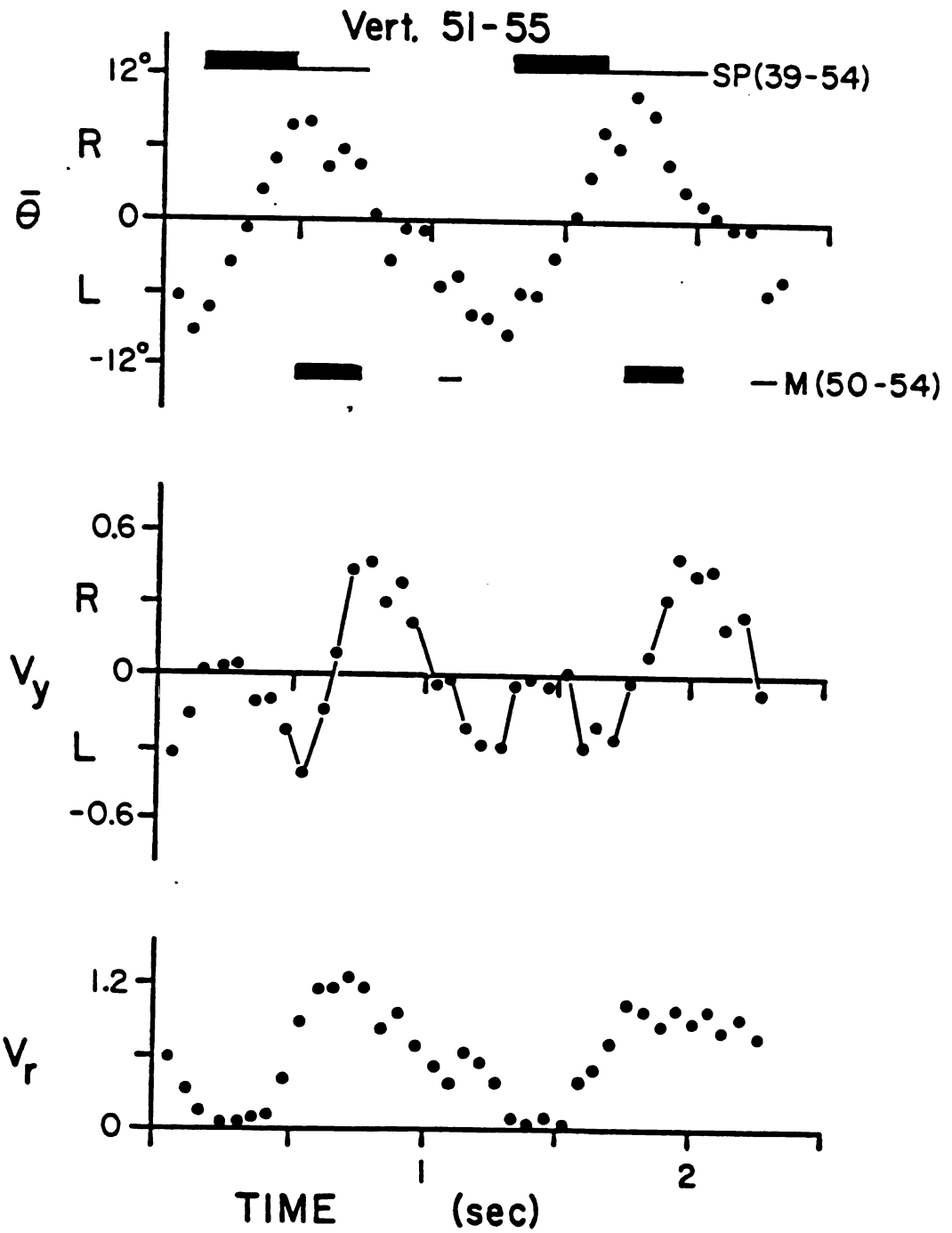

Figure 2.24. Emg and movement records from sequence 49.4 of Crotalus 6 performing right-handed sidewinding on sand. Notation is as in Figure 2.6.

activity of the left M began when the vertebrae were maximally convex to the left and continued until the vertebrae were almost straight. Some weak activity of the left M was evident just prior to static contact with the substrate.

Crotalus 6 also performed left-handed sidewinding, for which movement and emg records are illustrated in Figure 2.25. For vertebra 51, during the complete period of movement from .29 to 1.21 sec, values for mean V_x and CV of V_r were .67 TL/sec and 64%, respectively. Emg's were obtained from both the right SP and left M at vertebra 51 and from the left LD at vertebra 81. Both of the left muscles were active before during and after static contact as the vertebrae flexed from maximally convex to maximally concave to the left. The major activity of the right SP began well after static contact while the vertebrae were maximally convex to the right and ceased as this region became straight. Lesser activity of the right SP began almost exactly when static contact was intitiated and ceased slightly after static contact.

The phase lag between these two sites at vertebrae 51 and 81 (Figure 2.25) illustrates the posterior propagation of emg and mechanical events. Lag times between sites 1 and 2 for the first and second times of static contact were .43 and .42 sec, respectively. The overlap in activity of the left side muscles from the two sites suggests more than 30 adjacent muscle segments may be active simultaneously.

Crotalus 5 also performed left and right-handed sidewinding while moving on sand. The electrode site was at the 88th vertebra of this snake and muscles included the left and right SP and IC and the right LD. Activity of the left and right IC did not overlap during either left or right-handed sidewinding. The greatest overlap of major

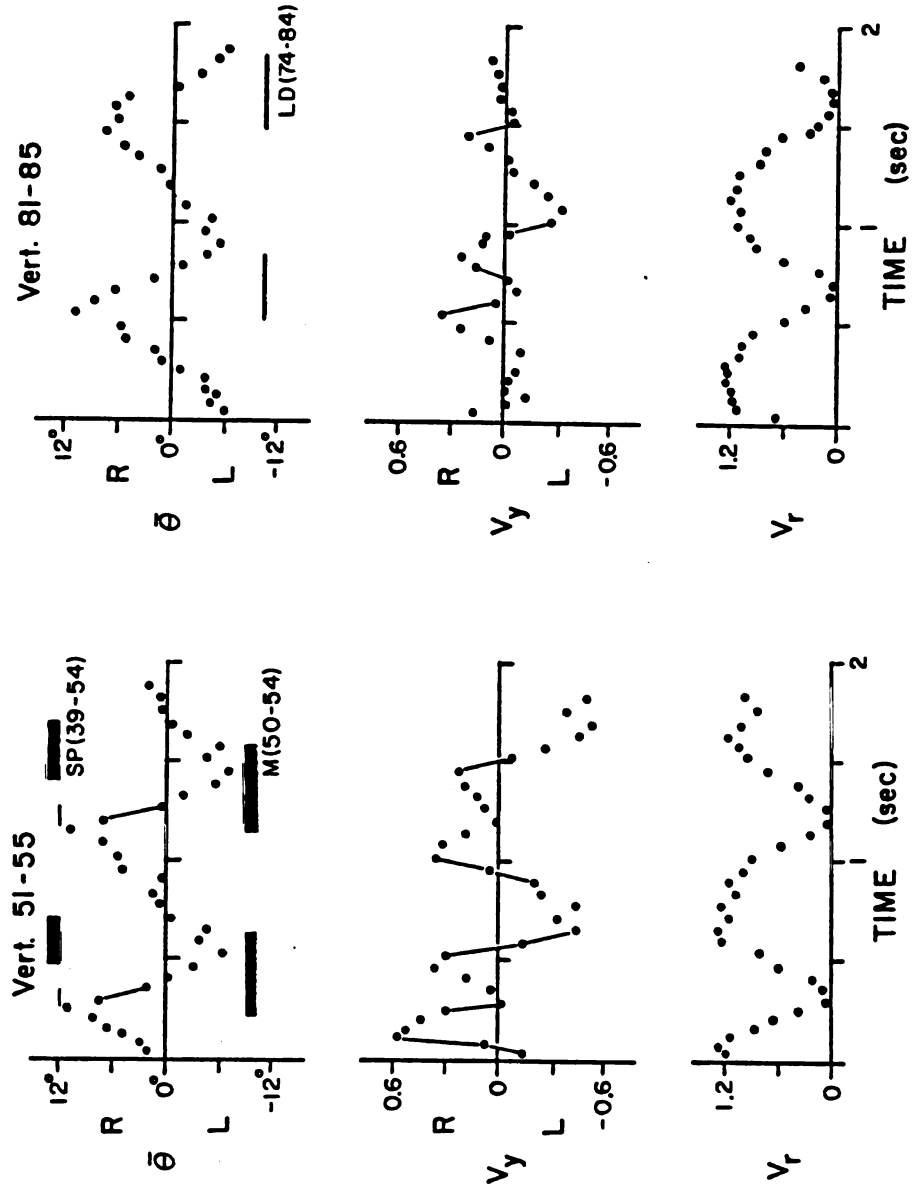

Figure 2.25. Emg and movement records for sequence 49.1 from two sites in Crotalus 6 performing left-handed sidewinding on sand. Notation is as in Figure 2.6.

activity occurred between the left and right SP during both left and right-handed sidewinding. This time of bilateral SP activity always began just after static contact when the vertebrae were being flexed and lifted away from the substrate. To a lesser extent, the LD could also be active during this time period of bilateral SP activity. Activity of the SP during the lifting phase occurred either as a continuation of SP activity (as seen in Figure 2.24) or as a distinct second contraction. As the vertebrae were being flexed to the right during right-handed sidewinding, the onset of activity of the right IC often lagged slightly behind that of the right SP and LD.

For the sidewinding of Crotalus muscles primarily had unilateral, descending contractions from maximal convexity to maximal concavity of the vertebrae, and bilateral activity occurred during the lifting phase. A postulated muscular mechanism of this mode will be discussed later.

DISCUSSION

Lateral Undulation

The only explicit predictions of a muscular mechanism of snake locomotion have been the models of lateral undulation proposed by Gray and Lissmann (1950) and Gray (1953). Gray and Lissmann (1950) used two experimental chambers to quantify forces involved in lateral undulation. In one set of experiments, snakes crawled through a channel with a series of right angle bends (Figure 2.26A). The movable sides of these channels allowed the determination of the normal forces applied against them. In order to progress, a snake must overcome the frictional forces resisting its forward movement. Snakes should overcome these resistive forces by pushing against the sides of the channel, generating reactive normal forces whose sum is sufficient to overcome frictional resistance. Gray and Lissmann found that the sum of these experimentally measured normal forces did indeed agree closely with the measured frictional resistance. Another important finding in this study was that forces were applied only to the sides of the channel labelled B, D and F in Figure 2.26A. Gray and Lissmann then examined the changing curvature of a snake within such a channel. As a region of the snake was flexed from straight to concave, the anterior-posterior length must decrease for the more lateral portions of the body forming this concavity (eg. see segments 15 1 to 13 1 in Figure 2.26A). Hence, Gray and Lissmann reasoned that muscles should be active in regions of the body where

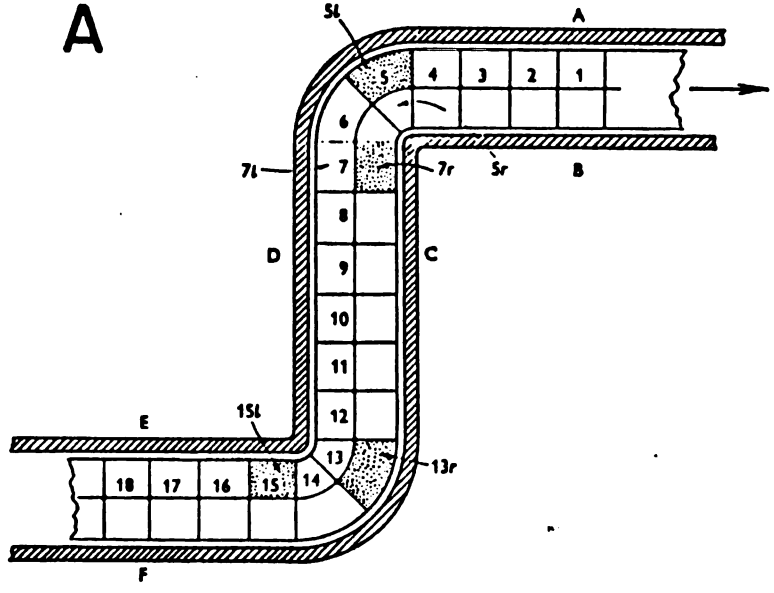

Fig. 8. (i) Diagram showing changes in length of the muscles when a snake is gliding past rectangular bends. *On entering a bend* the muscles on the inner side of the curve shorten whilst those on the outer side are stretched, e.g. the muscles of the right side shorten when a segment moves from position 7 to position 6; also, those of the left side when moving from position 15 to 14. The muscles of the left side are stretched when moving from position 7 to 6, and those of the right side on moving from position 15 to 14. *On leaving a bend* the muscles of the outer side of the bend shorten (5*l* and 13*r*), whilst those of the inner side (5*r* and 13*l*) are stretched.

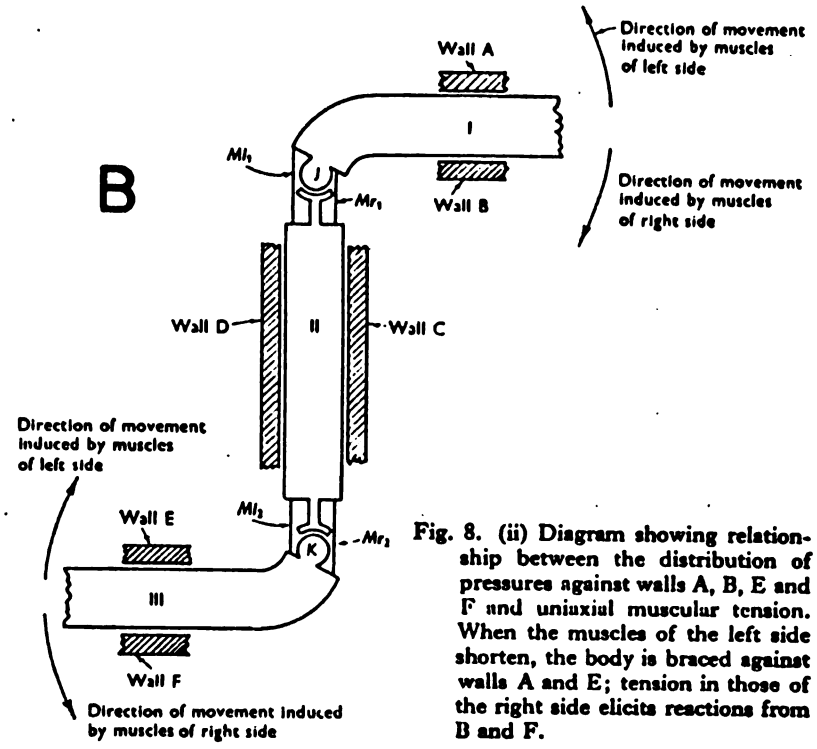

Fig. 8. (ii) Diagram showing relationship between the distribution of pressures against walls A, B, E and F and uniaxial muscular tension. When the muscles of the left side shorten, the body is braced against walls A and E; tension in those of the right side elicits reactions from B and F.

Figure 2.26. From Gray and Lissmann (1950). A. Figure 8(i) indicates changing lengths of muscles with shaded regions showing segments about to become shorter. B. Figure 8(ii) shows Gray and Lissmann's assumptions about sections of snakes functioning as lever arms.

shortening occurs. Gray and Lissmann then considered the lengths of snake between bends of a channel as lever arms, and they envisioned the muscles as contractile elements joining two such lever arms (Figure 2.26B). Thus, muscles should act on the vertebrae to produce a bending moment equal but opposite to the experimentally determined normal forces. Therefore, for the portion of the snake shown in Figure 2.26, right side muscle contraction would produce a pattern of forces consistent with that which was experimentally determined.

Using this reasoning, Gray and Lismann predicted the pattern of muscular effort shown in Figure 2.27 of a snake performining lateral undulation though a channel with several rectangular bends. A key feature of this prediction is that the muscular effort at a particular point in the channel remains constant. For example, for the region of the snake passing the second bend in the channel (between sections B and C), there is always a right side contraction. After the first point in time (shown as Figure 1), the more anterior muscle contractions are initiated when the body is straight, continue through the time of maximal concavity, and finally cease after the body is again straight. With the exception of the first bend (labelled E, F) in the channel shown in Figure 2.27, the straight portions of the channel are of equal lengths. Although the anterior regions of contracting muscle are of equal lengths, the most posterior region of muscle activity on the snake is longer than the other active regions (Figure 2.27). Furthermore, this most posterior block of muscles undergoes contractions beginning (posteriorly) when the body is straight, continuing through the time when the body is convex on the side of the active muscles, and continuing through a time of concavity not ceasing activity until the

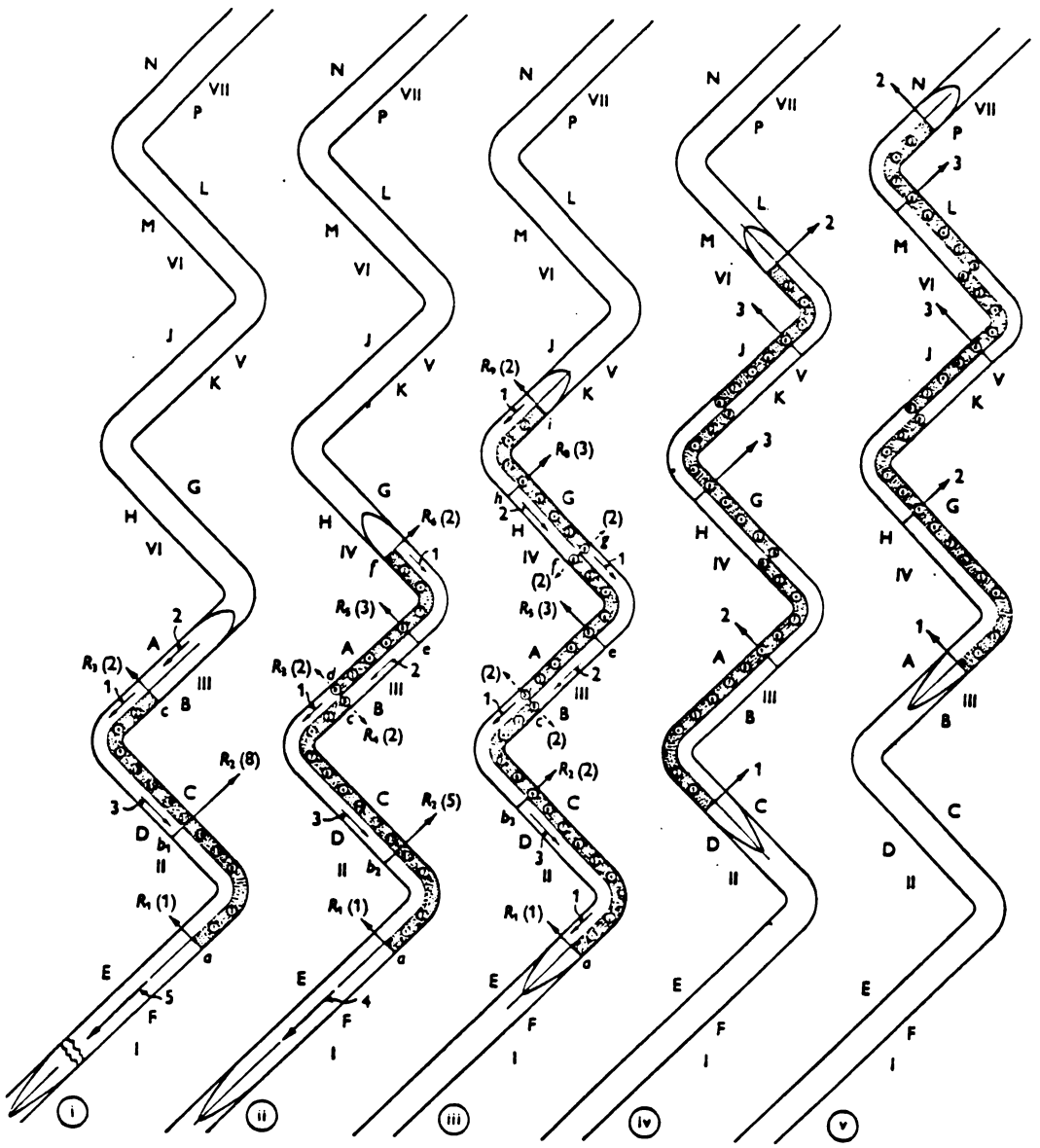

Figure 2.27. Figure 9 from Gray and Lissmann's (1950) model of the muscular mechanism of a snake performing lateral undulation through a channel with rectangular bends. Shaded areas indicate active muscles.

region is again straight (Figure 2.27). Therefore, although the predicted muscle activity is constant with respect to the substrate, it does not show a constant relationship to the mechanical events (flexion) within the body of the snake.

In a second experiment, Gray and Lissmann (1950) allowed snakes to crawl past a series of pendulums which could move freely in any direction. The displacements of the pendulums were recorded to determine the resultant forces applied by the snake while it performed lateral undulation. These resultant forces generated by the snake were always directed posterolaterally relative to the snake. Thus, reactive forces were directed anteromedially. When the reactive forces at each pendulum were resolved into forward and lateral components, Gray and Lissmann found the sum of the lateral components was usually zero, resulting in a net forward reactive force which propelled the snake.

Gray and Lissmann also considered the muscular mechanisms of hypothetical snakes crawling past various numbers of rigid pegs. Models were generated in an attempt to account for the forces which had been determined experimentally. For a snake gliding past a single peg on its left side, they suggested that left side muscle contractions begin in the region of the snake posterior to the peg and continues as the region becomes concave to the left while it passes the peg (Figure 2.28A). The contractions continue to occur after the snake has passed the peg and become convex. Muscle activy ceases about when the region has straightened. Gray and Lissmann also illustrated a hypothetical snake crawling past two pegs which were located on the concave side of the snake at the areas of maximum lateral displacement (Figure 2.28B). The proposed muscle activity was primarily on the concave side contacting

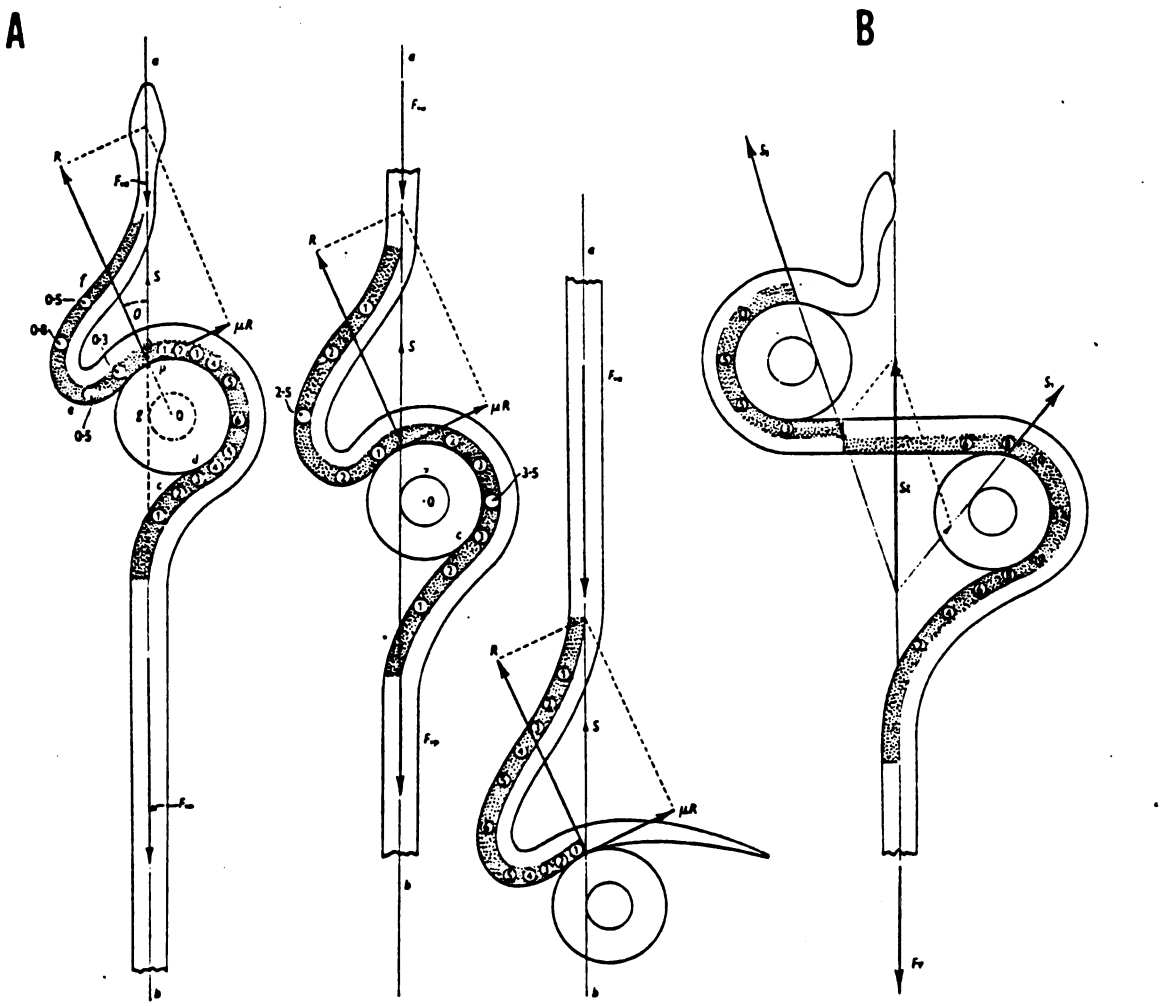

Figure 2.28. From Gray and Lissmann (1950). A. Figure 10 showing muscular mechanism for gliding past one peg. B. Figure 11 showing muscular effort for gliding past two pegs. Shaded areas indicate active muscles.

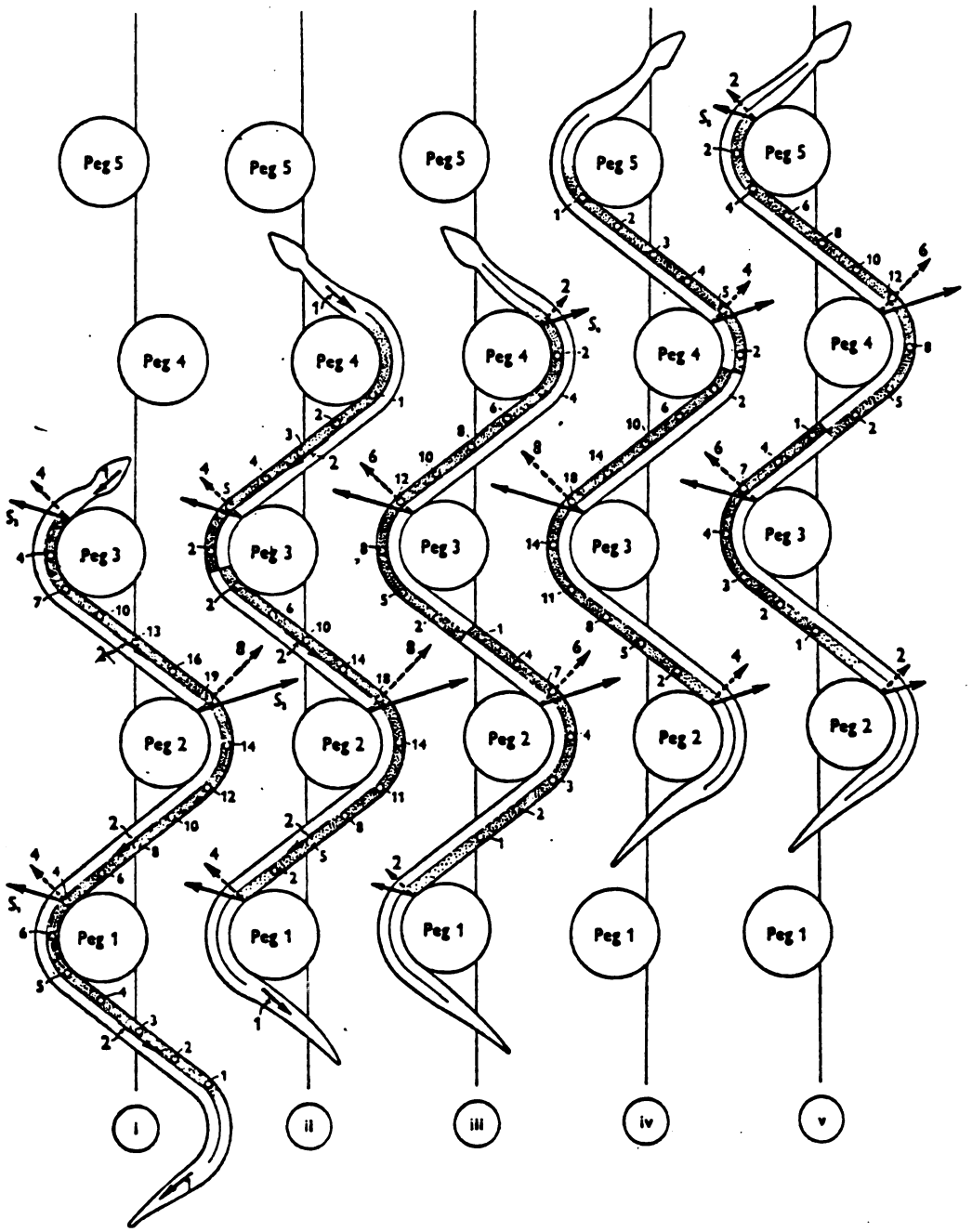

Figure 2.29. Figure 12 from Gray and Lissmann's (1950) model of the muscular mechanism of terrestrial lateral undulation. Shaded regions indicate active muscle.

the pegs.

Figure 2.29 illustrates Gray and Lissmann's model of muscle activity for a snake crawling past three to four pegs. In this figure, the pegs are located on the concave side of the snake at regions of maximum lateral displacement. As the snake initially contacts three pegs (Figure i), all activity is on the right side. The diagram indicates that the regions of active muscle travel posteriorly in the snake; therefore, the cycle of movement of a particular segment should be predicted by examining the posture of the body from posterior to anterior within a block of contracting muscle. For example, with the activity shown at time i, a segment should go through phases of straight, concave, straight, convex, and finally concave as peg 3 is contacted. The transition of right to left side activity provides a convenient event to follow posteriorly along the snake. At different times, this event occurs at regions that are concave right, straight and concave left. Examining the muscle activity at peg 3 shows right, transition from right to left, and left side activity. Therefore, for the illustrated model, the muscle contractions do not show a constant relationship to the substrate or to the mechanical events occurring within the body of the snake.

Gray (1953) discussed the general properties of undulatory propulsion. Among Gray's conclusions was that the general properties of undulatory swimming were the same as those of terrestrial locomotion, except that the wave of bending travels faster than the forward speed of the swimming animal. Thus, a component of motion is produced that is normal to the surface of each element of the swimmer's body. For his review of undulatory swimming, Gray provided a model of a muscular

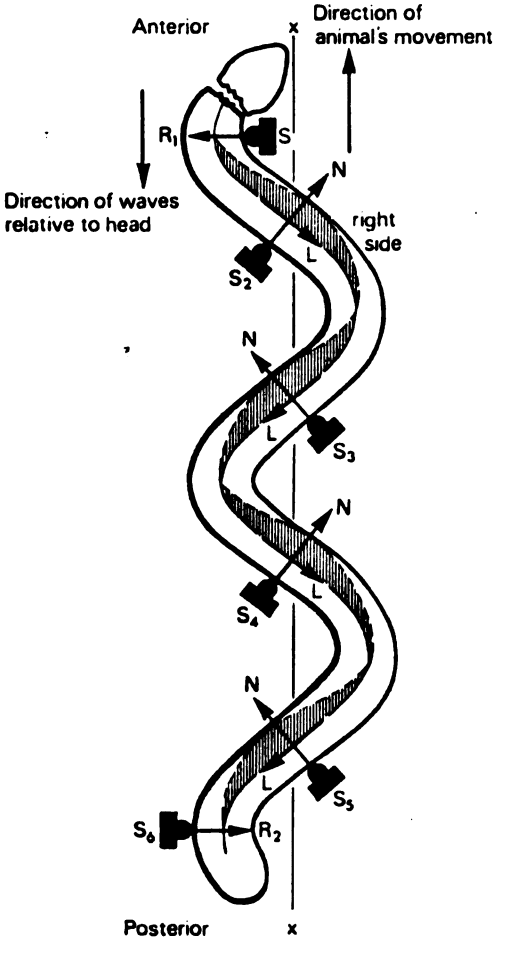

Figure 2.30. Figure 7 from Gray's (1953) model of the muscular mechanism of lateral undulation. Shaded areas indicate active muscles, and the width of these areas represents the degree of tension.

mechanism shown in Figure 2.30. Although Gray was discussing swimming, he included symbols (labelled S) to represent the pattern of application of external resistive forces. The described pattern of muscular effort consists of alternating, descending unilateral contractions. Activity begins when a region is maximally convex and continues until the region is maximally concave, and the greatest tension is generated midway through this cycle.

Thus, three models of the muscular mechanism of lateral undulation have been proposed (all by Gray and his co-workers). Common to all three is the posterior propagation of alternating, unilateral contractions of muscles which are assumed to span only one body segment. The model of Gray (1953) shows a constant relationship of muscle activity to mechanical events within the body of the organism, with contractions occurring from maximal covexity to maximal concavity. The model of a snake moving through a channel with rectangular bends (Gray and Lissmann, 1950) shows some consistency between muscle activity and the substrate, and most contractions include a cycle of straight, concave, and straight. The model for snakes moving past rigid pegs (also Gray and Lissmann, 1950) shows no consistent relationship between muscle activity and either the substrate or events within the body of the snake. In a later review of animal locomotion (Gray, 1968), these contradictions were not discussed.

The electromyographic studies of terrestrial lateral undulation were conducted with snakes crawling past a series of discrete pegs. For both Nerodia and Elaphe, muscle contractions began at maximum convexity and ceased at maximum concavity. This relation of emg to mechanical event remained constant along the length of the snake. Contractions were also

alternating, descending and unilateral. This supports Gray's (1953) model of lateral undulation. Surprisingly, the least applicable model was the one suggested for a snake moving past a minimal number of rigid pegs (Gray and Lissmann, 1950). A key factor affecting this model may have been the choice of snake postures for the analysis of forces. The pegs in this model were always located on the concave side of the snake at a region of maximum lateral displacement (Figure 2.29). Figure 2.31 illustrates representative postures of snakes moving past minimal numbers of pegs. These figures are from tracings of films from Gray and Lissmann (1950) and this study. In contrast to the model, pegs were consistently located about midway between regions of maximal lateral displacement. Gans (1974) stressed the need of anteromedially directed sufaces if a snake is to generate the reactive forces necessary for lateral undulation. Here, medial is considered towards the line bisecting distances between successive points of maximum lateral displacement (= overall direction of travel). The posture of the snake in Gray and Lissmann's (1950) model with pegs is not consistent with this requirement, whereas the posture of the snake in the tunnel in Figure 2.27 is. Perhaps this accounts for the greater accuracy of some predictions from the model of the snake in the tunnel.

Gray and Lissmann (1950) tended to stress concave region activity as shown in Figures 2.27 and 2.28 and for the anterior portion of the snake in Figure 2.29. They reasoned that this activity was necessary to move the snake around a region of maximum lateral displacement; therefore, they proposed that the muscles were often active throughout the time of maximal concavity rather than ceasing activity immediately after maximum flexion had been attained. In part, this may result from their tendency

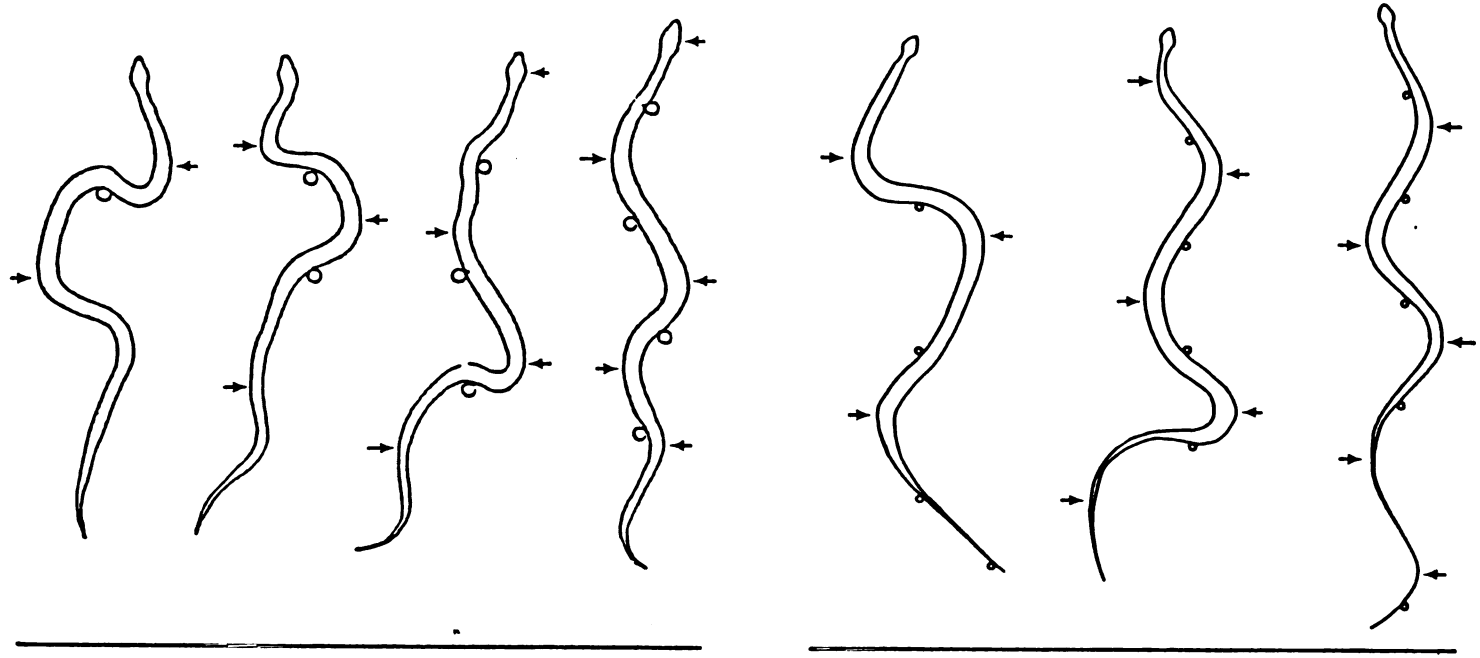

Figure 2.31. Representative postures of snakes moving past a limited number of pegs. At left, illustrations are modified from Figure 7 of Gray and Lissmann's (1950) tracings of films. At right are illustrations from tracings of films of Nerodia from this study. The circles represent pegs and the arrows indicate approximate regions of maximum lateral displacement.

to account for the position of an animal during a finite time interval rather than considering the dynamic, continuous nature of the movements characteristic of lateral undulation (Blight, 1977). During their approach to understanding snake locomotion, an attempt was first made to account for the behavior of small portions of the body. Gray and Lissmann assumed that the locomotor muscles spanned only one body segment. Although this was an unrealistic assumption for the larger epaxial muscles, many of the deeper muscles do span only a few vertebrae. Yet, emg's from such short muscles as the Mm. interarticularis superior and multifidus still correlated with convex to concave movements.

Not all of the aspects of the modelling of Gray and Lissmann were fully articulated. Of the assumptions that were stated, the posture of the snake on the substrate with pegs appears to have been the most serious flaw in their modelling process.

As shown by the electromyographic records, snakes swim by using alternating, descending, unilateral muscle contractions. The movement records indicate that a wave of lateral flexion is propagated posteriorly along the snake. However, during swimming, the relationship of the emg's to the mechanical events within the body is not constant. Instead, the emg's are propagated posteriorly faster than the mechanical wave. Therefore, there is a fundamental difference between the muscular mechanisms of aquatic and terrestrial lateral undulation and Gray's (1953) emphasis of the similarities between these two modes is not supported.

A large body of literature is available on the hydrodynamic theory of undulatory swimming (see Webb, 1975 for an extensive review). Most of this work has dealt with the locomotion of fishes, but the waveform of swimming snakes is very similar to that of fish performing anguilliform swimming (Gray, 1968). Much of this theoretically oriented work has predicted that an optimally efficient waveform for elongate swimmers would have regions of left and right flexion and an amplitude of undulations that increases from head to tail (Lighthill, 1960); hence, the similarity of hydrodynamic constraints has been stressed for various elongate-bodied swimmers. Because eels and snakes are both elongate-bodied swimmers, comparison of their muscular mechanisms of swimming is useful.

Grillner and Kashin (1976) used electromyography and cinematography to study the mechanism of eel swimming. Because they were most interested in the intersegmental coordination of swimming, they implanted electrodes at four longitudinal sites to determine the propagation of emg and mechanical waves. They found that for all points along the eel the phase lag of the emg's was less than that of the mechanical event within the body of the eel. Both the phase lag and duration of the emg's decreased with increased forward velocity of the eel. Anteriorly, the muscles were active during the transition from maximal flexion on one side to maximal flexion on the opposite side. Unfortunately, ambiguity in data presentation in Grillner and Kashin (1976) prevents a clear understanding of whether muscle activity occurred in concave or convex regions. The durations of the emg's in the eel were usually less than one-half of the period of activity. Thus, fundamental similarities appear to exist between the muscular

mechanisms of swimming in the eel and snake.

Grillner and Kashin (1976) found that that the difference in phase lag from anterior to posterior was constant both for emg and mechanical waves. In other words, waves (emg and mechanical) travelled posteriorly with a constant velocity, even though the two waves had different velocities with respect to each other. This constant phase lag in the eel differs from the findings for snake swimming. Table 2.4 indicates that the phase lag of posterior sites was usually less than or equal to that of the more anterior sites, indicating increased speed of emg and mechanical waves as they travel posteriorly. This observation is consistent with a description of the swimming of Nerodia and Elaphe which shows that the amplitude, wavelength and speed of the mechanical wave of lateral flexion increased from anterior to posterior along the snake (Jayne, 1985). Yet, sample sizes of the current study are admittedly small compared to those of Grillner and Kashin (1976). Furthermore, an exception to this trend occurred for the submerged swimming of a Nerodia. Presumably, the eels were performing submerged swimming, whereas the snakes usually swam at the water's surface. Therefore, this may be more of a difference between surface and submerged swimming rather than a difference caused by the contrasting morphologies of the eel and snake.

Blight (1977) emphasized the difficulty of predicting muscular mechanisms of undulatory swimming unless the active and the passive properties of the locomotor system are known. He modelled aspects of swimming based on various assumptions about the stiffness of the body of the swimmer. He considered stiffness-dominiated versus flexibilty-dominated systems. One may envision a straight rod at rest

in the water and a localized tension occurring on one side at the middle of the rod. Two different movements could result, depending on whether or not the rod was stiffness-dominated or flexibility-dominated. A stiffness-dominated rod would bend into a simple curve flexing towards the side of the applied tension. A flexibility-dominated rod would form a curve in its central portion, flexing towards the side of the applied tension; however, there would be two points of inflection, as the ends of the rod would bend in the opposite direction of the central region of applied tension. This would occur because the rod is not stiff enough to maintain the centrally generated concavity; instead the regions nearer the ends are dominated by the resistance of the water to their movement and they fold back on themselves, forming concavities facing the side opposite that where the central tension was applied. The important point is that identical applied forces could move two systems differently depending on the interaction of the resistive forces of the water with the stiffnesses of elongate bodies.

The underlying concept of stiffness discussed by Blight has great intuitive appeal for snakes which are elongate organisms with tremendous variation in their axial morphology. Blight dealt with such radically different chordates as Branchiostoma and newt and lamprey larva. Despite the different numbers of vertebrae in Nerodia and Elaphe (Table 2.1), no differences were found for their mechanisms of swimming as reflected by the relation of $\tilde{\theta}$ to emg. Assuming equal lateral flexion could be attained for each vertebral joint in both species, the greater number of vertebrae in Elaphe would seem to make it more flexible than Nerodia. However, given the overwhelming hydrodmechanical constraints that tend to unify elongate swimmers, the difference in flexibilty

between these two taxa may be trivial compared to those discussed by Blight.

Concertina Locomotion

A striking feature of concertina locomotion is the highly variable pattern of movement and muscular activity. In both Elaphe and Nerodia, emg's consistently correlated with flexion of the vertebral column towards the side of active contraction or the maintenance of a concave posture during static contact with the sides of the tunnel. However, the great variability makes a comprehensive model of this mode premature. This variation suggests muscle activity may occur in response to those variable regions which first establish static contact with the sides of the tunnel. Recently, Gans (1984, 1985) has stressed that the ability of an organism to perform a locomotor mode depends on the local feedback about the deformation of the trunk and its contact with the substrate. Presumably, a two-step process is involved. First, the ability to receive such local feedback should be important. Second, there must be suffficient plasticity in the neural pattern of control to make adjustments of muscle activity in response to this feedback.

The width of the tunnels used for concertina locomotion probably accounts for some variablilty seen in this mode. Gray (1946) found that as the width of the tunnel increased for a snake using concertina locomotion, the number of undulations and the number of cycles of movement per time decreased. Therefore, in order to make meaningful comparisons of the concertina locomotion of Nerodia and Elaphe, snakes must be filmed in tunnels of comparable width. Elaphe attains much greater lengths than Nerodia; hence some method of correcting for size is necessary before making interspecific comparisons. However, determining the tunnel width which best corrects for size is

problematic. As shown earlier (Table 2.1), Nerodia is relatively stouter, with a proportionately longer tail than Elaphe. It is not clear if dividing tunnel width by snake length or width would best indicate the relative size of the tunnel. Because of the different numbers of vertebrae in these two taxa, perhaps comparable tunnel widths would be those for which there were a constant number of vertebrae necessary to to extend between the sides of the tunnel. Tunnel width could also affect the portions of the snake that contribute propulsive forces. In wide tunnels (about 15cm) a substantial portion of the tail was often not pressed against the sides. In fairly narrow tunnels (about 8 cm) the complete length of the tail often made convolutions that pressed against the sides of the tunnel; however, the extent to which this region may contribute significantly to the locomotor forces of this and other modes remains unclear.

Sidewinding

Figure 2.32 provides a convenient summary of the postulated muscular mechanism of left-handed sidewinding of Crotalus cerastes. The shaded areas indicate activity of either SSP-SP, LD or IC. Because the muscle contractions are descending, the posterior and anterior edges of a shaded region represent the onset and offset of activity, respectively. During left-handed sidewinding, unilateral activity of the left side muscles (SSP-SP, LD and IC) flexed the vertebrae to the left as they were moved anteriorly towards a region of static contact. Left side activity of these muscles continued through and beyond static contact until the vertebrae were maximally flexed to the left. Right side activity (SSP-SP, M and some LD) began during or just after static contact with the substrate. Right side activity (including IC)

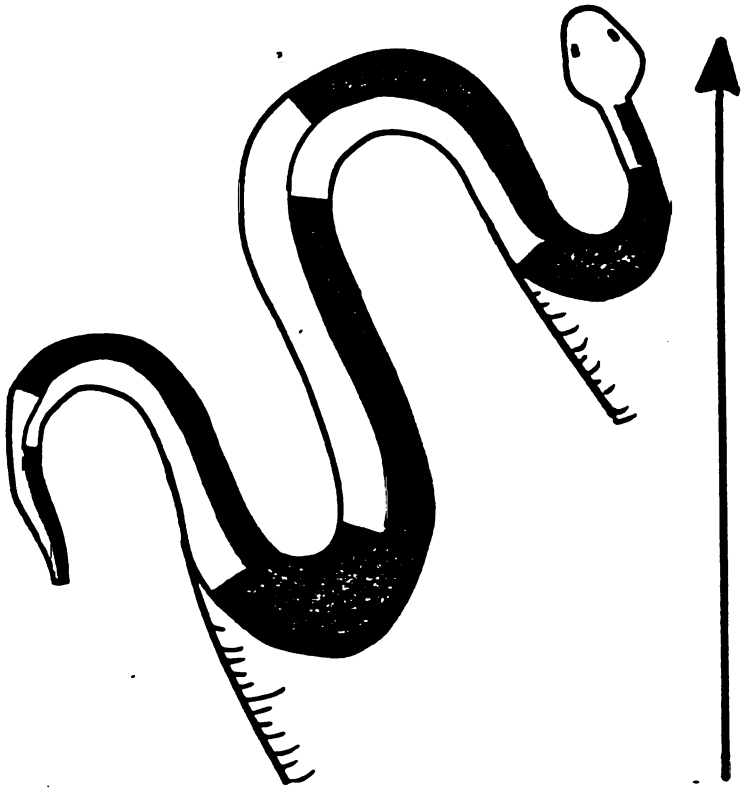

Figure 2.32. Working model of the muscular mechanism of left-handed sidewinding of Crotalus cerastes. Shaded regions indicate active contractile tissue. See text for more detailed description.

continued at least until the vertebrae began to flex to the right. Depending on the exact posture of the snake, right side activity could continue until the region was maximally concave to the right. This continuation of right side activity was more likely when the region approaching static contact was not flexed very tightly to the right. Right-handed sidewinding can be described by switching left and right in the above description.

The nonplanar movements used during sidewinding make this mode particularly interesting compared to the other modes of snake locomotion. Although this mode is often considered somewhat specialized, it occurs in a wide variety of taxa including booid and colubroid snakes (Gans and Mendelssohn, 1972). The viperid Crotalus cerastes and the colubrid Nerodia fasciata belong to two distinct lineages of snakes and yet they will both sidewind, although C. cerastes appears to be considerably more proficient at this mode than N. fasciata (Chapter 1). One often must harass Nerodia to elcit sidewinding, and this mode is most easily elicited from small individuals of this taxon. For larger Nerodia, it was more difficult to prompt good sidewinding on sand. For this reason, individuals were placed on the floor in order to obtain footage of this mode. Although no films were taken of C. cerastes sidewinding on the floor, individuals were allowed to crawl on the floor, and they readily performed sidewinding which was not discernably different from that performed on sand. Allowing for the different substrates, it is still instructive to compare the sidewinding of these two species.

Figures 2.22 - 2.25 illustrate the emg records during the sidewinding of these two species. Both species had substantial

bilateral activity of the SP. The M of Crotalus also overlapped strongly with the SP and M of the opposite side. No emg's were obtained from the M of Nerodia. In both species, the bilateral activity correlated with a time when lifting of the vertebrae was occurring. However, the lifting phase of Nerodia (near mid-body) was consistently before intiation of static contact, whereas the lifting in Crotalus occurred after static contact. In other words, the portion of Crotalus anterior to the region of static contact was being lifted, whereas dorsiflexion occured in the region of Nerodia posterior to and just on the area of static contact.

A postural difference between these two species may partially account for these differences. Chapter 1 discussed a significant difference between Nerodia and Crotalus for the angle of the track of static contact relative to the overall direction. This difference implied the posture of Crotalus facilitated a greater area of the body having static contact with the substrate. Figure 2.33 illustrates the postures during sidewinding of two snakes from which emg's were obtained. Figure 2.33A illustrates the posture of Nerodia on the linoleum floor. This snake usually had only one region of static contact with the substrate. At .87 sec, the Nerodia was establishing static contact between the neck and the substrate just after a brief period of backward sliding. At 1.48 sec, the Nerodia had a well-established region of static contact near mid-body. At 2.11 sec the snake had almost lost static contact near mid-body and would soon establish static contact with the neck region. Interestingly, the portion of the snake posterior to about the 100th vertebra never established static contact.

This posture of Nerodia was fundamentally different from that of

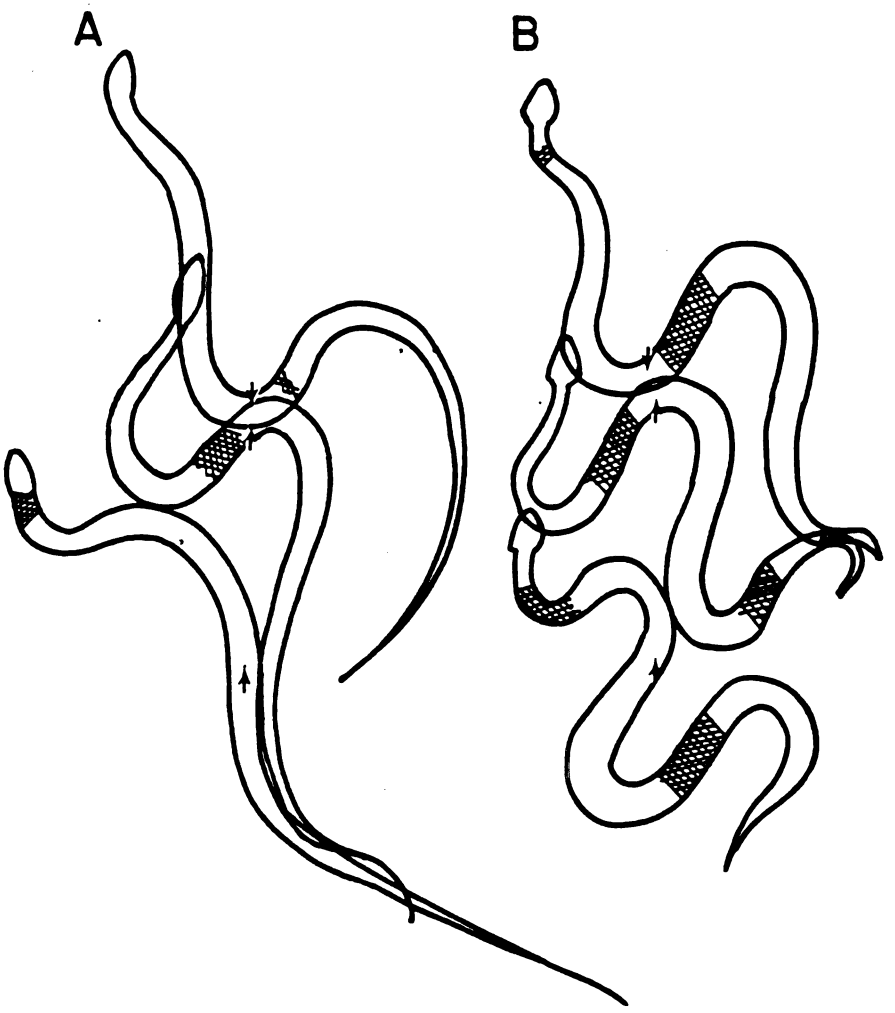

Figure 2.33. Representative postures of snakes performing right-handed sidewinding. Illustrations were made from tracings of films. A. From sequence 61.3 (Figures 2.22 and 2.23) of Nerodia on a linoleum floor. From bottom to top the images are from .83, 1.48 and 2.11 sec in the sequence. The arrows indicate the electrode site near mid-body (vertebra 66). B. From Crotalus 5 on sand. From bottom to top, the images are at 0, 1.08 and 1.75 sec. Cross-hatched regions indicate static contact with the substrate. Arrows indicate near mid-body (vertebra 70). See discussion for more complete explanation.

the Crotalus cerastes shown in Figure 2.33B. At 0 sec, the Crotalus had firmly established static contact with the neck region while a more posterior region also was in contact. At 1.08 sec, the snake had two well-established regions of static contact that were parallel to each other. At 1.75 sec, the snake was just beginning to contact the substrate with its neck, while it continued to maintain a large posterior region of static contact.

Hence the Nerodia tended to pivot about an anterior to central region of static contact, whereas the Crotalus moved its body between two extensive zones of static contact. Because Nerodia was on a hard substrate, it was not possible to determine from tracks the portions of the body that may have been dragged along the substrate. Because the tail accounts for different percentages of total length of Nerodia (25%) and Crotalus (8%), it would be interesting to determine if this difference is involved in the apparent dragging of the posterior region of Nerodia.

In some respects, momentary sliding contact in this sequence of Nerodia resembled the transitional, slide-pushing mode described recently by Gans (1984). However, Gans defined this mode by the continuous propagation of lateral flexions which slide over the substrate in a manner similar to the waves of lateral flexion that slip backward relative to the water during swimming. Hence, even if static contact was not established by the Nerodia in this sequence, the snake would still have had an asymmetric profile of V_y and a highly variable V_r (see early portion of Figure 2.22), neither of which are compatible with the description of slide-pushing. Furthermore, no lifting of the body was mentioned for slide-pushing.

As discussed in Chapter 1, the existence of a transitional mode combining lateral undulation and sidewinding could support the idea that sidewinding was derived from lateral undulation. Opinions differ about the relation of sidewinding to other locomotor modes. Gray (1946) and Brain (1960) suggested that sidewinding was derived from lateral undulation after they emphasized the continuous propagation of a wave of lateral flexion in both of these modes. Although Gans(1974) did not state that sidewinding was derived from concertina locomotion, he preferred to stress the commonality of static contact in these two modes.

The profiles of linear velocities used in this study tend to emphasize discontinuous movement of the snake because of the momentary static contact with the substrate seen in concertina and sidewinding. However, the profiles of $\bar{\theta}$ used in the emg analysis often revealed continuous transitions of the snake from concavity to convexity during sidewinding (Figures 2.24 and 2.25). As snakes contacted the substrate during sidewinding, the linear velocities would equal zero, but angular velocities (slope of 0 versus time) of the vertebral column changed continuously. Continuous change in angular velocities indicates the continous propagation of a wave of lateral bending, and this supports the suggestion of Gray (1946) and Brain (1960).

The electromyographic event most characteristic of sidewinding is bilateral activity of the SP. Figure 2.9 illustrates a sequence of terrestrial lateral undulation of Nerodia 36. During two cycles of activity in this sequence, there was some bilateral activity of the SP. Hence, bilateral activity can apparently be superimposed on a pattern of muscle activity characteristic of lateral undulation, and the extent of

this activity will determine whether sidewinding occurs. Muscle activity in sidewinding and lateral undulation ceases when a region becomes maximally concave, whereas concertina locomotion often has prolonged concave side muscle activity. This evidence may further support suggestion of the close relationship of sidewinding to terrestrial lateral undulation.

Anatomical Considerations

The extensive amount of overlap of serially homologous muscles may cause some concern that electrodes could have detected signals from nearby active segments while the segment actually containing the electrode was inactive. Similarly, the close proximity of adjacent bundles of non-homologous muscles could have caused spurious records ("cross-talk" of Mangun et al., 1981) to be detected from electrodes implanted in inactive muscles. For this latter case, if noise between adjacent non-homologous muscles were a problem, then the emg's from adjacent muscles (such as the SSP-SP and LD) would have similar onset, offset and similar times of maximum amplitude. As the sample emg's in Figure 2.23 show, differences in these aspects of emg's were detetected from electrodes in adjacent non-homologous muscles; therefore, this type of noise was not a complicating factor for this study. It is more difficult to evaluate the potential problem of noise between adjacent serially homologous segments. In one trial of concertina locomotion, two electrodes in the LD were within three vertebrae of each other, and differences in the onset and offset were detected between the two emg's. Although the emg signal is admittedly more complex than simple onset and offset, this does suggest that noise among adjacent serial homologs was minimal.

For smaller snakes, some attempts were made to manufacture electrodes of smaller size (about 0.8 mm stripped portion) to minimize the number of adjacent muscle segments contacting the electrode. However, in such smaller snakes (eg. NF36, NF 37 and NF39) two or three segments often contacted the electrode. Most muscle segments did not

have a perfect 1:1 ratio with the underlying vertebrae; instead contractile tissue forming a segment (defined by tendons) of the major muscles studied (SSP-SP, LD, and IC) usually arose from two or three vertebrae. Hence, even if an electrode were in a single segment, it is likely that the total contractile tissue forming a muscle segment is controlled by nerves from more than one body segment. The detailed studies of Gasc (reviewed 1981) give some indication of the patterns of innervation of the axial muscle segments of snakes. For example, in viperids each head of the iliocostalis is supplied from the nerve of a single body segment, whereas colubrids generally have a complex system in which branches from one nerve supply more than one muscle segment. Thus, the control of activity for a single muscle segment by nerves from several body segments appears likely. All of this emphasizes that undue precision should not be attributed the the emg's described herein. However, no major problems of technique were apparent, and the consistent mechanical correlates of emg in the region of the contractile tissue of muscle segments did indicate repeatability within and among the conspecific snakes used in this study.

Other aspects of snake axial musculature were difficult to assess accurately. Figures 2.2 to 2.5 are simplified illustrations of the axial muscles considered in this study. One of the most persistent complications of performing gross dissection of these muscles was that tendons often contributed to connective tissue that formed intermuscular septa and sheaths surrounding the longitudinal bundles of the major epaxial muscles. The sites of attachment for the anterior tendons of the M. longissimus dorsi were probably the most difficult to determine objectively. As described earlier, the medial tendon of the M.

longissimus dorsi of Crotalus cerastes has a distinct portion that continues anterodorsally; however, the more distal portion of this tendon is very diffuse, contributing to a sheath around the M. semispinalis-spinalis, before making a rather vague attachment along the neural spines of the vertebrae. Although not illustrated in Figures 2.2 and 2.3, the medial tendon of Nerodia and Elaphe contributes to a similar sheath, to a lesser extent. In all three of the studied taxa, the two septa between the SSP-SP and LD and the LD and IC were additional complicating factors. Traces of these intermuscular septa could usually be followed to bony attachments. To differing extents, these septa intermingle with the tendons that connect nonhomologous muscles. In all three of the studied species a very distinct tendon extends between the M. longissimus dorsi and the medial head of the M. iliocostalis. Yet, the variable nature of the septum between these two muscles made it difficult to determine if the origin of the M. iliocostalis is directly on a bone or if it attaches to a bone via the M. longissimus dorsi. Similarly, in Nerodia and Elaphe, the connection between the semispinalis and the M. longissimus dorsi is somewhat obscurred by an intermuscular septum. Hence, the question arises as to what the functional origin and insertion may be for these interconnected muscle segments.

If simultaneous activity of a set of interconnected segments occurs, then the set of contracting muscles might be considered a functional unit. Alternatively, if the interconnected segments of nonhomologous muscles are not active simultaneously, then the effective origins and insertions may be the bony element to which an attachment is most immediately made. For example, in Nerodia (Figure 2.2) the contractile

tissue of the LD is about eight vertebrae posterior to that of the connected SSP. The usual pattern of muscle activity involves descending contractions. Consequently, for joint function of the SSP and LD, the activity of the contractile tissue of the LD would be synchronous with a SSP eight vertebrae anterior to its location and would precede activity of the contractile tissue of the SSP at the same level of the body. Similarly, if the IC and LD function together, then LD activity at a given body segment should also precede that of the IC. Differential activity could not be observed between the SP and SSP for any of the studied snakes, and the LD never consistently preceded the activity of either head of the SSP-SP (Figures 2.6, 2.9, 2.11, 2.12, 2.19 and 2.22), implying that these two muscles may function independently for the studied taxa. Similarly, for planar movements, no consistent differences between the onset and offset of activities of the LD and IC (at the same body segment) were observed that would support their combined function.

The differential activity of the major muscles during sidewinding locomotion offered considerable insight into their function. Figure 2.22 illustrates a particularly good sequence of the activity of the SP, LD and IC during the sidewinding of Nerodia. The bilateral activity of the SP in Nerodia (and Crotalus) was associated with dorsiflexion of the vertebral column; however, the dorsiflexion in Nerodia apparently occurred more posteriorly within the vertebrae spanned by the SP. Perhaps the rather long anterior tendon of the SP in Nerodia (14) does not allow enough dorsiflexion along its entire length to permit the lifting of the portion of the snake anterior to the region of static contact. In contrast, Crotalus has a relatively short anterior tendon

of the SP (7) and the bilateral activity of this muscle correlated with lifting the vertebrae anterior to the region of static contact. Some additional evidence suggests a major role of the SSP-SP as a dorsiflexor. A few Crotalus cerastes became particularly agitated during filming, and they assumed defensively coiled positions by raising most of the anterior portion of their bodies in preparation to strike. Sustained low-level bilateral activity was recorded for the SSP-SP segments in the elevated regions of the snakes.

Another muscle apparently important for dorsiflexion is the M. multifidus (M). Recordings of this muscle during the sidewinding of Crotalus consistently correlated with dorsiflexion of the vertebrae. Fewer recordings from the M were obtained for Nerodia, and none was obtained during the sidewinding of this taxon. However, as illustrated in Figure 2.14 this muscle was almost continuously active in the most anterior region of a swimming Nerodia. As mentioned earlier, typical swimming posture of this species invloved elevation of the head and neck region above the surface of the water. It is also interesting to note that the activity of the M in this sequence did not follow a pattern ever observed for the SSP-SP during swimming. Although no recordings were obtained from the SSP-SP immediately superficial to the M segment, this indirect evidence of unusual activity suggests that the M may be able to function independently from the SSP-SP.

A comparison of the activity of the LD during the sidewinding of Nerodia versus Crotalus suggests that this muscle functioned similarly in these two species despite the different attachments of the medial tendon. Although the activity of the left LD of Nerodia overlapped with that of the right SP during right-handed sidewinding, overlap between

the left and right LD was minimal. This suggests that the left side muscles were primarily affecting flexion to the left as the simultaneous activity of the right SP added a component of dorsiflexion. The time of bilateral activity used to lift the trunk of Crotalus occurred after static contact rather than before it as in Nerodia. However, the left and right LD of Crotalus also showed effectively no overlap of activity, suggesting that the LD of Crotalus was also primarily a lateral flexor.

The proportions of tendon and contractile tissue within a muscle segment may effect the extent to which contractile tissue is stretched during vertebral flexion which could, in turn, affect the time of activity of different muscles at the same level of the body. Tendinous elongation within segments does vary among different muscles and among taxa, and this variation has been the object of considerable interest to workers studying snake anatomy and locomotion (Mosauer, 1935a; Auffenberg, 1961; Gasc, 1974; Ruben, 1977; Jayne, 1982). The length of the contractile tissue within a segment can be divided by the total length of a segment to provide an estimate of this tendinous elongation. For the SSP-SP of Nerodia, Elaphe and Crotalus, these values of percent muscle tissue per segment are about 25%, 28% and 32%, respectively. For the same three taxa, these values for the LD are 67%, 67% and 62%, respectively. The values of tendinous elongation of the IC of Nerodia, Elaphe and Crotalus were 67%, 67% and 84%, respectively. Hence, in all of the studied taxa, there was an increase in the proportion of contractile tissue within muscle segments proceeding from medial to lateral.

During the sidewinding of Nerodia (Figure 2.22), the relationships among the activities of the SP, LD and IC depended on the side of the

snake. On the right side during right-handed sidewinding, the order of onset of activity proceeded from SP to LD to IC. The time lag between firing of the LD and IC may suggest that the IC and LD were functioning as a combined unit. However, on the left side of the same snake onsets of LD and IC (at the same level in the body) were about simultaneous, and this seems to rule out the joint function of these two interconnected muscles. A closer examination of the activity of the IC in Nerodia (and Crotalus) during sidewinding reveals that the major activity of this muscle began about when the region was straight and continued until maximal concavity. This time of activity, combined with the lateral location of this muscle and its relatively high proportion of contractile tissue, suggests that there may be different optimal times for the various muscles to affect lateral flexion.

When Ruben (1977) compared the differences in tendinous elongation of muscle segments of Lichanura roseofusca and Masticophis flagellum, he was primarily interested in the interspecific differences that may be correlated with the habit of constricting prey. As he discussed, a greater proportional length of contractile tissue per segment would allow for the formation of curves with a smaller radius of curvature, and this would facilitate constriction. Although Ruben's comparison of a boid with a colubrid snake somewhat complicated his comparison, the relation of relative length of contractile tissue to the amount of lateral flexion was a useful concept. As shown above, some evidence indicates that different relative contractile tissue lengths of muscles within individual snakes may be related to their role of forming different lateral curvatures within the vertebral column. It would be particularly interesting to determine if the series of muscles from

medial to lateral (SSP-SP, LD and IC) have different optimal times of contraction beginining as a region is maximally convex and continuing until it is maximally concave. The activity of the IC primarily during times of concavity in a few sequences suggests that this could be a productive area for future work.

Because differential activity of the IC was clearly apparent in some sequences of snake locomotion and not in others, it is instructive to determine any common characteristics for those sequences that displayed such activity of the IC. Recalling that the IC showed greater activity during the time of concavity for its region, an examination of the regimes of lateral flexion during the different modes would seem likely to reveal some trends. Except for concertina locomotion, the magnitude of maximal right and left flexion was usually comparable within a sequence of a given mode for an individual snake. To minimize the effects of errors in determining maximum lateral flexion, for each sequence an average was taken of the absolute values of maximal right and left vertebral flexion. For concertina locomotion no clear pattern of symmetry was present in the plots of $\bar{\theta}$ versus time; therefore, the single greatest value of maximal $\bar{\theta}$ was noted for each sequence of this mode. Samples of these values of maximum $\bar{\theta}$ are listed in Table 2.5.

Maximum $\bar{\theta}$ of Nerodia during terrestrial lateral undulation was usually near 5°. Interestingly, the slowest sequence of this mode for Nerodia had the highest value of maximum $\bar{\theta}$. The overall value of CV of V_r of this rather slow sequence (number 53.2) was 41%, whereas smaller time intervals had values of this quantity small enough to indicate the mode was lateral undulation. Perhaps, there is a range of values of

Table 2.5. Average maximum $\bar{\theta}$. Abbreviations for locomotor mode are: LU, terrestrial lateral undulation; ALU, aquatic lateral undulation; C, concertina; and SW, sidewinding. Mean V_x is in TL/sec. Numbers in parentheses after angles indicate the vertebral number of the vertebra centered in the interval of the five vertebrae used to measure $\bar{\theta}$. See text for complete explanation.

Snake (Sequence)	Mode	V_x	Site 1	Site 2	Site 3	Site 4
NF35(53.7)	LU	.29	5.4°(71v)			
NF35(53.2)	LU	.11	7.5°(71v)			
NF35(53.3)	LU	.27	5.3°(71v)			
NF36(61.11)	LU	.47	4.1°(66v)			
EO18(60.2)	LU	.33	3.5°(111v)	3.8°(171v)		
NF34(47.2)	ALU	.81	2.9°(46v)	3.0°(70v)	2.8°(94v)	
NF38(64.16)	ALU	.67	3.3°(29)	3.9°(64v)		
NF39(65.1)	ALU	.74-1.16	3.8°(30v)	5.0°(64v)	4.3°(97v)	
EO20(64.5)	ALU	.63	1.3°(76v)	1.4°(116v)	1.6°(153v)	1.1°(192v)
EO19(63.1)	ALU	.78	1.6°(65v)	1.4°(119v)	2.3°(165v)	
NF33(47.3)	C	.07	11.0°(72v)			
EO15(43.4)	C	.05	15.0°(111v)	11.8°(135v)		
NF36(61.3)	SW	.27	7.0°(66v)			
CC6(49.4)	SW	.49	9.2°(53v)			
CC6(49.1)	SW	.67	8.4°(53v)	7.5°(83v)		

maximal $\bar{\theta}$ over which a constant V_r was most easily maintained during terrestrial lateral undulation. Maximal $\bar{\theta}$ of the Elaphe performing lateral undulation was sightly less than that of Nerodia; however, the complicating effects of peg spacing and snake size prohibit meaningful comparisons between these two taxa.

As mentioned previously (Table 2.3), the maximal $\bar{\theta}$ for a given region of a snake may vary through time and among different regions within the body of an individual snake. Allowing for this variation, Nerodia still showed consistently greater values of $\bar{\theta}$ (2.8° to 5.0°) than Elaphe (1.3° to 2.3°). These lower values for Elaphe are consistent with descriptions of the waveform described for the swimming of these two genera. Jayne (1985) found that the waveforms of swimming Nerodia fasciata and Elaphe guttata were nearly identical after correcting for the speed and size of swimming snakes. This similarity was somewhat puzzling because Elaphe has about twice as many body vertebrae as Nerodia; therefore, one might have intuitively expected Elaphe (with similar segmental lengths of major epaxial muscles) to have had a greater number of undulations than Nerodia. However, Elaphe had similar amplitudes and wavelengths for its undulations when compared to Nerodia. This indicates that Elaphe had nearly twice as many vertebrae in each half wave of its body. Thus, the values of $\bar{\theta}$ of Elaphe, which were about half those of Nerodia, agree very closely with these observations of waveform for the swimming snakes.

Few maximal values of $\bar{\theta}$ were determined for concertina locomotion. As discussed earlier, there were many complicating factors attributable to the widths of the tunnels confining the snakes using this mode. However, values greater than 10° were observed during this mode (Table

2.5), and these may have approached the upper limit for lateral flexion of the vertebrae of these snakes. Certainly, the indirect method of measuring lateral flexion must be remembered when considering these extreme values of $\bar{\theta}$. For a vertebral column of a Python, Gasc (1974) determinined maximal lateral flexion of about 8° per joint. Mosauer (1932) gave a value of about 25° for maximal lateral flexion between adjacent snake vertebrae, but he did not indicate the interspecific variation for the sample that he used to determine this value. Clearly, the mobility of the vertebral columns of intact snakes is an area that would profit from a detailed investigation.

Both Nerodia and Crotalus had moderately high values of $\bar{\theta}$ during sidewinding (Table 2.5). The value of 7.0° for Nerodia sidewinding was greater than that of Nerodia performing lateral undulation. The maximum measured values for $\bar{\theta}$ of Crotalus approached 10°. For large Crotalus cerastes, this would appear close to the upper limit for intact snakes. Some large Crotalus cerastes filmed in this study (e.g. CC5) flexed so tightly that the side of the animal was touching itself along the entire concave region of 180° arc. Only 20 to 22 vertebrae were required to form such an arc in this Crotalus, resulting in a value of about 9° for maximal $\bar{\theta}$. Hence, the relatively high values of lateral flexion observed in sidewinding snakes may have been limited by the overall shape of the body rather than the morphology of the vertebrae.

One of the most conspicuous examples of differential activity of the IC (with relatively greatest proportion of contractile tissue per segment) was seen during the sidewinding of Nerodia, for which relatively tight lateral flexions were observed. For sequences of other modes, examination of the relation of muscle activity to extreme lateral

flexion was inconclusive. However, the potentially different roles of the medial and lateral epaxial muscles should prove a productive area for future work. Depending on the forces required for constriction, a constricting snake may have a high proportion of contractile tissue in segments of the IC while having a relatively unspecialized SSP-SP that could initiate lateral flexion during locomotion, while the region is maximally convex. Unfortunately, dissection of the IC of many species is especially complicated. For the sake of convenience, Jayne (1982) used tendinous elongation of the SP as a general indicator of tendinous elongation of epaxial muscle segments. Although this may be true for many species, perhaps some of the most interesting species will prove to be those for which this relation does not hold.

To a great extent, the lateral displacement of the axial muscles is determined by the shape of the underlying vertebrae. For the three species of this study, gross differences the shapes of the vertebrae are apparent even in the limited view provided by Figures 2.2 to 2.4. More information is avaialable on the shape of snake vertebrae than on the movements allowed by them. Mosauer (1935a), Johnson (1955) and Gasc (1974) have all stressed the importance of the prezygapophysial region of the vertebrae. This area serves as the point of attachment for the SSP, LD and numerous smaller epaxial muscles (Mosauer, 1935a; Gasc, 1974). Johnson (1955) conducted a detailed comparative study of vertebral form of snakes and its correlations with phylogeny and habitat specialization. The only ratios of vertebral dimensions that showed significant differences among his habitat groups included the width across the prezygapophyses. Gasc (1974) carefully determined the major direction of the axial muscles of Python and constructed a

detailed model including orientation of each of the axial muscles and presumed cumulative resultant forces generated by the action of each of the major groups of axial muscles. Such a detailed analysis is beyond the scope of this study, but a major conclusion from this approach of Gasc's was the paramount role of the prezygapophysis as a lever arm for the transmission of muscular forces.

Gasc's detailed approach to modelling necessarily included many assumptions about the orientation of the muscle relative to the lever arms. Skeletal morphology clearly can limit the possible orientation of muscles. Mosauer (1935a) envisioned aspects of vertebral morphology as forming a number of tunnel-like structures which accommodated the major muscles and limited their movements. For example, the neural spines of the vertebra would prevent the SSP-SP on the convex side from forming a chord across the arc of the flexed vertebrae. Unfortunately, it is not at all clear to what extent a contracting muscle on the concave side may form a chord across the flexed vetebrae. The connective tissue sheaths around the major muscles are presumed to limit such lateral excursions during contraction. However, during the vigorous lateral flexion of some snakes such as Elaphe a bulge from the iliocostalis forms such a chord, albeit a shallow one. In fact, during the later portion of this study, I found that this was a handy landmark that could be used to facilitate implantation of electrodes into the IC. The formation of such chords alters the orientation of the muscle fibers relative to the lever arms, affecting vector analysis. Hence, the most useful aspect of such modelling may prove to be the a priori generation of more general hypotheses of muscle function which may then be tested with emg. As the current limited number of papers on the axial musculature of snakes

suggest, few workers have be able to determine the gross anatomy of this system with the detail of Gasc, let alone model such a complicated system.

Simple differences in the number of body segments are probably the easiest aspect of variation in the vertebral skeleton that can be dealt with. Variation in vertebral number, with its concomitant variation in packaging of the axial muscles, is a topic of central interest to the study of snake locomotion. Segmental length of axial muscles is not just correlated with the number of vertebrae. Instead, these two characters correlate with specialization for habitat and habits (Gasc, 1974; Jayne, 1982). The proliferation of serially homologous axial elements within snakes raises some interesting issues. For example, what is a functional unit in these many segmented, elongate organisms? One may consider individual serial homologs as the fundamental functional units. In another sense, an entire region of the body may also be considered a functional unit since it may be spanned by a single muscle segment. If there is a fudamental unit of nervous control, this may also define a functional unit. For example, a nerve impluse could be propagated along the animal causing the simultaneous activity of several body segments; therefore, the number of involved segments could be considered a functional unit.

Relevant to these issues is the number of adjacent muscle segments that are simultaneously active during snake locomotion. For modes other than concertina, it appears that there are continuous waves of descending stimuli. Electrodes could not possibly be put into all of the simultaneously active adjacent muscle segments, but the number of such adjacent segments can be determined indirectly. If overlap in

activity is observed for homologous muscles along the same side of the body at locations that are less than 180° out of phase, then one can deduce that all of the intervening segments are also active. Hence, a minimal number of active segments can be generated from information of two different longitudinal sites. A more exact estimate of the number of active adjacent segments can be obtained by using the velocity of the emg along the body of the animal. Approximate number of active adjacent segments will equal (duration of emg)(number of vertebrae between sites)/ (lag time of emg between two sites).

Because of some uncertainty of the nature of the propagation of the emg during concertina locomotion, the method using emg velocity was not used for this mode. However, as mentioned earlier, during concertina locomotion of E015 in sequence 43.4, overlap of activity was observed for two sites 24 vertebrae apart. For sequence 60.2 of the terrestrial lateral undulation of E0 18, an estimated 45 adjacent segments of the LD were active simultaneously. For the sidewinding of Crotalus 6, a block of 40 adjacent muscles was active.

By far the most information of this sort is available from the swimming Nerodia and Elaphe. The SSP-SP, LD and IC were simultaneously active at the same level of the body during swimming; therefore, when serially homologous muscles were not available between two sites, any one of these three muscles was used for the estimate. One complication for the sequences of swimming is that some of the lag times were very small. Hence, small absolute errors in determining this quantity will cause large relative error affecting the estimate of the number of active segments.

The smallest estimated number of active adjacent segments was 25 for the anterior region of Nerodia 38. For Nerodia 34 during sequence 47.2, estimates of active segment were 72 between sites 1 and 2 and 59 between sites 3 and 4. For Nerodia 34 during sequence 47.16, estimates for these same two regions were 64 and 52, respectively. Nerodia 39 decelerated during sequence 65.7. During the fastest portion of this sequence, the estimated numbers of active adjacent segments from sites 1 to 2 and sites 2 to 3 were 40 and 66, respectively. For these same two regions the values were 43 and 60, respectively, during the slowest portion of this sequence. Hence, for NF34 there was a consistent increase in the number of active adjacent muscle segments going from the anterior to posterior region. Thus, for Nerodia most estimates of the number of active adjacent segments fell within the range from 40 to 70.

For Elaphe 20, the values from sites 1 to 2, sites 2 to 3 and sites 3 to 4 were 40, 50 and 120, respectively. The somewhat unusual waveform of E020 was discussed earlier and may partially account for the seemingly low values from the anterior region of this snake. For the larger Elaphe 19, the values from site 1 to 2 and sites 2 to 3 were 72 and 110, respectively. Hence, both of the Elaphe showed an increase in the number of active adjacent segments from anterior to posterior, and the range of all values was from 40 to 120 active segments.

Thus, a difference in the swimming locomotion of Nerodia versus Elaphe finally seems to emerge. Namely, more adjacent muscle segments are active simultaneously in Elaphe compared to Nerodia. One possible confounding factor affecting this conclusion could be that "homologous" regions were not sampled from both taxa. However, an examination of the location of electrode sites listed in Table 2.2 rebuts this suggestion.

Paired comparisons can be made between Elaphe and Nerodia for regions of the snakes that occupy similar proportional positions, as measured by either vertebral counts or distance along the body. The difference in the number of active segments between these two taxa also coincided nicely with the similarity of waveform of the bodies of these swimming snakes, as was discussed earlier.

The posterior increase in numbers of active adjacent segments, correlated with the waveform of swimming snakes, suggests yet another difference between aquatic and terrestrial lateral undulation. During terrestial lateral undulation there is a relatively constant configuration of the body of a snake as it passes a particular lateral pivotal point. Furthermore, there is a fairly constant relationship of the emg to the flexion in the snake's body as it passes such a point (Figure 2.10). Therefore, during terrestrial lateral undulation a constant block of muscle activity may be propagated posteriorly, whereas the number of segments in such a block of active segments increases posteriorly in a swimming snake.

Because of variation in the duration of the emgs and errors in determining this quantity, the approach used in the study of eel swimming by Grillner and Kashin (1976) would be useful for finer resolution of some of the differences in the swimming of Elaphe and Nerodia. Grillner and Kashin obtained repeated trials of eels swimming at various velocities and then calculated regressions of phase lag as a function of body length. In my study, much variation in phase lag was evident, and this affected estimates of the number of active adjacent muscle segments. Unfortunately, Grillner and Kashin did not indicate the number of the body segment at the location of their electrode sites;

therefore, comparison of the number of active segments in swimming eels and snakes is not possible.

Thus, it appears that for all modes of snake locomotion large blocks of the major epaxial muscle segments are active simultaneously. Frequently, such blocks of simultaneous activity may exceed a third of the snake's body length. Furthermore, interspecific differences in the number of segments in such blocks were found when comparing swimming of Elaphe and Nerodia. Some question arises as to the fineness of control snakes may have over their locomotor movements.

Emg's of deeper and smaller epaxial muscles of snakes were only obtained incidentally in this study. Future work with the deeper muscles, combined with an increased comparative sampling of species, will undoubtedly be necessary to form a more cohesive framework for our understanding of the muscular mechanisms of snake locomotion.

CHAPTER THREE

MECHANICAL BEHAVIOR OF SNAKE SKIN

INTRODUCTION

The mechanical properties of skin are of interest to a wide variety of disciplines such as engineering, pathology, surgery and functional morphology. Although some mechanical testing of skin has been performed in vivo (Finlay, 1970), most knowledge is from in vitro testing (e.g. Lanir and Fung, 1974; Vogel and Hilgner, 1979). Such tests have provided the basis for current theories and models which assert that the mechanical behavior of skin is primarily determined by the network of collagen and elastin fibers in the dermis (Lanir, 1979). Because of the importance of the mechanical properties of skin to medicine, most information is available for mammalian skin which is usually from humans or from commmon laboratory animals such as rats, rabbits and cats.

Recent studies have examined the morphology and mechanical properties of the skin from other vertebrate classes. Motta (1977) described the arrangement of collagen fibers in the stratum compactum of sharks as forming layers of alternately oriented sheets that form helical paths around the body of the shark. After performing stress-strain tests on shark skin, Wainwright, et al. (1978) suggested that shark's skin functions as an exotendon for transmitting locomotor forces as well as providing reenforcement to resist the pressures encountered during lateral flexion. Using methodology similar to Wainwright et al. (1978), Hebrank (1980) found that eel skin was stiffer than shark skin and suggested similar functions.

Because most studies of the skin of squamate reptiles have dealt with the shedding cycle or the physiological importance of the integument (for recent review see Lillywhite and Maderson, 1982), the most detailed anatomical descriptions pertain to the epidermis and most superficial layers of the dermis. However, gross differences in the scalation of snakes have long been used in taxonomic studies and some recent studies (e.g., Jackson and Reno, 1975) have suggested some functional consequences for this variation. Other discussions of the epidermal morphology of snakes have generally emphasized interactions of skin and substrates such as frictional resistance and adhesive properties (Gans, 1974; Gans and Baic, 1977). The role of the distensibility of skin in accommodation of the large objects swallowed by snakes has also been discussed (Gans, 1974), but the relevance of mechanical behavior of skin to locomotion has received scant attention.

Of the major modes of snake locomotion, the mechanical function of the skin is probably most important for rectilinear locomotion. As described by Lissmann (1950), the skeleton of the snake using this mode moves forward with a rather constant speed relative to the substrate. In contrast, the ventral skin of the snake alternately establishes static and sliding contact with the substrate. Propulsive forces are generated while the skin is in static contact with the substrate. The recovery phase involves rapidly accelerating the skin forward relative to the skeleton and substrate in order to establish the next region of static contact from which the snake can propel itself. The cutaneous and costocutaneous muscles of snakes cause the contraction of the skin and movement of the skin relative to the skeleton, respectively. Hence, the skin undergoes successive extensions and contractions resulting from

the activity of these muscles during rectilinear locomotion. The sites of insertion and mass of the cutaneous and costocutaneous musculature vary widely among snakes and in some cases this variation is correlated with specializations in habitat and locomotion (Buffa, 1904; Gasc, 1974; Voris and Jayne, 1976). Because of these variations in the gross morphology of the skin and associated musculature, it is desirable to know if there may be correlated differences in the stiffness of the skin.

This study investigates the mechanical properties of snake skin during uniaxial tensile loading. The stiffness of snake skin is compared within and among species and correlations between skin stiffness and gross anatomy of the skin and associated musculature are discussed.

MATERIALS and METHODS

Species were chosen for this study based on their availablity and specializations in the gross morphology of the skin and associated musculature that are indicative of specializations in habitat and locomotion. With respect to skin and costocutaneous musculature, Nerodia fasciata pictiventris (Florida banded water snake) is an anatomically generalized colubrid snake that is semi-aquatic to terestrial. Ahaetulla prasina (vine snake) is an extremely slender colubrid snake that is highly arboreal. Completely aquatic snakes were represented by the booid Acrochordus granulatus (file snake) and the hydrophiids (sea snakes) Hydrophis melanosoma and Enhydrina schistosa. These three species can only move on land with great difficulty and the speeds attained during terrestrial locomotion are generally very slow (Smith, 1943). The genus Laticauda (sea krait) forms a distinct group of the hydrophiids that are primarily aquatic but frequently do leave the water. Nerodia, Ahaetulla and Laticauda all have a 1:1 correspondence between the number of vertebrae and the number of ventral scales (Alexander and Gans, 1966). The ventral scales of these three taxa are much wider than the dorsal scales and are of sufficient width so that they are the only (or primary) surface of the snake that contacts a flat substrate when the snake is in a normal posture. Acrochordus, Hydrophis, and Enhydrina have lost the 1:1 correspondence between vertebrae and ventral scales (Alexander and Gans, 1966; Voris,

1975), and in these snakes, the width of the ventral scales is no greater than that of the dorsal scales. In Ahaetulla, Hydrophis and Enhydrina the mass of the costocutaneous musculature is extremely reduced compared to the more normal condition displayed in the other taxa of the study (Voris and Jayne, 1976).

Table 3.1 lists the species studied and the method of storage of the specimens before the preparation of the skin samples. All individuals used in this study had been kept in captivity for a minimum of three weeks before dying from unknown causes or being killed by an intracardial injection of sodium pentabarbitol solution. No samples were used if gross examination revealed scars or infected areas. All strips of skin removed from snakes were approximately 110 x 15 mm and the long axis of each sample was always oriented longitudinally. Within each snake, samples were removed from three different dorsal-ventral positions: mid-ventral, mid-dorsal, and ventrolateral. The position of the mid-ventral and mid-dorsal samples always included the dorsal and ventral midlines, respectively, regardless of the species. The mid-ventral samples usually included a substantial portion of the region of insertion of the M. costocutaeous inferior. The location of the ventrolateral samples varied among species because this sample included the region of insertion of the M. costocutaneous superior whose location varies widely among species. Table 3.1 lists the positions of these ventrolateral samples by indicating the dorsal scale rows contained in the sample. Dorsal scale rows were counted starting with the ventral scale as zero and proceeding dorsally. Ventrolateral samples were removed from the left and right sides at the same anterior-posterior position in order to provide replication of a particular anatomical

Table 3.1. Specimens used for uniaxial loading of skin. SVL = snout-vent length in mm. Unless otherwise stated snakes died of unknown causes while in captivity. All refrigeration was 1°C and frozen storage was -5°C. R,L = dorsal scale rows included in right and left ventrolateral samples of skin.

Species (Individual)	Comments
Nerodia f. pictiventris (NfA)	female, SVL = 750, killed with injection, tests within 5 hr of death, R,L = 1 - 3
Nerodia f. pictiventris (NfB)	female, SVL = 710, killed with injection, tests within 5 hr of death, R.L = 1 - 3
Ahaetulla prasina (ApA)	female, SVL = 1000, tests within 8 hr of death, R,L = 0 - 2
Ahaetulla prasina (ApB)	female, SVL = 1050, refrigerated within 2 hr of death, tests within 24 hr of death, R,L = 0 - 2
Laticauda colubrina (LcA)	female, SVL = 1100, skin removed within 12 hr of death and kept refrigerated in saline solution for 3 days before tests, R,L = 4 - 6
Hydrophis melanosoma (HmA)	female, SVL = 820, frozen with 8 hr of death, tests within 1 week of death, R,L = 5 - 9
Enhydrina schistosa (EsA)	male, SVL = 720, frozen within 8hr of death, tests within 2 weeks of death, R,L = 6 - 10
Acrochordus granulatus (AgA)	female, SVL = 560, frozen within 8 hr of death, tests within 1 week of death, R,L = 24 - 37

region. The samples were removed from one of four different anterior-posterior positions. Sites 1 and 2 were located about 240 to 120 mm and 120 to 0 mm anterior to midbody, respectively.. Sites 3 and 4 were 0 to 120 mm and 120 to 240 mm posterior to midbody, respectively. Table 3.2 lists all of the samples that were tested using the following abbreviation scheme for each sample. The first three letters of a sample indicate the species and individual (Table 3.1). The numeral indicates the anterior-posterior site of the sample and the last letter designate the dorsal-ventral position (V, mid-ventral; D, mid-dorsal; R or L, right or left ventrolateral). For example, ApB2L indicates skin from Ahaetulla prasina B at site 2 in the left ventrolateral region.

After each strip of skin had been removed from the snake, I used my fingers to remove excess adhering musculature. Each strip of skin was trimmed to resemble an hour glass. The ends of the sample tapered towards the middle to from a central rectangular portion approximately 70 x 7 mm. The expanded ends of the samples were gripped with emory cloth glued to a clamp that was tightened with screws. The clamps were oriented so that the sample was vertical during the loading test. Ringer's solution was used to keep the samples wet during preparation and testing. For each sample, Vernier calipers were used to measure the width to the nearest 0.1 mm and minimum and maximum thickness to the nearest 0.05 mm. "Mean" thickness was estimated by averaging minimum and maximum thickness.

Skin samples were loaded uniaxially in the longitudinal direction using an Instron® servo-hydrolic materials testing machine with a 443 N load cell. A Nicolet digital oscilloscope was used to store the load

and extension of each sample as digital data with a density of 200 load-extension data points/ sec. Load was measured to the nearest 0.044 N and extension was measured to the nearest 0.032 mm. Data were transferred to a pdp 11 computer for analysis and plotting. The initiation of loading of the sample was determined after examining a plot of the digital data on an oscilloscope, and sample length at load initiation was divided into sample extension to calculate strain. Because of the difficulty in determining the thickness of the skin and because of the goal of determining the functional consequences of differences in the skin, load per unit width was used for primary comparison of different samples. Stresses (load per cross-sectional area) in the samples were calculated primarily to facilitate comparisons with other studies and to clarify certain interspecific differences.

In order to compare the overall similarities among different tests, plots were made of load/width versus percent strain. Manipulation of freshly killed Nerodia revealed the skin of an intact snake may undergo a maximal longitudinal strain of about 10 to 15%. Thus, for each plot, the load/width was determined at 10 and 15% strain to estimate loading at physiologically encoutered strains. A computer algorithm was used to find the maximum slope of each plot by determining the least squares regressions for succesive windows of 75 data points which included the last 2% strain for that sample. Maximum slope was used as an indicator of the maximum stiffness of the material and the strain at each region of maximum stiffness was recorded to the nearest 1%. The beginning of failure was defined as the point after which the slope continuously decreased and this occurred at the same point in time as the maximum stiffness. The end of failure was indicated by a load of zero. The

area under each plot from load initiation to the end of failure was calculated by a computer algorithm and this quantity was used as a relative indicator of the energy at failure. Because strain rate is known to affect the stiffness of skin (Lanir and Fung, 1974), all tests were performed at 5% strain/ sec as a representative physiological value.

RESULTS

Table 3.2 partially summarizes the results of the uniaxial loading of the skin samples. Within individuals and among species, substantial differences are apparent for the loads at 10% strain, 15% strain, beginning of failure and the end of failure. The strain at the end of failure showed varied from 17 to 69% and maximum stiffness varied from 0.047 to 2.388 N/mm%.

Figure 3.1 illustrates representative loading curves for the skin of Nerodia. For comparable regions within the bodies of two Nerodia of similar sizes, the loading curves were comparable for load per unit width at given strains, stiffness and strain at failure (Table 3.2). For ventral samples listed in Table 3.2, loads at 10% and 15% strain averaged .12 and .30 N/mm, respectively. The ventrolateral samples listed in Table 3.2 averaged loads of .11 and .37 N/mm, and the two dorsal samples of Nerodia (Table 3.2) had average loads of .90 and 2.22 N/mm at strains of 10% and 15%, respectively. Dorsal skin samples possessed the greatest average maximum stiffness (.433 N/mm%) compared to values of .130 and .197 N/mm% for the ventral and ventrolateral samples. Skin from all three different sample areas generally failed at about 30% strain.

Comparing the two individuals of Ahaetulla prasina, the loading characteristics of samples from different individuals were most similar for those from the dorsal region. The average loads at 10 and 15%

Table 3.2. Summary of uniaxial loading of snake skin samples. All loads are in N/mm. Stiffness is in N/mm% and maximum stiffness occurred at the strain during beginning of failure. See materials and methods for explanation of sample labels.

Sample	Test	Skin Thickness mm mean(range)	Load at Strain 10%	15%	Begin Fail Load(Strain)	Max. Stiff.	Max. Load	Energy(Strain) at Failure
NfA1V	9	.73(.30-1.15)	.10	.30	1.48(29%)	.097	1.78	-(33%)
NfB1V	27	.80(.30-1.30)	.10	.24	1.91(35%)	.188	2.02	35.0(37%)
NfA2V	11	.75(.35-1.15)	.12	.39	.98(21%)	.100	.98	-(21%)
NfB2V	31	.93(.30-1.55)	.17	.25	1.25(24%)	.126	1.36	16.3(26%)
NfA1L	8	.60(.20-1.00)	.05	.22	1.68(29%)	.153	1.95	-(31%)
NfA1R	7	.55(.30-.80)	.05	.27	2.10(30%)	.171	2.10	24.4(30%)
NfA2R	10	.53(.25-.80)	.29	.71	2.31(33%)	.149	2.31	-(33%)
NfB2L	33	.53(.25-.80)	.08	.24	1.83(30%)	.159	1.96	24.6(32%)
NfB2R	34	.48(.25-.70)	.20	.76	3.99(29%)	.352	4.06	56.2(32%)
NfB1D	28	.35(.20-.50)	1.01	2.34	5.61(24%)	.419	5.65	81.0(26%)
NfB2D	32	.48(.25-.70)	.78	2.10	7.39(29%)	.447	7.39	108.8(29%)
ApA1V	12	.28(.15-.40)	.40	.60	.50(12%)	.097	.60	6.1(15%)
ApB1V	19	.28(.15-.40)	.69	1.35	.97(12%)	.142	1.48	13.8(17%)
ApB3V	23	.28(.15-.40)	.06	.41	.99(19%)	.133	1.90	25.7(28%)
ApB2L	21	.20(.15-.25)	.19	.41	.55(18%)	.052	.77	16.1(28%)
ApB2R	22	.18(.10-.25)	.21	.41	.61(19%)	.047	.69	13.6(27%)
ApA4R	18	.18(.10-.25)	.07	.16	.71(31%)	.047	.96	26.1(42%)
ApB4L	25	.18(.10-.25)	.17	.42	1.29(28%)	.070	1.39	28.6(31%)
ApB4R	26	.15(.10-.20)	.13	.42	.95(23%)	.075	1.29	24.2(31%)
ApA1D	13	.13(.10-.15)	.26	.48	1.04(25%)	.061	1.23	23.4(29%)
ApB1D	20	.13(.10-.15)	.18	.28	.92(34%)	.046	1.15	32.4(43%)
ApB3D	24	.13(.10-.15)	.20	.30	1.32(35%)	.075	1.53	31.5(38%)

Table 3.2 (cont'd)

Sample	Test	Skin Thickness mm mean(range)	Load at Strain 10%	15%	Begin Fail Load(Strain)	Max. Stiff.	Max. Load	Energy(Strain) at Failure
LcA2V	6	.83(.60-1.05)	1.00	3.36	28.04(35%)	1.530	33.51	747.4(43%)
LcA1L	4	.80(.55-1.05)	.23	.68	21.30(35%)	1.769	24.69	335.1(37%)
LcA1R	3	.93(.70-1.15)	.29	.89	4.90(28%)	.386	4.90	58.1(28%)
LcA2D	5	.80(.40-1.20)	2.52	8.88	24.30(23%)	2.338	33.18	58.3(29%)
HmA1V	47	.38(.25-.50)	.06	.19	8.17(51%)	.430	9.32	199.6(54%)
HmA2V	54	.28(.20-.35)	.16	.45	6.01(38%)	.403	6.27	121.0(41%)
HmA3V	52	.40(.25-.55)	.04	.09	3.84(55%)	.206	3.88	82.8(56%)
HmA1L	48	.25(.20-.40)	.03	.08	4.84(50%)	.330	3.27	110.9(55%)
HmA1R	46	.30(.25-.35)	.04	.08	2.42(49%)	.179	2.54	62.5(54%)
HmA2L	49	.33(.15-.50)	.03	.07	4.26(60%)	.200	4.26	87.5(60%)
HmA2R	51	.40(.25-.55)	.04	.08	3.33(51%)	.207	3.76	73.3(54%)
HmA1D	45	.28(.20-.35)	.07	.19	6.55(43%)	.372	6.55	107.6(43%)
HmA2D	53	.35(.25-.45)	.10	.33	4.38(37%)	.476	5.68	100.5(41%)
HmA3D	50	.28(.20-.35)	.12	.42	5.33(31%)	.473	5.65	67.3(32%)
EsA1V	35	.35(.25-.45)	.03	.05	1.27(46%)	.063	1.69	69.5(62%)
EsA2V	41	.48(.35-.60)	.04	.10	1.66(45%)	.082	3.17	120.2(69%)
EsA1L	37	.35(.20-.50)	.04	.10	.87(37%)	.049	1.19	36.0(50%)
EsA1R	36	.45(.35-.55)	.03	.06	.62(36%)	.042	1.05	31.7(53%)
EsA2L	42	.40(.30-.50)	.03	.06	1.00(56%)	.031	.99	39.6(64%)
EsA2R	40	.38(.25-.50)	.03	.06	.78(41%)	.037	.88	24.9(49%)
EsA1D	38	.33(.15-.50)	.02	.06	.82(52%)	.032	.92	30.5(59%)
EsA2D	39	.35(.25-.45)	.03	.09	.99(41%)	.041	1.11	43.8(56%)
EsA3D	44	.33(.15-.50)	.04	.08	1.04(46%)	.042	1.18	46.7(60%)

Table 3.2 (cont'd)

Sample	Test	Skin Thickness mm mean(range)	Load at Strain 10%	15%	Begin Fail Load(Strain)	Max. Stiff.	Max. Load	Energy(Strain) at Failure
AgA1V	56	.48(.25-.70)	.06	.17	2.67(42%)	.126	3.17	63.8(49%)
AgA2L	57	.43(.25-.60)	.10	.23	2.07(45%)	.092	2.15	53.0(47%)
AgA2R	58	.35(.25-.45)	.02	.04	2.47(51%)	.123	2.62	65.4(57%)
AgA1D	55	.23(.15-.30)	.04	.10	.93(53%)	.038	.98	63.8(59%)

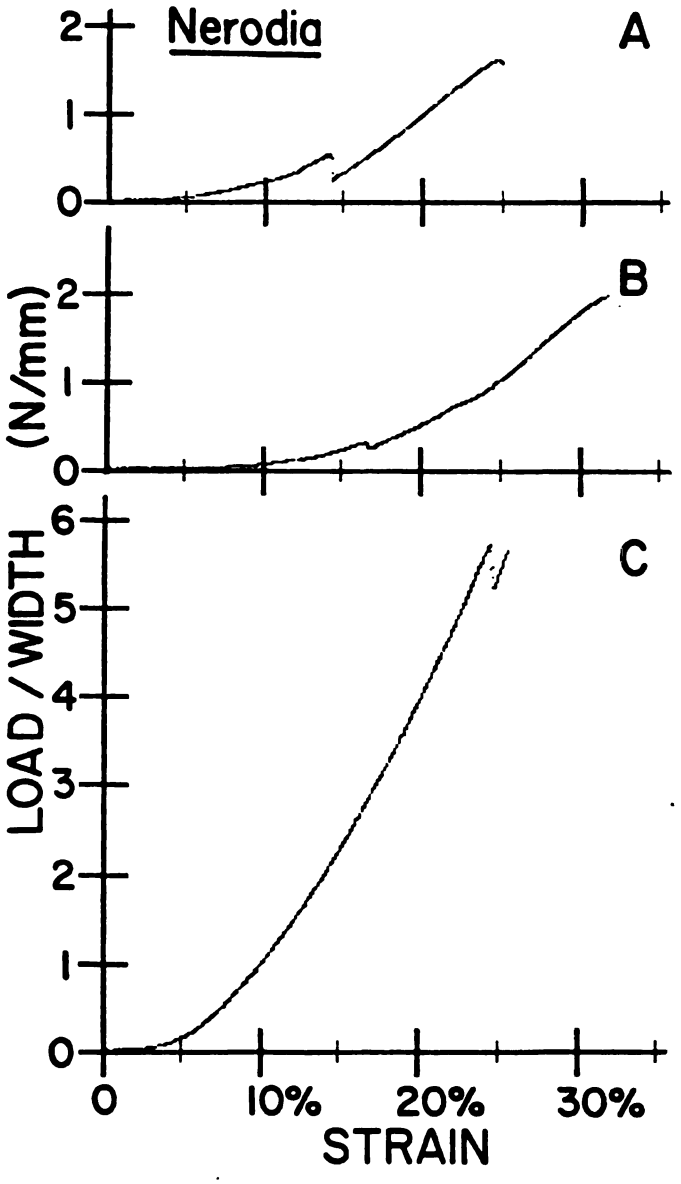

Figure 3.1. Loading curves for skin from Nerodia fasciata pictiventris. A: ventral sample NfB2V, B: ventrolateral sample NfB2L and C: dorsal sample NfB1D.

strain were quite similar for the ventrolateral (.15; .36 N/mm) and dorsal (.21; .36 N/mm) samples compared, to the slightly higher average loads of .38 and .79 N/mm for the ventral samples (Table 3.2). Skin samples from the ventral region had the greatest average maximum stiffness (.124 N/mm%) compared to the similar values of .058 and .061 N/mm% for the ventrolateral and dorsal samples. For Ahaetulla prasina B ventrolateral samples were tested from two anterior-posterior positions (2 and 4). The loading curves were nearly identical between replicates from a single anterior-posterior position (Table 3.2). However, the more posterior samples did not fail until a slightly greater strain than the more anterior samples, and as a result, they attained greater maximum stiffness and maximum load (Figure 3.2). Samples of the skin from Ahaetulla generally failed near 30% strain.

Figure 3.3 illustrates loading curves for samples of skin from Laticauda. The dorsal skin of Laticauda colubrina had loads of 2.52 and 8.88 N/mm at 10 and 15% strain compared to values of 1.00 and 3.36 N/mm for the ventral sample and average values of .26 and .78 N/mm for the ventrolateral samples (Table 3.2). Failure usually occurred near 30% strain. Laticauda had skin much stiffer than any other species in this study with maximum values of 1.53, 1.77 and 2.34 N/mm% for the ventral, ventrolateral and dorsal regions, respectively.

Representative loading curves for the skin of Hydrophis melanosoma are illustrated in Figure 3.4. The ventrolateral skin from Hydrophis melanosoma showed only slight variation in the loads at 10 and 15% strain (Table 3.2), with averages of .04 and .08 N/mm. The other two sampling regions had greater variation in these values (Table 3.2) and averaged .09 and .24 N/mm for the ventral samples and .10 and .31 N/mm

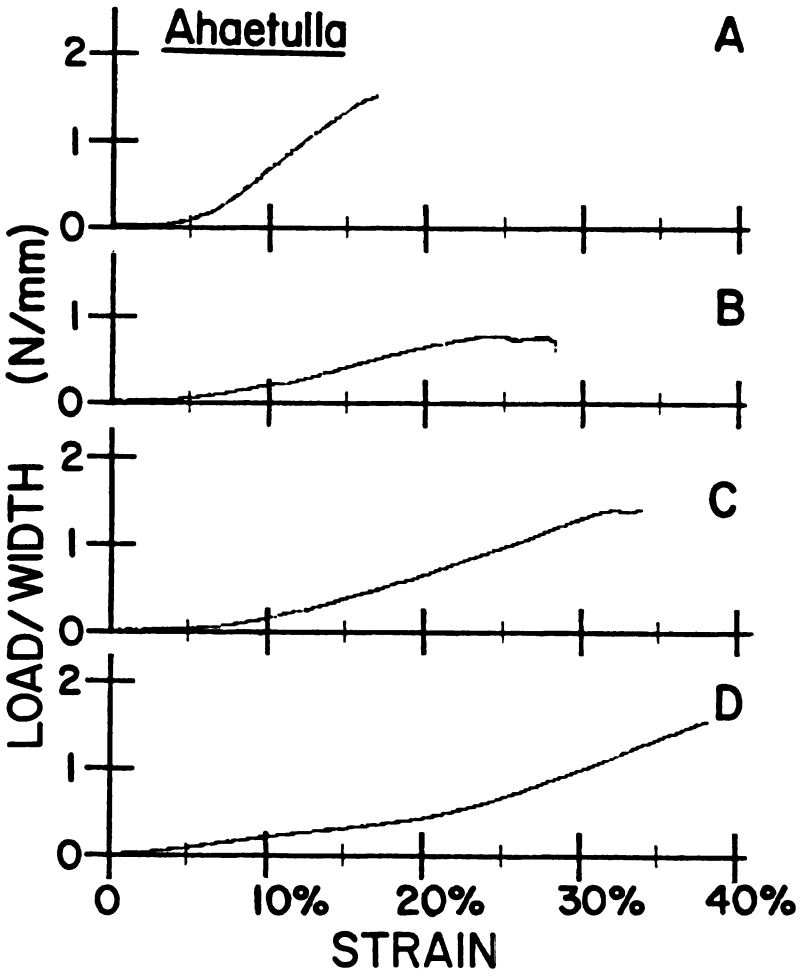

Figure 3.2. Loading curves for skin from Ahaetulla prasina. A: ventral sample ApB1V, B: ventrolateral sample ApB2L, C: ventrolateral sample ApB4L and D: dorsal sample ApB3D.

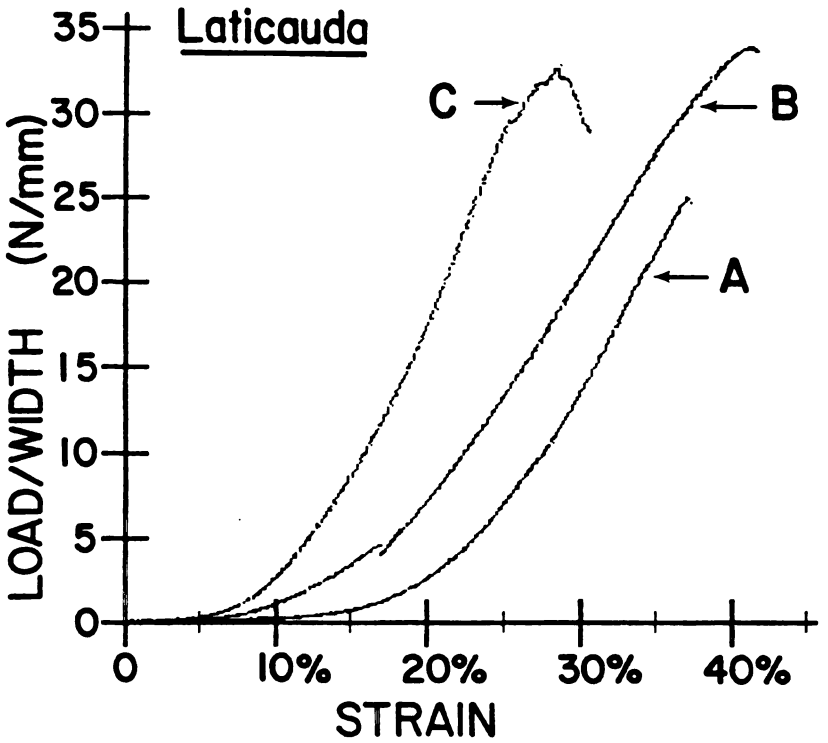

Figure 3.3. Loading curves for skin from Laticauda colubrina. A: ventral sample LcA2V, B: ventrolateral sample LcA1L and C: dorsal sample LcA2D (Note vertical scale is different from all other figures).

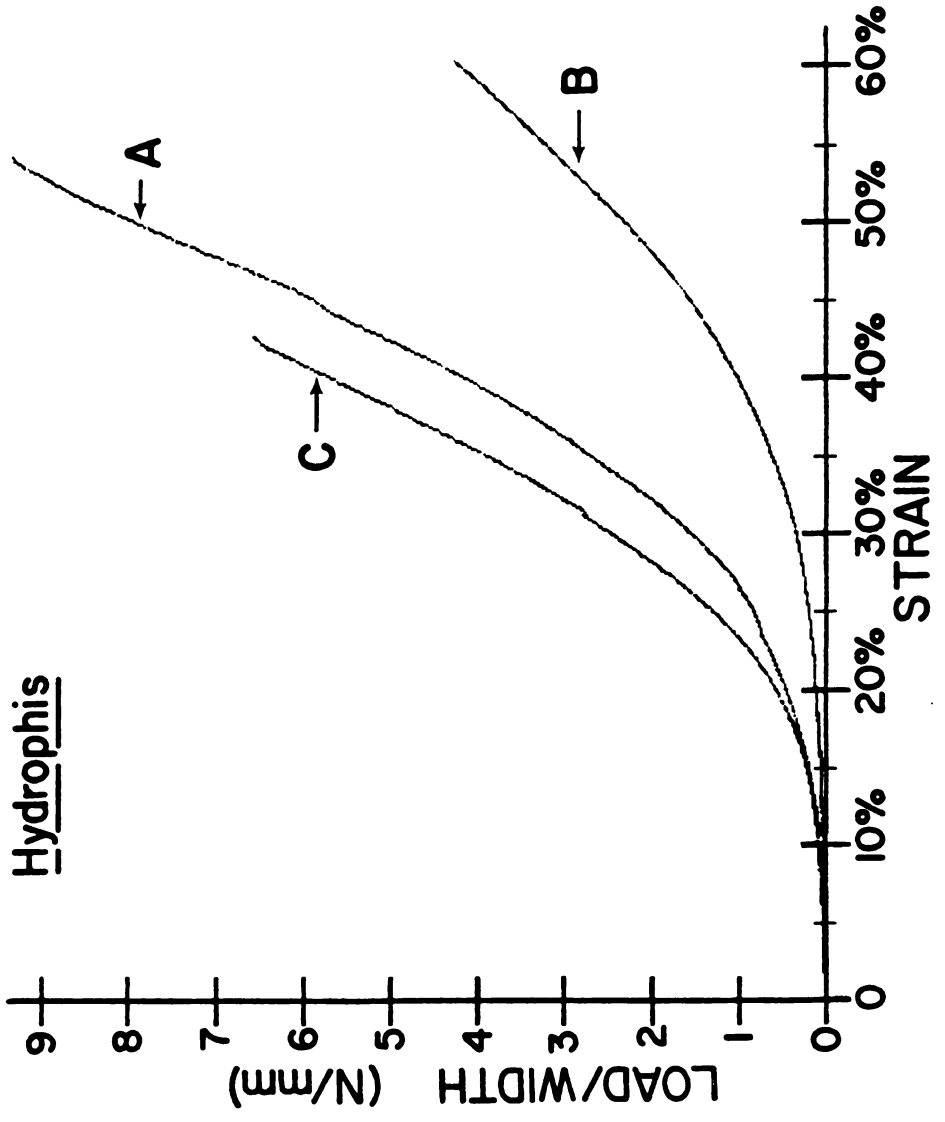

Figure 3.4. Loading curves for skin from Hydrophis melanosoma. A: Ventral sample RmA1V, B: Ventrolateral sample RmA2L and C: dorsal sample RmA1D.

for the dorsal samples. The ventrolateral samples of skin had the smallest average maximum stiffness (.229 N/mm%), compared to values of .346 and .440 N/mm% for the ventral and dorsal samples, respectively. Half of the samples of the skin from Hydrophis did not begin to fail until strains greater than 50%. Although the end of failure was consistently at a greater strain for the ventrolateral samples compared to the dorsal samples, the average maximum load of the ventrolateral samples was less than that of the dorsal samples (3.46 vs 5.96 N/mm). The average maximum load of the ventral samples was 6.49 N/mm.

Figure 3.5 shows representative loading curves for the skin of Enhydrina schistosa. The average loads of the skin of Enhydrina schistosa at 10 and 15% strain were always very low and similar for the ventral samples (.04; .08 N/mm), ventrolateral samples (.03; .07 N/mm) and dorsal samples (.03; .08 N/mm). The ventral samples had the greatest average maximum stiffness (.073 N/mm%) compared to values of .040 and .038 N/mm% for the ventrolateral and dorsal samples, respectively. Five of the nine samples did not begin to fail until strains were greater than 45% and the end of failure occurred at strains greater than 55% for six of the samples (Table 3.2).

Figure 3.6 illustrates loading curves for the skin of Acrochordus granulatus. The skin of this species had relatively small average loads at 10 and 15% strain for the ventral sample (.06; .17 N/mm), the ventrolateral samples (.06; .14 N/mm) and the dorsal sample (.04; .19 N/mm). The dorsal sample had the smallest maximum stiffness (.038 N/mm%) compared to .126 N/mm% for the ventral sample and an average of .108 N/mm% for the ventrolateral samples. The beginning of failure occurred at strains greater than 45% for three of the four sample of

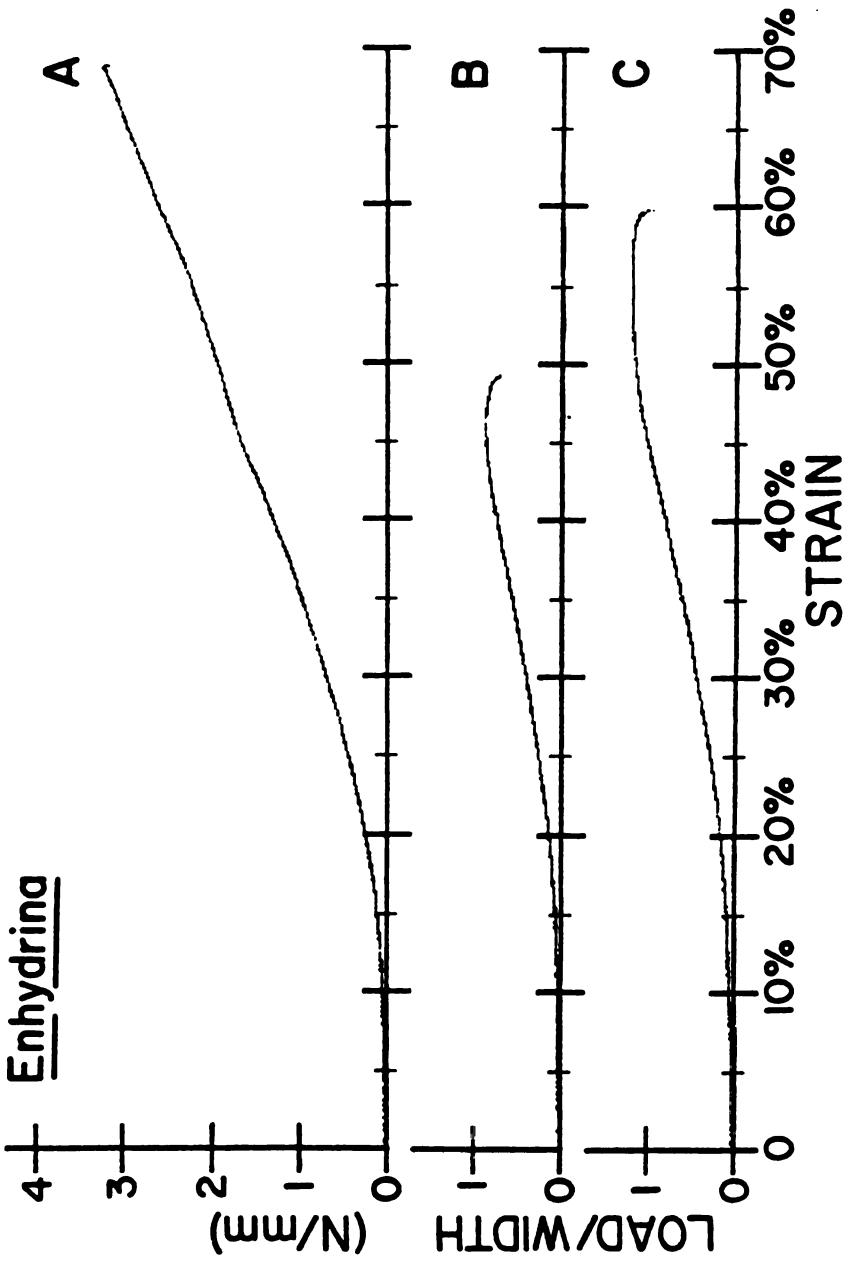

Figure 3.5. Loading curves for skin from Enhydrina schistosa. A: ventral sample EsA2V, B: ventrolateral sample EsA2R and C: dorsal sample EsA3D.

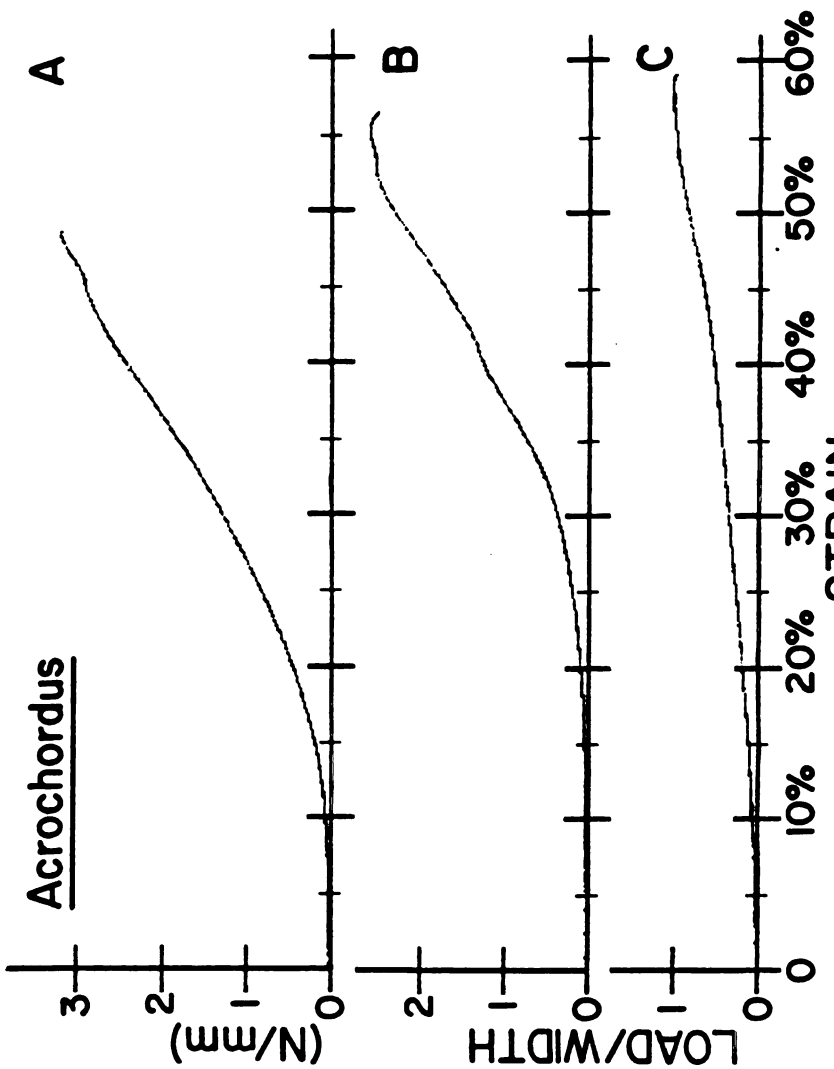

Figure 3.6. Loading curves for skin from Acrochordus granulatus. A: ventral sample AgA1V, B: ventrolateral sample AgA2R and C: dorsal sample AgA1D.

skin from Acrochordus (Table 3.2).

All skin samples failed in the relatively thin region between scales. Because of the greater thickness of scales within the skin, one might expect that samples with the least number of scales per unit area would be most resistant to deformation. Table 3.3 lists estimates of the number of scales in a 7 x 70 mm strip of skin for each sample region of each species that was tested. No clear correlations are apparent when the sizes of scales are compared with loads or stiffnesses at given strains. For example, within both Nerodia and Ahaetulla, the mid-ventral skin samples had the largest scales. However, the mid-ventral skin of Nerodia was the anatomical region of least stiffness, whereas within Ahaetulla the ventral skin was generally stiffer than the ventrolateral and mid-dorsal skin. As a group, the taxa with the smallest scales (Hydrophis, Enhydrina and Acrochordus) generally had skin which had small slopes of the loading curve. However, when the different sample regions are compared within each of these taxa, increased scale size does not consistently predict increased loads or stiffness.

The species used in this study generally attain adult lengths of about one meter. Hence, for snakes of similar size, load/width of skin is a convenient measure to compare both the resistance generated by the skin during lateral flexion and the ability of the skin to transmit locomotor forces. For a given width of skin, the rate of loading during a constant strain rate may differ from two primary causes. Differences in either the structure of the individual collagen fibers or in the overall thickness of the collagen fiber matrix will alter the resistance of the skin to stretching. Although the scales of snake skin cause

Table 3.3. Approximate number of scales in longitudinal strips of skin 7 x 70 mm.

SPECIES	SAMPLE		
	VENTRAL	VENTROLATERAL	DORSAL
Nerodia f. pictiventris	12	36	36
Ahaetulla prasina	14	42	56
Laticauda colubrina	14	42	42
Enhydrina schistosa	120	120	120
Hydrophis melanosoma	96	120	120
Acrochordus granulatus	1764	1274	764

heterogeneity in thickness, dividing load/width by "mean" thickness approximates stress. Different stresses of samples at a given strain should indicate qualitative differences in the structure of the collagen fibers.

"Mean" thickness of the skin samples did vary considerably (.13 - .93 mm) among and within species (Table 3.2). However, the variation within species was often not sufficient to alter the ranking of the different anatomical regions with respect to stress compared to the rankings based on load/width. For example, within Laticauda, Hydrophis and Enhydrina there were no clearcut differences among the thicknesses of skin from the ventral, ventrolateral and dorsal regions (Table 3.2). Therefore, the conversion of loads to stress for these snakes was accomplished by using a nearly constant conversion factor.

In contrast, skin from the ventral region of both Nerodia and Ahaetulla was noticably thicker compared to skin from the ventrolateral and dorsal regions. Consequently, greater differences became apparent when comparing maximum stress of the three different regions within both taxa (Table 3.4) than when the maximum loads/width were compared for the three regions (Table 3.2). For example, in Nerodia mean maximum stress showed more than an eight-fold difference between the ventral and dorsal samples (1.9 vs 15.8 N/mm^2), whereas mean maximum load/width varied only by a factor of about four (1.5 vs 6.5 N/mm%).

The mean maximum stiffness of Ahaetulla skin from different regions varied from .058 to .124 N/mm%, whereas these quantitites only varied from .334 to .467 N/mm^2 after correcting for thickness of the skin. The stresses at 15% strain were also relatively uniform among the three different regions within Ahaetulla (2.07 to 2.81 N/mm^2). Hence, the

Table 3.4. Mean values of stress and stiffness for uniaxial loading of snake skin samples. Means were calculated for homologous samples listed in Table 3.2. All stresses are in N/mm^2. Stiffness is in $N/\%mm^2$ and maximum stiffness occurred at the strain during beginning of failure. See text for more complete explanation.

Sample	Stress at Strain 10%	15%	Begin Fail Stress	Maximum Stiffness	Max. Stress	Energy at Failure
Nf Ventral	.15	.38	1.77	.159	1.94	31.2
Nf Ventrolateral	.26	.85	4.58	.379	4.75	70.1
Nf Dorsal	2.26	5.54	15.72	1.064	15.77	229.1
Ap Ventral	1.37	2.81	2.93	.443	4.74	54.3
Ap Ventrolateral	.86	2.07	4.72	.334	5.87	124.3
Ap Dorsal	1.64	2.72	8.41	.467	10.03	223.8
Lc Ventral	1.20	4.05	33.78	1.843	40.37	900.5
LclL	.29	.85	26.63	2.211	30.86	418.9
Lc Dorsal	3.15	11.10	30.38	2.923	41.48	72.9
Hm Ventral	.28	.78	17.52	1.029	18.87	388.1
Hm Ventrolateral	.11	.25	12.17	.760	10.97	275.1
Hm Dorsal	.32	1.04	18.31	1.459	19.93	303.9
Es Ventral	.09	.18	3.58	.177	5.79	227.2
Es Ventrolateral	.09	.18	2.11	.102	2.63	84.5
Es Dorsal	.09	.23	2.80	.113	3.16	118.9
Ag Ventral	.13	.35	5.56	.263	6.60	132.9
Ag Ventrolateral	.15	.32	5.94	.283	6.25	155.1
Ag Dorsal	.17	.43	4.04	.165	4.26	277.4

variation in skin thickness seems to account for much of the variation in the loading among the different samples within Ahaetulla. Similarly, the relative thinness of Ahaetulla skin probably accounts for the rather small loads at the beginning and end of failure compared to those of other species.

Laticauda had the thickest ventrolateral and dorsal skin of any of the studied taxa and only Nerodia had ventral skin of comparable thickness to that of Laticauda (Table 3.2). However, even after converting load/width to stress, Laticauda still had the greatest maximum stiffness (1.84 to 2.92 N/mm^2), stress at beginning of failure (26.6 to 33.7 N/mm^2) and maximum stress (30.9 to 41.5 N/mm^2). Because the thickness of the skin of Laticauda is insufficient to account for differences, Laticauda probably has substantially different dermal collagen fibers compared to any of the other snakes of this study.

Of all the samples, the skin of Hydrophis, Enhydrina and Acrochordus generally had the smallest loads and stresses at 10 and 15% strain (Tables 3.2 and 3.4). Although most Hydrophis skin samples had low initial rates of loading, the ventral (18.9 N/mm^2) and dorsal (19.9 N/mm^2) samples attained mean maximum stresses that were only exceeded by the skin of Laticauda. As Table 3.4 indicates, the ventrolateral and dorsal samples of Enhydrina skin had the two smallest values of mean maximum stiffness (.102; .113 N/mm^2).

DISCUSSION

The mechanical properties of snake skin are somewhat intermediate to those of mammalian skin and eel and shark skin. Mammalian skin usually loads very slowly at low strains. For example, Veronda and Westman (1970) subjected cat skin to longitudinal uniaxial tensile loading and stress remained less than about .1 MN/m^2 for strains less than 45%. Vogel and Hilgner (1979) recorded stresses less than .1 MN/m^2 at 10% strain and a stress of about 3 MN/m^2 at 40% strain during the longitudinal uniaxial loading of rat skin. In this study, stress of snake skin at 10% strain was generally greater than .1 MN/m^2 and ranged as high as 3.15 MN/m^2 for the dorsal skin of Laticauda (Table 3.4). When Wainwright et al. (1978) prestressed shark skin in the circumferential direction at .3 and 2.8 MN/m^2, longitudinal stresses were .25 and 1.6 MN/m^2, respectively, at 10% strain. Hebrank (1980) found that eel skin loaded in the direction of the dermal collagen fibers had the highest early loads (1.5 MN/m^2 at 5% strain), and uniaxial loading in the longitudinal direction gave the lowest early loads (<.1 MN/m^2 at 10% strain).

The maximum stiffnesses (in $MN/\%m^2$) of snake skin in Table 3.4 can be converted to E, the elastic modulus, by multiplying by 100, and this value corresponds to the mean terminal elastic modulus calculated by Hebrank (1980) for eel skin. E for longitudinally stressed snake skin, in the stiffest region of the loading curves, varies from about 10 to

300 MN/m^2. Maximum stiffness of the samples of snake skin occurred at strains ranging from 12 to 60% (Table 3.2). Hebrank (1980) recorded a mean terminal E of 3.54 MN/m^2 for longitudinally stressed eel skin, and this occurred at the highest strain used by Hebrank which was some 50%. Terminal E can also be estimated from the stress-strain curves available for mammalian skin. Terminal E of cat skin subjected to static longitudinal loading is about 58 MN/m^2 and occurs at some 100% strain (Veronda and Westman, 1970). Terminal E of rat skin loaded uniaxially with a strain rate of 2.7% strain/sec is 26.3 MN/m^2 and occurs at a strain of 63.8% (Vogel and Hilgner, 1979). Because increased strain rates increase the stiffness of skin during testing (Lanir and Fung, 1974), detailed comparisons of these E values are not possible. However, it is interesting to note that the range of values of terminal E of snake skin nearly spans the reported range of values of such widely divergent taxa as fish and mammals. Furthermore, restraint of the sides of the skin orthogonal to sides undergoing loading significantly increases the stiffness of the skin (Lanir and Fung, 1974; Wainwright et al., 1978; Hebrank, 1980). Thus, the stiffness of the skin in intact snakes may be even more variable than indicated by these in vitro tests.

The loading curves of snake skin were usually smooth lines; however, slight discontinuities in these lines were common. These discontinuities were most noticeable for the ventral and ventrolateral samples of Nerodia skin (Figure 3.1), but they were also evident in certain tests of the skin of Ahaetulla (Figure 3.2 and others) and of Laticauda (Figure 3.3). Usually there was just one such discontinuity within a test and this usually occured near 15% strain. Vogel and Hilgner (1978) observed a similar phenomenon for uniaxial loading of

mammalian skin and they termed this the "step phenomenon". Vogel and Hilgner usually observed several of these "steps" within a single test and the "steps" were generally confined to the lower strain (<50%) regions of curves. These steps may be considered either as transient loss of stress or as a gain in strain. As Vogel and Hilgner discussed, the simplest model that explains the behavior of skin consists of a spring in series both with a dash-pot and a Kelvin element (a spring in parallel with a dashpot). The step phenomenon can be explained if there are several springs of different elasticity in parallel within the Kelvin element. Hence, the failure of one of these springs would cause a step (Vogel and Hilgner, 1978). During the tests of snake skin the stratum corneum was often observed breaking and peeling away from the deeper layers of the skin before they failed. This failure of the stratum corneum probably corresponds to the step observed near 15% strain. Thus, although the collagen fibers most likely dominate the mechanical behavior of snake skin, the stratum corneum, which probably has a different elastic modulus than collagen, may contribute significantly to the low strain properties of snake skin.

The loading curves of ventrolateral and ventral skin were usually most similar within species of snakes with well developed costocutaneous muscles. For example, the ventrolateral and ventral samples of Nerodia skin were very similar both in the early loads and maximum stiffness compared to the much stiffer skin from the dorsal region (Figure 3.1). The ventrolateral and ventral samples of Acrochordus skin also attained very similar maximum stiffness compared to the dorsal skin (Figure 3.6). All three samples of Laticauda skin had similar maximum stiffness, but the early loading was most similar between the ventral and ventrolateral

samples (Figure 3.3). The costocutaneous inferior and superior muscles move the skin relative to the skeleton during the propulsive and recovery phases of rectilinear locomotion (Lissmann, 1950). Thus, one might expect that the skin forming the insertions for these two muscles should have more similar mechanical properties than skin lacking insertions of costocutaneous and cutaneous muscles.

The simple superficial morphology of the skin, such as scale size, is a poor predictor of the loading and stiffness of skin (Tables 3.2 and 3.3). Thus, the apparently reasonable suggestion that increased numbers of scale rows facilitate distension of skin during swallowing (Pough and Groves, 1983) now appears premature. An additional factor contributing to the regional differences in skin stiffness may be the extent of the mid-dorsal and mid-ventral septa. For example, in Nerodia the mid-dorsal septum of connective tissue firmly attaches the skin to the neural spines of the underlying vertebrae. Hence, after removing the mid-dorsal skin samples of Nerodia, a slight thickening of connective tissue was present, and this thicker mid-dorsal region may have dominated the behavior of the sample during loading. In contrast to Nerodia, the mid-dorsal skin of Acrochordus is only very weakly attached to the vertebrae and this was the region of least stiffness within Acrochordus. Acrochordus, Enhydrina and, to some extent, Hydrophis are laterally flattened with a pronounced mid-ventral keel. Gross examination the mid-ventral keel of these snakes reveals a slight proliferation of connective tissue that contributes to the keel and this is likely to cause increased stiffness. Future study of the nature of the dermal collagen fibers and the thickness of the skin between scales (i.e., the hinge region) should prove useful for predicting the

stiffness of snake skin.

Skin commonly exhibits anisotropic behavior (e.g., Vogel and Hilgner, 1978; Hebrank, 1980). Perhaps the localized thickenings of snake scales cause anisotropy of snake skin which may be important for allowing such different roles as accommodation of ingestion of large objects and the transmission of locomotor forces. The use of certain large species of snakes in future studies would facilitate determination of anisotropy.

Lissmann (1950) analyzed films of the rectilinear locomotion of a Boa constrictor and suggested a muscular mechanism for this mode. Lissmann suggested that the cutaneous musculature contracts to produce the maximal shortening of the ventral skin, whereas the costocutaneous muscles move the skin relative to the skeleton. Hence Lissmann's proposed mechanism assumes no elastic recoil of the skin. Future work combining electromyography with mechanical testing of snake skin should clarify the interesting relations of muscular and passive mechanisms of skin movement during the rectilinear locomotion of snakes.

This study indicates substantial differences in the mechanical behavior of snake skin. Despite some superficial similarities in the appearance of snakes, snakes occupy a great diversity of habitats. The skin of snakes probably serves several functions associated with this variety of habitats, and this may include acting as a physiological barrier or a transmitter of locomotor forces. For example, the primarily aquatic Laticauda provides a marked contrast to the almost exclusively arboreal Ahaetulla. The skin of Laticauda was much thicker and stiffer than that of the very thin and light-bodied Ahaetulla. Perhaps this difference reflects the protective function of skin or

perhaps it indicates different function in locomotion. Future integrated studies of muscle function and dermal morphology and mechanical behavior should clarify some of the reasons for this variability.

SUMMARY

Each of the approaches used in this study of snake locomotion revealed some significant interspecific differences. Cinematographic analysis of the movement of unrestrained snakes showed that Nerodia fasciata could perform faster terrestrial lateral undulation than Elaphe obsoleta. Both Crotalus cerastes and Cerberus rynchops were proficient sidewinders, but each species performed this mode in a slightly different fashion. Nerodia fasciata could be induced to sidewind but this was more easily performed by smaller snakes of this species. The postures used during the sidewinding of snakes also varied among these three species.

Activity of major epaxial muscles during snake locomotion usually began when regions were maximally convex and ceased when the region was maximally concave on the side of the active muscle. Most muscle activity occurred as alternating, descending unilateral contractions. Bilateral activity of muscles from the transverso-spinalis group correlated with dorsiflexion of the vertebrae during sidewinding. However, this bilateral activity occurred at different times with respect to the movement profiles when comparing Nerodia to Crotalus. Despite the different anterior site of attachment of the M. longissimus dorsi of Crotalus compared to Nerodia, no differences in activity of this muscle were observed between these two taxa. Muscular activity during aquatic lateral undulation differed from that of terrestrial

lateral undulation because the wave of muscle activity was propagated faster than the mechanical wave of flexion within the snakes' bodies. Estimates of the number of active adjacent muscle segments revealed that during swimming more adjacent muscle segments were simultaneously active in Elaphe than in Nerodia.

The loading behavior of skin subjected to uniaxial tension varied widely among the studied species of snakes. Variation was found among species for the load/width of sample at low strains and for the maximum stiffness attained by a sample. Superficial morphology such as the number of scales per unit area was an inadequete predictor of the mechanical behavior of snake skin. The mid-ventral and ventrolateral samples of skin were from the regions of insertion for the costocutaneous inferior and superior muscles, whereas the mid-dorsal sample never included any area of attachment of these muscles. For Nerodia, which has rather generalized morphology of the costocutaneous muscles, skin samples from the ventrolateral and mid-ventral regions displayed very similar mechanical properties, whereas the mid-dorsal skin sample was stiffer than both of these. Laticauda and Acrochordus are two highly aquatic taxa with well developed costocutaneous muscles, but the skin of Laticauda was the stiffest of any studied whereas that of Acrochordus had some of the lowest recorded stiffnesses. Enhydrina and Hydrophis are fully aquatic, whereas Ahaetulla is highly arboreal. All three of these taxa have reduced costocutaneous musculature and they generally had skin of low stiffness in the low-strain region of the loading curve.

Even the limited comparative scope of this study was able to detect functional differences among taxa. The next challenge is to attempt to

put these functional differences into a biologically meaningful perspective. Additional comparative information will be necessary to do this adequately; however, some promising directions for this additional work are suggested.

The different methods of sidewinding were an unexpected finding in this study. The emphasis on categorizing snake locomotion by the nature of force transmission provides a convenient conceptual framework, but it may also potentially obscure some interesting differences among taxa. Gans and Mendelssohn (1972) found that sidewinding was widespread among advanced snakes, and they even obtained footage for the rather awkward sidewinding of a boid. This may lead one to conclude that sidewinding is primitive for the colubroid snakes. However, if different patterns of movement and muscle activity are found within the colubroids it may be that sidewinding is one of the many characters of coubroid snakes that have evolved independently several times.

Interestingly, the skin of aquatic snakes encompassed an enormous range of functional variablity. Among terrestrial snakes there is relatively uniform appearance of the ventral scales, which are the primary surface contacting the substrate (Gans, 1974). The diversity of size and shape of the ventral scales of the fully aquatic sea snakes seems to exceed that of all terrestrial taxa combined (e.g. see illustrations in Smith, 1926, 1943). Perhaps the role of the ventral skin in bearing the weight of the snake and providing directionally dependent frictional resistance (Gray and Lissmann, 1950) has constrained morphological diversity of skin among non-aquatic species of snakes. Similarly, the constraints of non-aquatic locomotion may limit variation in the tensile properties of snake skin. To resolve this

issue, it is clearly desirable to obtain a much larger sample of species without the predominance of morphological extremes used in this study.

Even if functional consequences are found for the morphological diversity of the locomotor apparatus of snakes, an additional issue of the biological role of the locomotion of snakes needs to be addressed. The role of locomotion in predation is one area worth investigation to determine the biological relevance of such laboratory measures as maximum forward velocity. The distinction has long been made between sit and wait predators versus actively foraging predators. Certain viperids seem to exemplify the sit and wait strategy (e.g. Reinert, 1985). Other snakes such as Masticophis seem to show adaptations for the extended periods of activity necessary for a more active foraging strategey (Ruben, 1976). Recently, work on the role of locomotion in predation for other vertebrates such as fish (Webb, 1976) and lizards (Huey and Hertz, 1984) has stressed the importance of acceleration as well as maximum speed in predator prey encounters. Consequently, determination of maximum accelerations attained by snakes, especially certain slender-bodied lizard predators, should clarify the importance of locomotor ability during predation. Comparison of accelerations between lizards and snakes could also reveal some intriguing ecological limitations (or advantages) of being limbless.

Locomotor ability of snakes is also likely to be important in situations not involving predation. Seasonal movements of more than 400 m are well documented for snakes moving to and from hibernacula (Klauber, 1972). Other snakes such as Crotalus cerastes may travel distances in excess of 300 m in a single evening, although the speed and purpose of such forays is not known (Mosauer, 1933). For aquatic snakes

the ability to maintain purposeful movement over a range of water currents may be important. The only truly pelagic sea snake, Pelamis platurus, can often be found stranded on beaches after stormy conditions (Kropach, 1975). Furthermore, the feeble movement displayed by most hydrophiiinae when placed on land suggests that specialization for some locomotor modes may preclude the use of other modes.

Many insights into snake locomotion have been gained by careful laboratory study. The secretive existence of certain species of snakes will probably continue to make field studies of them infeasible. Yet, many other species of snakes are conspicuously present in a variety of habitats, and combined laboratory and field investigations of these species should be able to clarify the biological importance of locomotor performance and different locomotor modes.

BIBLIOGRAPHY

BIBLIOGRAPHY

Albright,R. G., and E, M, Nelson. 1959. Cranial kinetics of the generalized colubrid snake Elaphe obsoleta quadrivittata. II. Functional morphology. J. Morph. 105:241-291.

Alexander, A. A., and C. Gans. 1966. The pattern of dermal-vertebral correlation in snakes and amphisbaenians. Zoologische Mededelingen 41(11):171-190.

Auffenberg, W. 1961. Additional remarks on the evolution of trunk musculature in snakes. Am. Midl. Natl. 65:1-19.

Bennet, S., T. McConnell and S. L. Trubatch. 1974. Quantitative analysis of the speed of snakes as a function of peg spacing. J. Exp. Biol. 60:161-165.

Brain, C. K. 1960. Observations on the locomotion of the Southwest African adder, Bitis peringueyi (Boulenger), with speculations on the origin of sidewinding. Ann. Transvaal Mus. 24:19-24.

Bellairs, A. 1970. The life of reptiles. Universe Books, New York.

____. 1972. Comments on the evolution and affinities of snakes, p.157-172. In: Studies in vertebrate paleontology, K A. Josey and T. S. Kemp (eds.). Winchester Press, New York.

Blight, A. R. 1977. The muscular control of vertebrate swimming movements. Biol. Rev. 52:181-218.

Broadley, D. G. 1983. FitzSimons' snakes of Southern Africa. Delta Books, Johannesburg.

Buffa, P. 1904. Ricerche sulla muscolatora dei serpenti e considerazioni sulla locomozione di questi animali. Dall'l stituto di Zoologia e Anatomia comparata della R. Universita di Padova.

Cundall, D. 1983. Activity of head muscles during feeding by snakes: A comparative study. Amer. Zool. 23:383-396.

Duellman, W. E. 1979. The numbers of amphibians and reptiles. Herp. Rev. 10(3):83-84.

Finlay, B. 1970. Dynamic testing of human skin in vivo. J. Biomechanics 3:322-327.

Gans, C. 1961. The feeding mechanism of snakes and its possible evolution. Amer. Zool. 1:217-227.

____. 1962. Terrestrial locomotion without limbs. Amer. Zool. 2:167-182.

____. 1974. Biomechanics an approach to vertebrate biology. Univ. Mich. Press, Ann Arbor.

____. 1984. Slide-pushing - a transitional locomotor method of elongate squamates, p.13-26. In: Symp. zool. Soc. London No. 52 . M. W. J. Ferguson (ed.). Academic Press, London.

____. 1985. Limbless locomotion - a current overview. In: Proceeding International Symposium on Vertebrate Morphology. Forschritte der Zoologie, Gustav Fischer Verlag, Stuttgart and New York.

____. and D. Baic. 1977. Regional specialization of reptilian scale surfaces: relation of texture and biologic role. Science 195(4284):1263,1348-1350.

____. and H. Mendelssohn. 1972. Sidewinding and jumping progression of vipers, p.17-38. In: Toxins of Animal and Plant Origin, Vol. 1. A. de Vries and E. Kochva (eds.). Gordon and Breach, London.

Gasc, J. P. 1967. Introduction a l'etude de la musculature axiale des Squamates serpentiformes. Mem. Mus. Natl. Hist. Nat. Ser. A Zool. 48:69-124.

____. 1974. L'interpretation fonctionelle de l'appareil musculosquelettque de l'axe vertebral chez serpents (Reptilia). Mem. Mus. Natl. Hist. Nat. Ser. A Zool. 83.

____. 1981. Axial musculature, p.355-435. In: Biology of the Reptilia Vol. 11. C. Gans and T. S. Parsons (eds.). Academic Press, New York.

Gray, J. 1946. The mechanism of locomotion in snakes. J. Exp. Biol. 23:101-120.

____. 1953. Undulatory propulsion. Quart. J. Micro. Sci. 94:551-578.

____. 1968. Animal locomotion. Weidenfield and Nicholson, London.

____. and H. W. Lissmann. 1950. The kinetics of locomotion of the grass snake. J. Exp. Biol. 26:354-367.

Grillner, S., and S. Kashin. 1976. On the generation and performance of swimming in fish, p.181-201. In: Neural control of locomotion. R. M. Herman, S. Grillner, P. S. Stein and D.G. Stuart (eds.). Plenum Press, New York.

Haas, G. 1962. Remarques concernant les relations phylogenetiques des diverses familles d'ophidiens fondees sur la differenciation de la musculature mandibulaire, p.215-241. In: Problem actuels de paleontologie. (Evolution des vertebres). Colloques internationaux du Centre National de la Rechereche scientifique, 104.

Hebrank, M. R. 1980. Mechanical properties and locomotor functions of eel skin. Biol. Bull. 158:58-68.

Heckrote, C. 1967. Relations of body temperature, size, and crawling speed of the common garter snake, Thamnophis s. sirtalis. Copeia 1965:759-763.

Hertel, H. 1966. Structure form and movement. Rheinold, New York.

Hoffstetter, R., and J. P. Gasc. 1969. Vertebrae and ribs of modern reptiles, p.201-302. In: Biology of the Reptilia Vol. 1. C. Gans, A. Bellairs and T. S. Parsons (eds.). Academic Press, New York.

Huey, R. B., and P. E. Hertz. 1984. Effects of body size and slope on acceleration of a lizard (Stellio stellio). J. Exp. Biol. 110:113-123.

Jackson, M. K., and H. W. Reno. 1975. Comparative skin structure of fossorial leptotyphlopid and subfossorial colubrids. Herpetologica 31:350-359.

Jayne, B. C. 1982. Comparative morphology of the semispinalis-spinalis muscle of snakes and correlations with locomotion and constriction. J. Morph. 172:83-96.

____. 1985. Swimming in constricting (Elaphe g. guttata) and nonconsticting (Nerodia fasciata pictiventris) colubrid snakes. Copeia 1985:195-208.

Johnson, R. G. 1955. The adaptive and phylogenetic significance of vertebral form in snakes. Evolution 9:267-288.

Kardong, K. V. 1977. Kinesis of the jaw apparatus during swallowing in the cottonmouth snake, Agkistrodon piscivorus. Copeia 1977:338-348.

Klauber, L. M. 1972. Rattlesnakes. Univ. Cal. Press, Berkeley.

Kropach, C. 1975. The yellow-bellied sea snake, Pelamis, in the Eastern Pacific, p.185-216. In: The biology of sea snakes, W. A. Dunson (ed.). University Park Press, Baltimore.

Lanir, Y. 1979. A structural theory for the homogeneous biaxial stress-strain relationships in flat collagenous tissues. J. Biomechanics 12:423-436.

____. and Y. C. Fung. 1974. Two dimensional mechanical properties of rabbit skin - II Experimental results. J. Biomechanics 7:171-182.

Lighthill, M. J. 1960. Note on the swimming of slender fish. J. Fluid Mech. 9:305-317.

Lillywhite, H. B. and P. F. A. Maderson. 1982. Skin structure and permeability. In: Biology of the Reptilia, Vol. 12 C. Gans and F. H. Pough (eds.). Academic Press, New York. pp. 397-442.

Lissmann, H. W. 1950. Rectilinear locomotion in a snake (Boa occidentalis). J. Exp. Biol. 26(4):368-379.

Mangun, G. R., R. M. Ulkey, B. Young, and G. E. Goslow, Jr. 1981. "Cross-talk" in electromyograms: a precautionary note (abstract). Amer. Zool. 21:1039.

Marx, H., and G. B. Rabb. 1972. Phyletic analysis of fifty characters of advanced snakes. Fieldiana Zool. 63.

Mosauer, W. 1932. On the locomotion of snakes. Science 76:583-585.

____. 1933. Locomotion and diurnal range of Sonora occipitalis, Crotalus cerastes, and Crotalus atrox as seen from their tracks. Copeia 1933:14-16.

____. 1935a. The myology of the trunk region of snakes and its significance for ophidian taxonomy and phylogeny. Publ. Univ. Cal. Los Angeles Biol. Sci. 1:81-121.

____. 1935b. How fast can snakes travel? Copeia 1935:6-9.

Motta, P. J. 1977. Anatomy and functional morphology of dermal collagen fibers in sharks. Copeia 1977:454-463.

Pope, C. H. 1967. The giant snakes. Alfred A. Knopf, New York

Pough, F. H. and J. D. Groves. 1983. Specializations of the body form and food habits of snakes. Amer. Zool. 23:443-454.

Reinert, H. K., D. Cundall and L. M. Bushar. 1984. Foraging behavior of the timber rattlesnake, Crotalus horridus. Copeia 1984:976-981.

Ruben, J. A. 1976. Aerobic and anaerobic metabolism during activity in snakes. J. Comp. Physiol. 109:147-157.

____. 1977. Morphological correlates of predatory modes in the coachwhip (Masticophis flagellum) and rosy boa (Lichanura roseofusca). Herpetologica 33:1-6.

Savitzky, A. H. 1983. Coadapted character complexes among snakes: fossoriality, piscivory, and durophagy. Amer. Zool. 23:397-409.

Smith, M. A. 1926. A monograph of the sea-snakes. Oxford Univ. Press, London.

____. 1943. The fauna of British India, Reptilia and Amphibia, Vol. 3. Serpentes. Taylor and Francis, Ltd., London.

Thomas, R. G., and F. H. Pough. 1979. The effect of rattlesnake venom on digestion of prey. Toxicon 17:221-228.

Underwood, G. 1967. A contribution to the classification of snakes. British Museum Nat. Hist., London.

Varkey, A. 1979. Comparative cranial myology of North American natricine snakes. Milwaukee Public Museum Publ. Biol. Geol. (4).

Vogel, H. G. and W. Hilgner. 1979. The step phenomenon as observed in animal skin. J. Biomechanics 12:75-81.

Voris, H. K. 1975. Dermal scale-vertebrae relationships in sea snakes (Hydrophiidae) Copeia 1975:746-757.

____. and B. C. Jayne. 1976. The costocutaneous muscles in some sea snakes (Reptilia, Serpentes). J. Herpetology 10(3):175-180.

____., and H. H. Voris. 1983. Feeding strategies in marine snakes: an analysis of evolutionary, morphological, behavioral and ecological relationships. Amer. Zool. 23:411-425.

Wainwright, S. A., F. Vosburgh and J. H. Hebrank. 1978. Shark skin: Function in locomotion. Science 202(17):747-749.

Wall, F. 1919. A popular treatise on the common Indian snakes. J. Bombay Natl. Hist. Soc. 26:88-93.

Webb, P. W. 1975. Hydrodynamics and energetics of fish propulsion. Bull. Fish. Res. Bd. Canada. (190).

____. 1976. The effect of size on the fast-start performance of rainbow trout Salmo gairdneri and a consideration of piscivorous predator-prey interactions. J. Exp. Biol. 65:157-177.

Young, J. Z. 1981. The life of vertebrates. Oxford Univ. Press, London.